MORPHOMETRIC ANALYSIS OF NEURAL TISSUE

FOLLOWING THE LONG-TERM IMPLANTATION OF

NERVE CUFFS IN THE CAT FORELIMB

by

David Alexander Crouch

B.Sc. (Hon.), University of Guelph, 1992

THESIS SUBMITTED IN PARTIAL FULFILLMENT

OF THE REQUIREMENTS FOR

THE DEGREE OF MASTER OF SCIENCE

in the

School of Kinesiology

© David Alexander Crouch, 1997

SIMON FRASER UNIVERSITY

September 1997

Canadä

APPROVAL

NAME: David Alexander Crouch

DEGREE: Master of Science

TITLE OF THESIS: MORPHOMETRIC ANALYSIS OF NEURAL TISSUE
FOLLOWING LONG TERM IMPLANTATION OF
NERVE CUFFS IN THE CAT FORELIMB

EXAMINING COMMITTEE:

Chair: Dr. T. Milner

_____
Dr. J.A. Hoffer
Senior Supervisor
Professor and Director
School of Kinesiology, SFU

_____
Dr. D. Finegood
Associate Professor
School of Kinesiology, SFU

_____
Dr. J. Anthony
Laboratory Instructor
School of Kinesiology, SFU

_____
Dr. S. Chadan
Adjunct Professor
School of Kinesiology, SFU

_____
Dr. Glen Tibbits
External Examiner
Professor, School of Kinesiology, SFU

Date Approved: _____05 Sept 1997_____

ii

Abstract

Tripolar circumferential recording nerve cuffs that allow for the derivation of pressure and touch related information from cutaneous and proprioceptive nerves in the cat paw have been designed in our laboratory. At present, there is conflicting evidence with respect to the safety of nerve cuff implantation. We were unable to extrapolate any conclusions about the safety of our nerve cuffs from past literature for two reasons. First, our cuff design was different from the cuffs used in past studies and, second, previous morphometric studies possessed a number of methodological limitations that made their findings inconclusive.

As part of this thesis, a computer based experimental methodology was developed to carry out the quantitative assessment of neural tissues following the long-term (183 to 373 days) implantation of circumferential slit tube type nerve cuff electrodes on the median nerve of the cat forelimb. Morphological assessment was made by comparing a given cat's implanted limb with its own contralateral unoperated control limb. This thesis addressed many of the weaknesses found in previous studies in the literature. It was unique in trying to correlate morphometric variables with changes in compound action potential (CAP) data recorded over the implant period.

Four key messages emerged from this thesis. First, our nerve cuffs were found to be associated with small but statistically significant decreases in axon diameter, fiber diameter, and myelin thickness. Second, cuffed axons located near the perimeter of the nerve experienced somewhat larger differences (as compared to control) than did axons located closer to the center of the nerve. Third, all axon sizes showed the same magnitude of difference with respect to control (i.e. larger axons did not seem to be affected more than smaller axons located in the same cross section). Finally, morphometric differences with respect to control were found to be correlated with CAP changes but this correlation was opposite to what was expected. CAP amplitudes exhibited statistically significant ($p < 0.05$) negative correlations with fiber diameter and myelin thickness differences measured in the Perimeter Zone.

Quotation

"I am so smart, S-M-R-T, smart"

Homer Simpson

Acknowledgments

I would like to take this opportunity to thank the myriad people who helped get me through this phase of my education. Of course, my lab mates deserve recognition for "being there" during the good times and the bad. In absolutely no particular order: Kev, for being the Kamloops version of myself; Sheila for being the kick in the butt that I needed on occasion; Paul for being the artsy-est Engineer in the world; Klaus for helping me steer the Titanic and for introducing me to a man named Duke; Andy for giving me the space that I needed to complete my opus; Morten for being my co-mechanic and co-pilot on numerous adventures and last, but not least, Catharine, Josh and Tiffany for their wonderful care of the animals. Special thanks go to Sophie Dunbar for her caring and understanding during the final grind to the finish.

Thanks go to Dr. Glen Tibbits for allowing me to utilize his lab, framegrabber and computer during the data collection phase of this experiment. Farhad also deserves credit for introducing me to the wonders of the ALI macro language. I wouldn't have even been brave enough to attempt some of the programs that I was able to create without his initial assistance.

I would also like to thank Rob Balshaw of Simon Fraser University's Statistical Consulting Service and Kevin Wainwright for valuable statistic related input.

Finally, I would be remiss if I didn't thank (sic) the British Leland Motor Company (Triumph Division) for creating the most effective thesis diversion known to man.

Table of Contents

Table of Figures

List of Tables

1. INTRODUCTION

1.1 General

The incidence and prevalence of spinal cord injuries has grown in recent years. This situation has profound implications for our society as a whole but, more importantly, it requires that dramatic adjustments be made by individual victims. Spinal cord lesions lead to permanent loss of sensation and voluntary muscular control below the site of the injury. These compromised faculties require spinal cord injured patients to undergo tremendous adaptations in locomotion, personal care and lifestyle.

The permanent nature of spinal cord injuries results from the fact that central nervous system (CNS) neurons (Fig. 1), which project within the spinal cord, have limited capacities for regeneration. CNS neurons can regrow 1 or 2 millimeters out from the proximal end of a lesion but they tend to form neuromas rather than reestablish useful connections. Recent research tends to indicate that CNS glial cells, in particular oligodendrocytes, play key roles in preventing CNS neuronal regrowth.

Peripheral nervous system (PNS) neurons, on the other hand, show remarkable abilities for regeneration. PNS axons can survive lesions to the CNS and can continue to function even if disconnected from their distal targets (Davis et al., 1978; Stein et al., 1980). Limited success has also been observed in reconnecting severed whole nerve trunks in the periphery (Lundborg 1987, 1988). A different glial environment (Schwann cells) appears to be responsible for the improved regenerative capacity of the PNS over the CNS.

The loss of voluntary muscular control in spinal cord injured patients belies the fact that these muscles can usually be induced to contract following the application of an externally derived current source. In a rehabilitative environment, the current source can be applied to the motor nerves that innervate the muscle or, more commonly, the current is applied directly into the muscle belly via wire electrodes. Direct electrical stimulation of nerves or muscles in spinal cord injured patients is called Functional Electrical Stimulation (FES). Intended applications of this approach have ranged from the restoration of gait in paraplegics (Popovic, 1992; Tashman and Zajac, 1992; Nathan,1993) to the enhancement of hand grasp in

1

quadriplegics (Peckham and Keith, 1992; Franken et al., 1994; Haugland et al., 1995; Prochazka, 1996).

Central Nervous System

Brain

Motor Region

Sensory Region

Thalamus

D.C.N.

Spinal Cord Lesion

Peripheral Nervous System

Skin

Cutaneous mechanoreceptor

Spinal Cord

Muscle

Muscle spindle

α motor neuron
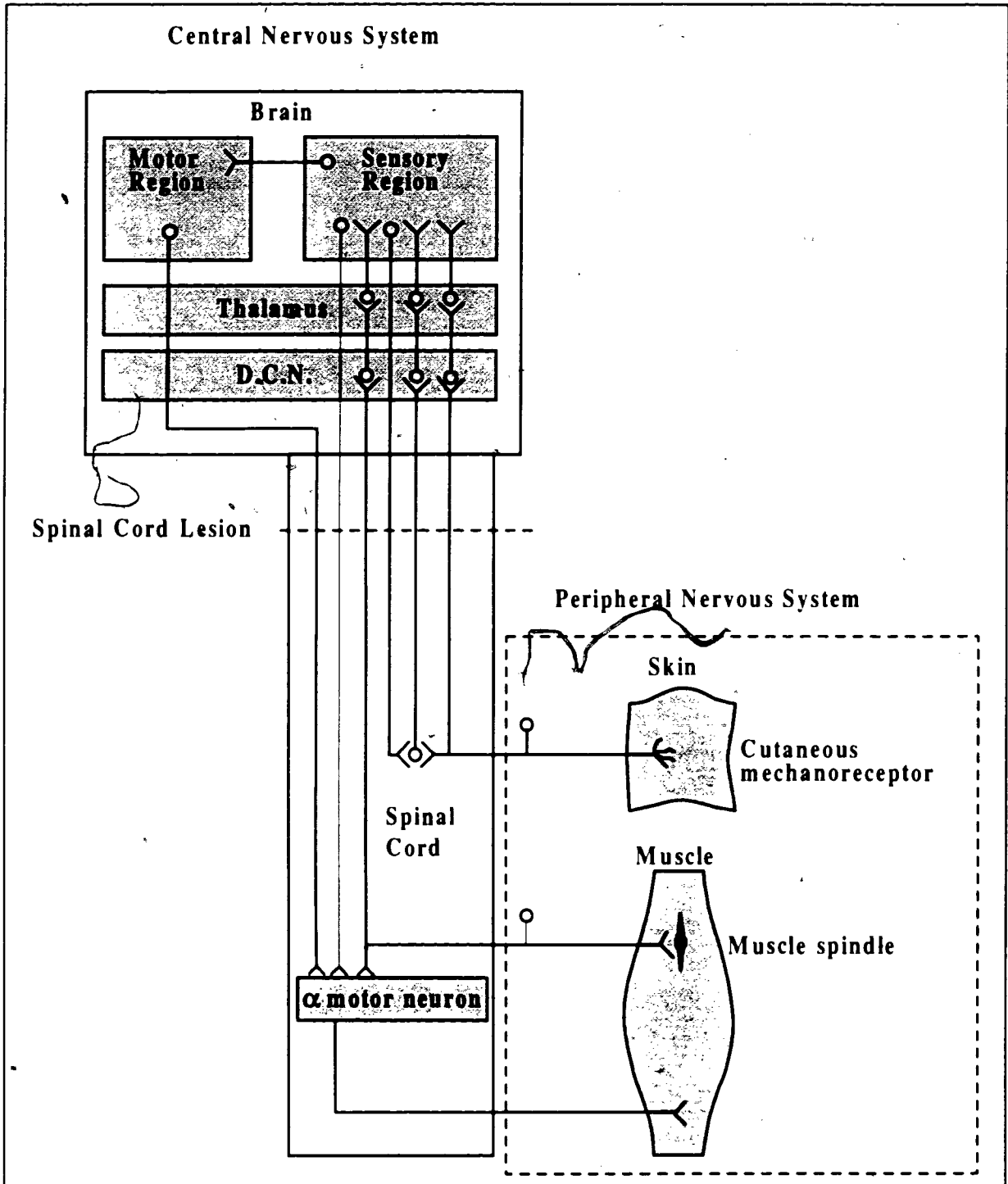
Figure 1: Central Nervous System to Peripheral Nervous System connections. Modified with permission from Christensen, 1997. D.C.N. = dentate caudate nucleus.

Control strategies for FES devices remain fairly crude. Open loop muscle stimulation has been attempted with limited success (Bucket, Peckham and Strother, 1980; Franken et al., 1994) but closed loop feedback systems have shown great promise (Hoffer and Haugland, 1992; Sinkjaer et al., 1992; Sinkjaer et al., 1994).

The advantages of closed loop control strategies combined with the fact that sensory receptors (touch, pain, proprioception and thermal) (Fig. 1) can survive following a CNS injury have led to the exploration of the possibilities of neurally based feedback mechanisms for FES devices. More specifically, recent research has been focused on utilizing nerve recording cuff electrodes to obtain afferent information from intact skin receptors so that neurally based closed loop control of FES systems can be implemented (Hoffer and Haugland, 1992; Haugland and Hoffer, 1994a; Haugland and Hoffer, 1994b; Haugland et al., 1994; Strange et al., 1995a; Strange et al., 1995b; Strange and Hoffer, 1996).

Our laboratory has specialized in the use of nerve cuffs to record natural activity patterns from anesthetized and freely moving subjects. We have chosen to utilize circumferential tripolar nerve cuffs because of their ease of implant, their durability during long term implant and their excellent ability to differentiate neural signals from surrounding EMG noise (Hoffer, 1990). It is anticipated that the information gained from our work will allow finer closed loop control of FES systems in the future.

2. BACKGROUND AND SIGNIFICANCE

2.1 Nerve Cuffs

Nerve cuffs have been used for decades for the stimulation of whole nerves. A number of nerve cuff designs have been tested. Waters et al. (1985) used bipolar cuff electrodes to alleviate the symptoms of foot drop. Kim et al. (1976,1983) and Glenn and Phelps (1985) used bipolar electrodes of various designs to stimulate phrenic nerves in humans. Agnew et al. (1989) used helical electrodes to stimulate peroneal nerves in cats. A complete review of all cuff designs is beyond the scope of this document but the reader is directed to Naples et al. (1990) for a discussion of the relative merits of some of the different designs.

Nerve cuff recording electrodes tend to differ from the majority of the cuff designs used for stimulation in that longer cuff lengths and better insulation between the nerve and surrounding tissues are required. Recording cuffs typically consist of an insulating silicone tube containing several circumferential metal electrodes (multistranded, flexible Teflon-coated stainless steel wire) placed around a length of peripheral nerve. The basic design, fabrication and surgical installation of nerve cuff recording electrodes was reviewed in detail by Hoffer (1990). The cuff closing mechanism has been revised to increase its ease of implantation and reliability (Kallesoe et al., 1996; see Appendix 4).

A properly sealed insulating cuff serves to resolve the small action currents generated by nerve fibers by constraining the current flow within a long, narrow resistive path. The insulating cuff also reduces the pickup of electromyographic (EMG) potentials generated by nearby muscles as well as signals generated by other current sources outside the cuff. The rejection of unwanted signals from outside of the cuff is maximized by utilizing a 'balanced tripolar' electrode configuration (Hoffer, 1975; Stein et al., 1975; Stein et al., 1977).

A number of factors must be considered during the design, fabrication and implantation of circumferential nerve cuffs. First, nerve cuff materials must have chemical and biological compatibility with the implant subject. That is to say, nerve cuffs must be biologically inert with respect to surrounding tissues and must not provoke an immune response. Second, cuffs must be mechanically compatible. Smooth, pliable materials are preferred over rougher or stiffer substances. Third, nerve cuffs must show geometric compatibility. Sharp edges and

4

jutting shapes must be avoided. Finally, it is advantageous to avoid placing the implant close to joints. The movement in these areas causes the cuff to exert excessive mechanical stress on the nerve. Leadout wires from the cuff are also subjected to excessive strain and shear forces when they are located too close to highly mobile joints.

2.2 Neural Anatomy

2.2.a General Organization

Peripheral nerves are composed of a variable number of longitudinally arranged tubular substructures called fascicles (Fig. 2). Fascicles tend to contain the same group of axons throughout the course of the nerve but intrafascicular exchanges of axons are not uncommon.

A dense, connective tissue sleeve, called the epineurium, holds the fascicles together as a bundle (Fig. 2). The thickness of the epineurial layer can vary between nerves as well as along the length of any given nerve. The epineurium has a protective function for the underlying neural tissue in that it acts as a cushion against externally applied forces. As such, epineurial connective tissue thickness is greatest at or near joints.

Each fascicle is surrounded by a connective tissue layer called the perineurium (Fig.2). Perineurial cells are tightly interdigitated such that they act as a diffusion barrier to most high molecular weight substances. Short slips of perineurial connective tissue follow epineurial blood vessels as they penetrate the perineurium.

The endoneurium is a loose collagenous structure that surrounds the individual axons of a fascicle (Fig. 2). The endoneurium contains numerous intercellular spaces, fibroblasts, mast cells and a capillary network (Lundborg, 1988).

5
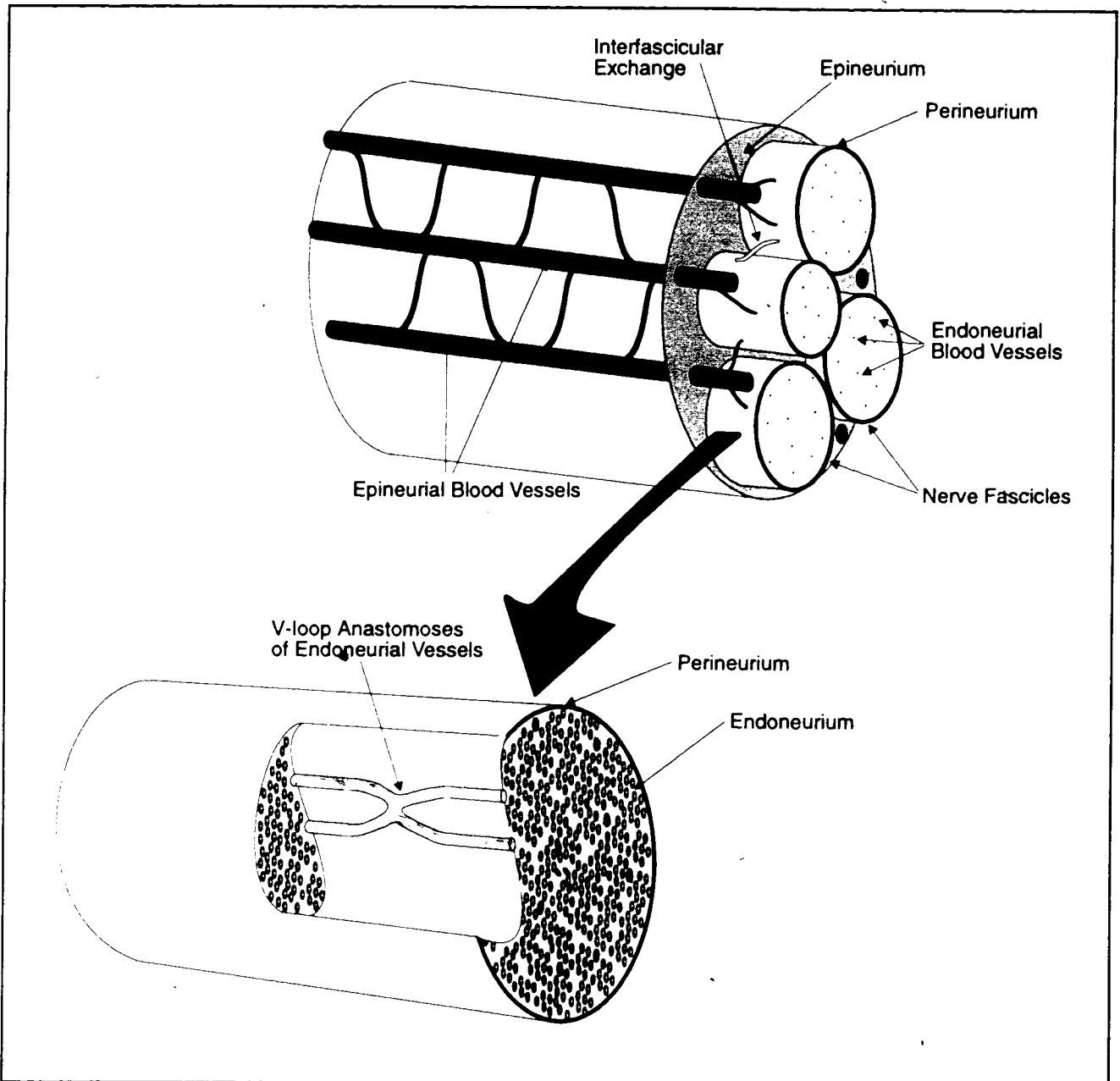
Figure 2: Diagram of the vascular system of a typical nerve. Note the extensive anastomoses between different vessels.

2.2.b Neural Vasculature

Examination of the blood flow within a peripheral nerve yields a number of important observations (Lundborg, 1975, 1987, 1988):

●anastomoses in the epineurium are extensive (Fig. 2).

•anastomoses between the epineurium and endoneurium are extensive (Fig 2). Epineurial vessels pierce the perineurium in an oblique fashion that may create a valve-like mechanism when intrafascicular fluid pressures rise.

•within each fascicle, the vascular bed is predominantly composed of capillary sized vessels.

•typically, endoneurial vessels run parallel to the course of the nerve but, quite often, these vessels loop back to form 'double-V-loop anastomoses' with other vessels. This rich, redundant supply of blood means that it is very difficult to cut off the circulation within a fascicle (Fig. 2).

•the vasa nervorum receive sympathetic innervation and, therefore, the blood flow within nerves can be modulated.

•nerves can be mobilized over several centimeters without seriously interrupting blood flow within a nerve.

•the perineurial connective tissue layer is quite impermeable to most substances. This means that diffusion through the perineurium occurs at a very low rate.

The aforementioned observations are significant when one is considering the implantation of nerve cuffs into an experimental subject. While the findings suggest that nerves should be fairly robust with respect to surgical mobilization and interruption of intrafascicular blood flow, they also suggest that an adequate blood supply is critical to the survival of nervous tissue. This dependence on an adequate blood supply is not unique to nervous tissue but nerves may be more susceptible to changes in flow than other kinds of tissue. Direct pressure on a nerve as low as 30 mmHg is sufficient to significantly impair nerve venular blood flow (Rydevik et al., 1981). Furthermore, pressures as low as 50 mmHg can impair blood flow within the arterioles and capillaries (Rydevik et al., 1981). To put these figures into perspective, 30 mmHg is the level of pressure that is typically seen in carpal tunnel syndrome patients (Lundborg et al., 1982). Clearly, it is essential to be aware of blood flow maintenance issues when installing any devices near or around a peripheral nerve.

2.3 Implications of Nerve Cuffs Implanted on Whole Nerves

A number of issues have been identified in the nerve trauma observed following some cuff implantation procedures. These include surgical trauma, pulls to the leadout wires, direct compression by the cuff, anoxia/ ischemia, permeability changes and edema, changes to axonal transport and changes to the cell body. It should be noted that, despite the fact that the following factors are separated into individual categories, there is a strong interdependence among them. The purpose for their separation is to illustrate the diversity of factors that can combine to cause damage to neural tissue during the type of long term implantation protocol utilized in this experiment.

2.3.a Surgical Trauma

When implanting a nerve cuff electrode on a peripheral nerve, the nerve is freed gently from surrounding tissues such that the longest possible free length is created without causing the obstruction, occlusion or severing of any of the nutrient arteries or nerve branches (Hoffer, 1990).

Lundborg has shown that rabbit sciatic nerves can be mobilized cleanly from the surrounding tissue and vasculature for up to 15 cm before any appreciable decrease in blood flow is observed (Lundborg, 1975). Our laboratory has tried to stay within these limitations by being careful to avoid damaging the existing vasculature during surgery and by not creating free lengths greater than 4 cm during cuff implantation.

Nerves can be damaged by excessive stretching and faster rates of stretching have been shown to increase the level of eventual damage (Sunderland, 1968). If the rate of stretching is slow, actual physical disruption of the connective tissue elements does not occur until the nerve has been stretched 70% greater than its initial length (Haftek, 1970) but serious blood flow changes have been observed with stretches that only increase the nerve length by 15% (Lundborg and Rydevik, 1973). It should be stated, however, that the Lundborg and Rydevik (1973) study defined damage as a permanent change in blood flow following a 30 minute period of stretching. Clearly, other ischemic and anoxic factors would also come into play that

might exacerbate the effect of these stretches. The surgical nerve mobilization performed as part of our cuff implantation procedure required only minimal stretching lasting for very brief periods (approximately 10 seconds at the most) and would not involve these confounding factors.

Any tissue disrupted during surgical intervention can be expected to experience some transient post-surgical inflammation. However, if a nerve is mobilized with minimal traction and it is handled gently throughout the procedure, then the level of post surgical edema should be minimal (Lundborg, 1975). We utilized nerve cuffs that were 20-30% larger than the nerve as a precaution against compression related damage during the post-surgical inflammatory period.

2.3.b Leadout Wires

It is imperative in a chronic nerve cuff implantation that the leadout wires coming from a cuff be of sufficient length to ensure that some slack exists in the wires between the nerve cuff and the backpack (Hoffer, 1990). It is possible that, with insufficient wire slackness, joint movements can be transmitted directly to the device. Our surgical protocol called for the inclusion of slack along the path of the wire to prevent the occurrence of lead pulls (Fig. 3).

2.3.c Compression

Unlike the long-term effects of edema, direct, acute compression injuries (as measured by changes in fast axonal transport) can be reversed quickly (within 1 day) if the severity of the compression is kept at a low level (<50mmHg) (Rydevik et al., 1980). Higher levels of compression can cause edema that might take several weeks to dissipate. Not surprisingly, it has also been demonstrated that both the magnitude and the duration of the applied compression play a role in determining the severity of the injury (Rydevik and Lundborg, 1977). While a nerve compression lasting 2 hours at a given pressure may cause little damage, a similar pressure applied for 6 hours can be significantly more harmful. The severity of the compression can also determine the type of axonal damage that may occur. Severe pressure

can cause axonal degeneration while less severe constriction may lead to local demyelination. (Powell and Myers, 1986). Essentially, high pressure ligatures cause reactions that are indifferentiable from a nerve axotomy (Lundborg, 1987).
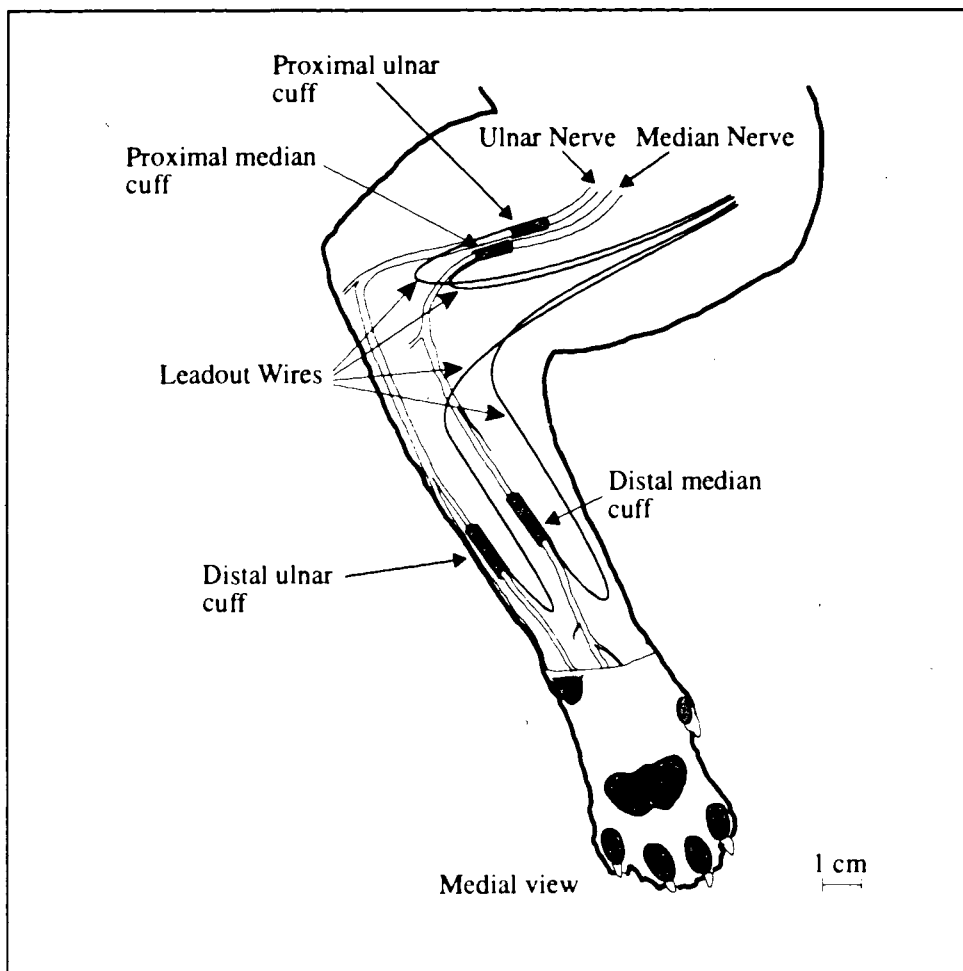
Figure 3: Medial view of the cat forelimb showing the placement of the nerve cuffs and the paths taken by the leadout wires. Leadout wires run subcutaneously for the majority of their course. Note the proximally located loops of wire that are designed to provide strain relief to the system through the normal range of joint motion. Modified with permission from Strange et. al., 1996.

With chronic, moderate levels of compression, there does not appear to be a reduction in the number of nerve fibers in the compressed region but the spectrum of fiber sizes becomes very different (Aguayo, Nair and Midgely, 1971). The fiber size distribution under a chronic compression is modified such that fewer large diameter fibers are observed as compared to the

uncompressed, contralateral, control side (Aguayo, Nair and Midgely, 1971). These findings are consistent with studies performed on axotomized animals (Gillespie and Stein, 1983).

While some damage can be observed throughout the entire nerve, other aspects are restricted to the site where the insult was introduced. This distinction is important because local damage seems to play a greater role in determining the level of neural damage (in direct compression models) than does the ischemia which results from the compression (Lundborg, 1975). Extreme levels of compression can cause a displacement of the nodes of Ranvier (Fig. 4) such that the nodal gap becomes completely obliterated by the invagination of one paranodal region's myelin sheath into the paranodal region on the opposite side of the node (Ochoa et al., 1972). Conduction velocity is reduced as a result.

Nodal displacement appears to be due to the local differences in pressure between adjacent internodes. Displacement was only observed at the edges of the pressure cuff and was not seen under the center of the cuff (Ochoa et al., 1972). Nerve modeling work done by Lundborg (1988) supports this hypothesis. Nodes were displaced differently depending on which side of the pressure cuff they were situated (Ochoa, and Marotte, 1973). The proximal side of the lesion showed swelling on the proximal side of the node while areas distal to the lesion showed swelling at the distal side of the node.
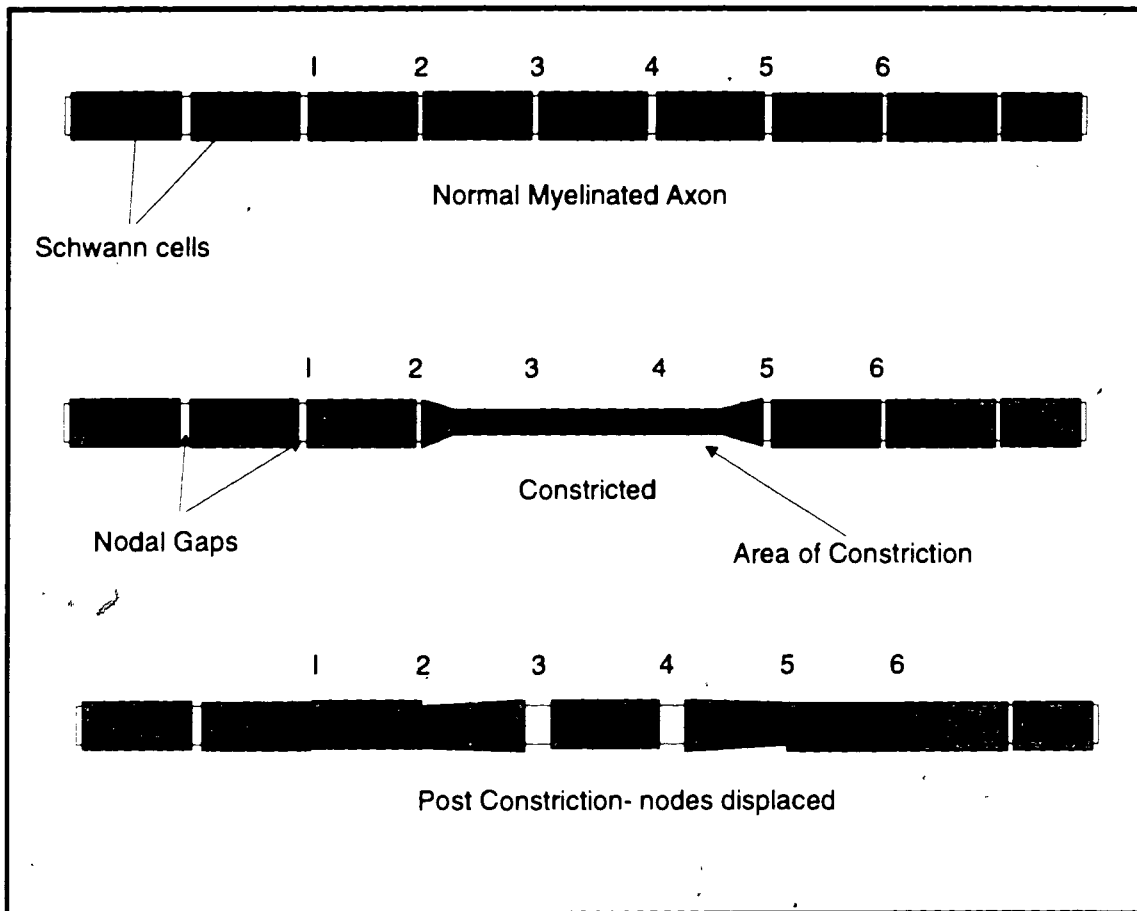
Figure 4: Schematic representation of the effect of local compression on an axon. Note there is relatively even spacing between the Schwann cells prior to the application of the constriction (*top*). Following constriction, nodes are displaced away from the site of the compression except for the nodes directly under the constriction (*nodes 3 and 4*). Note that nodes closer to the edge of the pressure cuff (*nodes 2 and* 5) are displaced more than those located further from the edge (*nodes 1 and* 6). In fact, the Schwann cells nearest to the site of compression tend to invaginate into the Schwann cell next to them. Note that the dimensions of the axons are not drawn to scale in order to aid in the clarity of representation.

2.3.d Anoxia/ Ischemia

In many compression studies, it is difficult to partition the effects of anoxia from the effects of local damage since one is often concomitant with the other. There are models, however, that have shown that anoxia alone may damage the endoneurial blood vessel epithelia such that the blood-nerve barrier function is compromised (Rydevik and Lundborg, 1977). The integrity of the blood-nerve barrier is essential to the maintenance of the osmotic balance in the endoneurial space. Damaged blood vessels lead to the creation of endoneurial

edema. Another problem which can arise specifically from long periods of ischemia (>4 hrs) is the formation of microthrombi and microemboli (Lundborg, 1975, 1987, 1988). Prolonged oxygen deprivation leads to the cessation of axonal flux which, in turn, leads to axonal swelling that triggers the formation of microthrombi and microemboli (Dahlin and McLean, 1986; Lundborg, 1987).

2.3.e Permeability Changes and Edema

Compression trauma to a nerve (~50mmHg) can cause an increase in the permeability of intraneural microvessels within that nerve (Rydevik and Lundborg, 1977). This reaction is similar to the response of many other tissues following a local traumatic event. Permeability changes are greatest at the edges of the pressure cuff (Rydevik and Lundborg, 1977). These data are consistent with the notion that there is an exaggerated pressure differential at the edge of any pressure cuff applied to the nerve (Ochoa et al., 1972; Lundborg, 1987). Increased permeability occurs in two stages: one immediate and one delayed by approximately 2 weeks. It has been suggested that the early changes are probably due to: 1) direct trauma that compromises the integrity of the blood-nerve barrier and/or 2) the release of endogenous mediators such as histamine or serotonin (Lundborg, 1975). The secondary wave of increased permeability may be due to immature regenerating vessels that have not fully developed an effective barrier or it is possible that degenerating axons may be releasing some kind of mediator (Lundborg, 1975). Macrophages and mast cells which arrive on the scene in the early phagocytic stage following injury also have a permissive effect on the blood-nerve barrier.

Given that neither the capillary nor the arteriolar blood flow within the nerve change at low levels of pressure (Rydevik et al.,1981) and that the perineurium is a relatively impermeable structure both to influx and efflux of fluid (Lundborg, 1975, 1987, 1988), it can be expected that the blocking of venous return might lead to significant endoneurial edema within the fascicles. In addition, the impermeability of the perineurium means that any edema formation will be difficult to dissipate. There are no lymph vessels within the endoneurium so the only method of fluid reuptake is through the endoneurial capillaries.

13

While many of the aforementioned studies have looked at the development of edema following the imposition of external trauma to the nerve there are other studies that examine the role of edema alone on nerve function. The development of a galactose neuropathy (hypergalactosemia) model has shown that hypergalactosemic rats experience chronic intraneural edema that leads to ischemia and eventual neural degeneration despite the fact that no external forces are applied to the nerves (Myers and Powell, 1984). It is also worth noting that long standing edemas may be invaded by white blood cells and fibroblasts such that fibrotic scars may be formed in the edematous tissue. Increased fibrosis will lead to a further increase in the pressure being applied to the axons.

2.3.f Axonal Transport

It has been shown that the interruption of axonal transport is the signal that leads to the degradation of distal axons and somatofugal atrophy of proximal axons following the more severe forms of compression neuropathy (Weiss and Hiscoe, 1948; Droz, 1969).

Fast axonal transport is an active, energy dependent process which carries out the transport of synaptic vesicles (for review see Vallee and Bloom, 1991). Ischemia inducing events will tend to reduce or obliterate vesicular transport within the neuron.

Slow axonal transport can be inhibited at low compressive pressures as well (Dahlin et al, 1984; Dahlin and McLean, 1986). Since slow axonal transport carries cytoskeletal building blocks within the axon, ischemic events in one area may prevent the transport of cytoskeletal elements to parts of the axon which are more distally located. This situation may make the distal segments more susceptible to ischemia or compression related damage and, thus, a cycle of degeneration could be initiated.

2.3.g Changes to the Cell Body

Compression of the axonal region of a nerve can cause changes in the cell body of the neuron (Dahlin et al., 1987) that are consistent with cell body changes that occur following axotomy (Grafstein, 1975). These changes include the movement of the nucleus to the periphery of the cell body and the dispersal of the Nissl substance (a process often called

chromatolysis). One difference, however, is that, in compression neuropathies, the cell body volume tends to get smaller while with axotomy the cell bodies tend to swell (Dahlin et al., 1987; Grafstein, 1975).

2.3.h Differential Damage

Comparison of Larger and Smaller Fibers

Previous research has shown that larger myelinated axons (>10 μm) are damaged more extensively than smaller myelinated and unmyelinated fibers following compression-type injuries (Ochoa et al., 1972; Stein et al., 1977; Stein and Oguztöreli, 1978; Lundborg, 1987). The work in our laboratory is primarily directed at recording the activity of skin and muscle mechanoreceptors in the paws of cats. Virtually all of these receptors are within the Aα and Aβ fiber groups (6-20 μm axon diameter) (Martin and Jessell, 1991). Thus, the axons of primary interest to our lab are the very same ones that are most likely to be damaged by compression.

Location of Axons Within a Nerve Cross Section

During nerve compression, axons that are radially located near the periphery of the nerve may be subject to greater damage than those axons that are closer to the center of the nerve (Aguayo et al., 1971). It has been suggested that axons near the outer edges may experience greater compression from the nerve cuff than do those located in the interior (Lundborg, 1987).

2.4 Previous Long-term Nerve Cuff Implant Studies

The accumulated evidence regarding the safety of long-term nerve cuff implantation is conflicting.

Some studies have concluded that nerve cuffs are completely safe. Naples et al. (1988) used self adjusting spiral nerve cuffs during 7 month implantation on median and ulnar cat

nerves. Following completion of the implant period, a gross histological assessment determined that no cuff related damage had occurred to the nerves. Assessment methods in this study were on a pass/fail (damage/no damage) basis and no quantification of the results was reported. Krarup and Loeb (1988) implanted circumferential nerve cuffs into the hindlimbs of cats. The cuffs were implanted for up to 119 days and the nerves were examined using morphometric analyses (the sizes and shapes of the axons were measured). These investigators examined 500-600 fibers and extrapolated their results to the entire nerve (about 8000 axons). They observed that only 1 to 2% of fibers were undergoing degeneration and they noted that the nerves were basically in good health. Glenn and Phelps (1985) studied the phrenic nerves of 77 human patients who had been implanted with unipolar and bipolar cuff phrenic nerve stimulating electrodes for time periods up to 16 years. They observed that a thick fibrous capsule ensheathed the nerve and the nerve cuff but that no neurophysiological damage (defined as the continued function of the nerve cuff) appeared to have occurred.

Some studies have shown that the long-term installation of nerve cuffs can cause changes to the implanted nerves that are difficult to characterize as either safe or damaging. Waters et al. (1985) corrected footdrop with a bipolar stimulating cuff electrode in the peroneal nerve of 7 human patients who used the stimulator for 10.1 to 12.3 years. Prior to cuff removal, extensive fibrosis was observed around the cuff as was substantial adherence to surrounding tissues. These investigators noted, however, that seroma formation between the cuff and the nerve was a more serious consequence of the implant because seromas had greater potential to cause compression of the nerves. Despite these concerns, it should be noted that Waters et al. (1985) did not experience any difficulties in stimulating the nerves through the cuffs. Kim et al. (1983) used phrenic nerve stimulation to aid in the diaphragm pacing of quadriplegic humans. These researchers paced their patients with bipolar stimulating cuff electrodes for 4 to 374 days but the cuffs were implanted anywhere from 273-986 days. Consistent with other studies, they observed a dense fibroadipose tissue layer around the cuffs. A focal loss of myelin was observed in only 2 of the 34 cases and they concluded that the cuff implants were generally safe.

A number of studies have shown evidence that suggests that nerve cuffs can cause significant trauma to the nerve. Stein et al. (1977) used silastic tube circumferential nerve cuffs for long-term (6 month) recording of nerve signals. A decreased density of axons was

observed in the implanted nerve as compared to the control limb. The fiber distribution was altered such that there were fewer larger fibers than in the control nerves. This difference was interpreted as a decrease in size of the largest axons in the nerve and not a reduction in the total number of axons. In another related study, Stein et al. (1980) used nerve cuffs to record from the hindlimbs of cats. They observed that some nerves stopped conducting following implantation of the nerve cuffs. These nerves demonstrated substantial recovery following repair surgeries designed to reposition the cuffs. Kim et al. (1976) implanted bipolar platinum ribbon electrodes encased in silicone rubber onto the phrenic nerves of 7 human patients. Nerve stimulation was carried out for periods up to 4 years. They observed the characteristic dense fibrous coating around the cuff and, despite the fact that stimulation was successful, there were indications of demyelination in some fascicles while other small fascicles were completely demyelinated. It was hypothesized that the mechanical factors associated with the presence of the cuff were more important in the mechanism of damage than was the stimulation protocol.

There are a number of reasons that the accumulated literature regarding long-term nerve cuff implantation leads to few conclusions with respect to this thesis project:

- First, previous studies were inconsistent in their determination of damage. Some studies showed severe nerve damage following a cuff implant while others noted little or no morphological changes.

- Second, previous studies utilized cuff designs that were different from the advanced designs currently in use in our laboratory. Our patented design (Kallesoe et al., 1996) has been engineered to increase the safety of implantation as compared to previous designs. In addition, most of the studies found in the literature have utilized stimulating cuffs. Our cuffs are used primarily as recording devices. The significance of these differences is difficult to estimate.

- Third, most of the previous studies have not used adequate morphometric methods. Most studies of nerve health have previously been judged solely on qualitative measures. Of the few studies that have tried to quantify the changes that occur to a nerve following a cuff implant, all have used sampling techniques of a few hundred axons to determine the health of the rest of the nerve cross section. Nerve cross

sections have been shown to be extremely heterogeneous with definite, non-random distributions of fiber sizes being present throughout the nerve (Torch et al., 1989).

- Finally, no studies have looked at the fate of cuffed nerves in the forelimb of the freely moving cat. This animal model is unique in that the elbow and shoulder joints of the cat are highly mobile and the loads supported by forelimbs, particularly during jumping and landing, are considerably higher than those observed in the more commonly studied cat hindlimb.

2.5 Neurophysiological Determinants of Nerve Health

Compound action potentials (CAPs) are commonly utilized in the determination of nerve health (Fig. 5). A CAP is generated by the electrical stimulation of a nerve bundle with an electrode. The stimulus pulse simultaneously excites all the axons in the nerve bundle and, as a result, each axon is induced to undergo an action potential (AP). The sum of all these simultaneous APs is recorded by another electrode and the resulting signal is termed a CAP. In our experimental model, the proximal cuff served as the stimulating electrode (Fig. 3) and the distal electrode was used to record the signal. Four main parameters: fiber diameter, cuff inside diameter, cuff length and interelectrode distance determine the shapes and amplitudes of the axonal potentials recorded (Marks and Loeb, 1976). The aggregate electroneurographic (ENG) activity recorded from a nerve depends on the number of active fibers and is usually dominated by the activity of the largest axons. The signal is biased in favor of superficially located axons (Marks and Loeb, 1976).
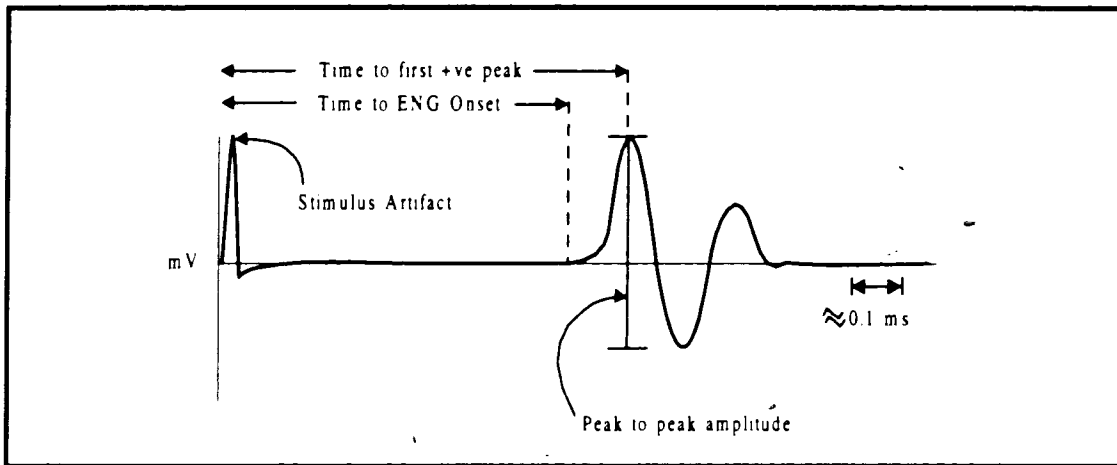
Figure 5: Sample of a typical compound action potential (CAP). The amplitude of the ENG peaks is highly variable so the y-axis has been left without units.

This study will utilize the time to onset of the first positive peak of a CAP recording, time to first positive CAP peak and the peak to peak amplitude of that CAP as the main indices of neural function (Fig. 5). The time to the first positive peak is related to the speed at which the fastest axons in the nerve are conducting and any increase in the time to the onset of this peak can indicate the loss of larger fibers within the nerve (Stein et al., 1980). The peak to peak amplitude is related to the number of large fibers in the nerve as well as to the number of large fibers close to the surface of the nerve. The CAP amplitude may also be influenced by such external factors as a change in the electrical impedance within the cuff (due to connective tissue growth for example), the condition of the cuff (i.e. if all the wires are intact) and the temperature of the recording site.

During chronic implantation, signals recorded from circumferential nerve cuffs may show changes in signal amplitude over time. These can be due, in part, to changes in the ability of the devices to record neural signals (Stein et al., 1978) or there can also be changes in the signal output from the nerves themselves (Davis et al., 1978). When the conduction velocities of the nerves and the amplitude of the CAP signal show concomitant decreases, it is possible that the experimental regimen may be causing damage to the nerves on which the cuffs are implanted (both symptoms indicate atrophy or loss of large, fast conducting axons). The CAP data recorded for the subjects of this thesis indicate that our cuffs may be causing damage to the nerves (Strange et al., 1995a; Strange et al., 1995b). It is important to be able

19

to correlate these electrophysiological measures of decreased function with a given degree of anatomical change. Until this study, no direct (i.e. histological) data about the anatomical integrity of cuffed nerves existed. This thesis provides a morphometric method for determining this information.

2.6 **Purpose of this Study**

Four primary questions are examined in this thesis:

1. Are there quantifiable morphological differences between control and cuffed nerve cross sections?

2. If morphological differences do exist, are larger axons in a given cross section damaged more than the smaller axons in the same nerve?

3. If morphological differences do exist, are the axons of the Perimeter Zone more severely affected than the axons located in the Inner Zone?

4. If morphological differences do exist, can these changes be correlated to CAP changes recorded during the implant regime?

3. MATERIALS AND METHODS

The processing and analysis of neural tissues for morphometric studies (Auer, 1994; Mezin et al., 1994; Mize, 1983) is very labour intensive. Because of this challenge, past researchers have used random samples of "representative" fields from whole nerve cross sections. In many cases, as few as 200 axons from a typical nerve cross section (of 8,000 axons) were sampled. As has been mentioned previously, this methodology is flawed due to the extremely heterogenous nature of nerve cross sections population (Torch et al., 1989). This study measured all axons from a given nerve cross section to eliminate any concerns about sampling errors.

3.1 Experimental Animals and Animal Care

Purpose bred neutered adult male cats (Liberty Labs, Liberty Corner, N.J.) were utilized in this study. Cats were group housed and were allowed to move freely about within their enclosure. Activities of daily living for the animals included climbing a wire fence, leaping from up to 1.5 m high shelving units and treadmill walking for 15 minutes per day. All experiments conformed to established animal care protocols and all experiments received university ethics approval

3.2 Cuff Design

A complete description of the design and construction of the slit-tube type circumferential nerve cuff electrodes utilized in this experiment is beyond the scope of this document. A brief description is included in Appendix 4 and interested readers are directed to Hoffer (1990) and Kallesoe et al. (1996) for more thorough examinations of the pertinent issues.

3.3 Surgical Methodology

3.3.a Pre-medication for all Anesthetized Procedures

All cats were given prophylactic antibiotics, 2 ml Cefadroxil oral liquid was given 24 hours prior to surgery and then continued daily for seven days post operative.

A mixture of Ketamine (10mg/kg @ 100mg/ml), Acepromazine (0.05 mg/kg @ 10mg/ml) and Atropine (0.02mg/kg @ 0.5mg/ml) was given via an intramuscular injection to facilitate intubation.

3.3.b Surgical Anesthesia Protocol

Ten to twenty minutes following pre-medication, a 1% to 1.5% mixture of Halothane in pure oxygen was administered via intubation. Depth of anesthesia was monitored closely by a veterinary technician with the aid of a CO_2 output monitor, blood pressure doppler, temperature probe and an esophageal stethoscope. An intravenous catheter was installed in the unoperated forelimb and a lactated ringers solution drip maintained hydration. A urinary catheter was installed to monitor urinary output/kidney function. Eye ointment was applied to prevent corneal drying. All surgical protocols were carried out in an aseptic surgical suite. A heated table and and hot water blanket were used to maintain body temperature.

3.3.c Post-Surgical Medication

Temgesic (0.01mg/kg @ 0.3mg/ml) with Acepromazine (0.02mg/kg @ 1mg/ml) was administered by intramuscular injection approximately 20 minutes prior to extubation. An injection of Temgesic alone was given subcutaneously 10-12 hours later. Temgesic acted as an analgesic while Acepromazine allowed for a more relaxed post surgical recovery response. A second combination of Acepromazine with Temgesic was used, when warranted, 10-12 hours post surgery.

3.3.d Cuff Installation

Nerve cuffs of the design described by Kallesoe et al. (1996) were manufactured in our laboratory and were implanted in a total of 9 cats. Of these, three cats received implants above the elbow (proximal) and below the elbow (distal) on both the median and ulnar nerves of the left forelimb (Fig. 6). Two cats received proximal and distal circumferential nerve cuffs on the ulnar nerve while simultaneously having a circumferential nerve cuff implanted on the proximal radial nerve and on the distal portion of the radial nerve (Fig. 6). A patch electrode was implanted on the distal radial nerve of NIH 12. This electrode was different from the nerve cuffs in that it was simply a flat silastic sheet that had electrodes sewn into its surface. Four cats received a proximal and distal circumferential nerve cuff on the median nerve and the same radial nerve treatment mentioned above. One cat (NIH 15) had nerve cuffs implanted on the small muscle nerves of flexor digitorum profundus (FDP) and extensor digitorum longus (EDL). Refer to Table 1 for a summary of cuff placements.

In all cases, the greatest possible nerve free length was mobilized away from surrounding tissues prior to cuff installation. Care was taken to ensure that nutrient arteries to the nerve and nerve branches leaving the main nerve trunk were not disrupted. Care was also taken not to unduly stretch the nerve.

Subject	Median	Ulnar	Radial	FDP and EDL
NIH-9	YES	YES		
NIH-10	YES	YES		
NIH-11	YES	YES		
NIH-12	YES		YES	
NIH-13		YES	YES	
NIH-14		YES	YES	
NIH 15	YES		YES	FDP YES EDL YES
NIH 16	YES		YES	
NIH 17	YES		YES	

Table 1: Summary of 9 implants showing the nerve cuffs implanted in each case.
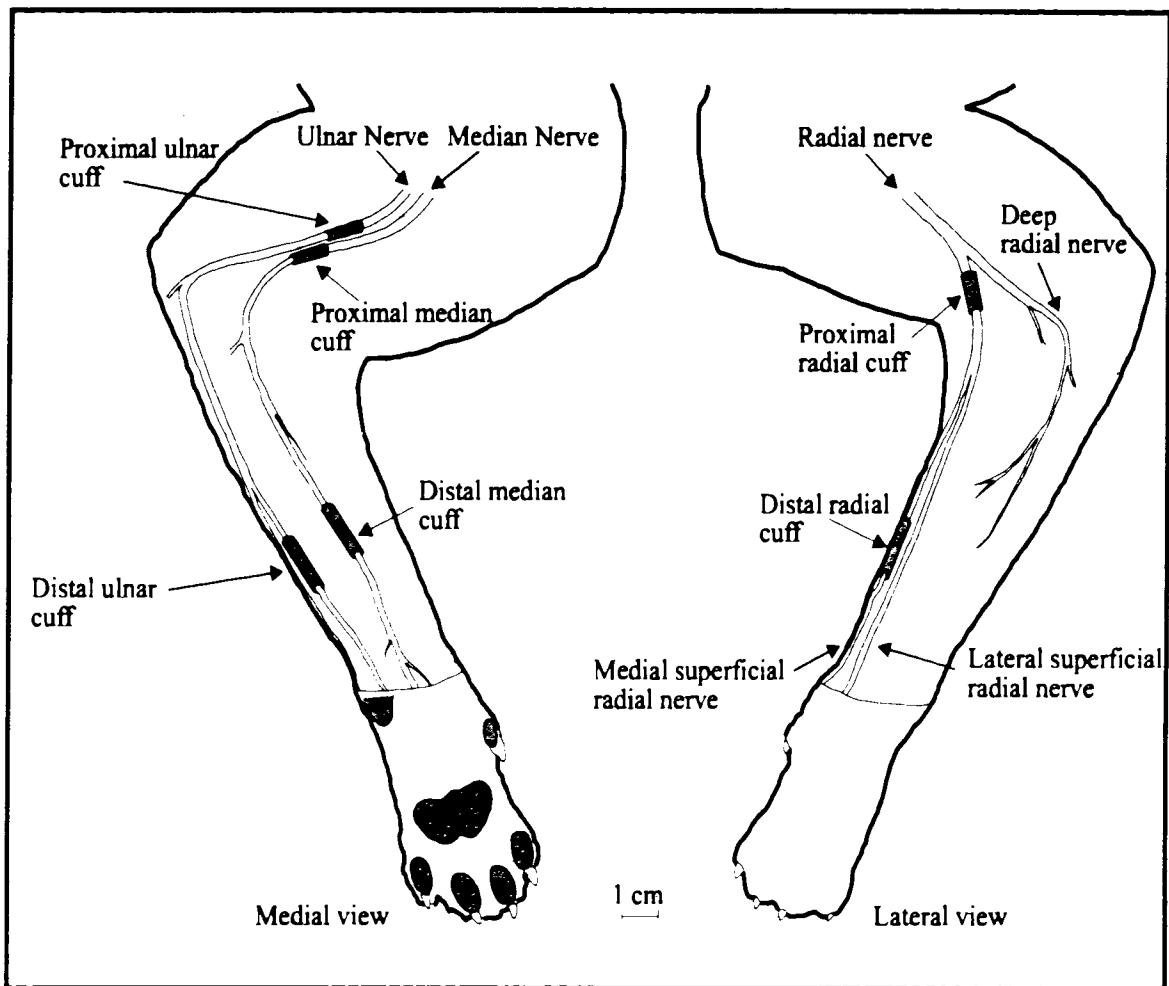
Figure 6: Schematic representation of nerve cuff placement. Modified with permission from Strange et al. (1996).

3.4 Sample collection

Under general anesthesia, nerve cuffs were taken off of the intact nerves. One cm tissue samples were taken from the cuff locations on both of the median and ulnar nerves. Samples were taken from both the proximal and distal locations (Fig. 6). A total of four samples were harvested from the implanted limb of each cat (2 cuff locations from 2 nerves). Control samples were taken from the contralateral, unoperated limb in locations that were judged to be equivalent to the cuff positions on the implanted side (2 control locations from each of 2 nerves). Thus, 8 tissue samples were taken from each cat.

Animals were sacrificed with a lethal dose of 100 mg Pentobarbitol per kilogram while still under general anesthesia.

3.5 Embedding and Staining

Two different tissue preservation techniques were used in this study. Nerve samples from NIH 9, NIH 10, NIH 11 and NIH 13 were fixed by immersion in Karnovsky's fixative (Karnovsky, 1965; Appendix 1). Following attempts to section and stain these samples, it was determined that the fixative was not performing well in our application. Axons exhibited shrinkage and severe distortion while the tissue block, as a whole, showed poor preservation. As a result of these shortcomings, the samples from NIH 9, NIH 10, NIH 11 and NIH 13 were not used in any further analysis. Nerve samples from NIH 12, NIH 14, NIH, 15, NIH 16, and NIH 17 were fixed and embedded using the techniques of Dyck et al. (1980) and Bancroft and Stevens (1990).

Briefly, the technique was carried out as follows: one centimeter long fresh nerve samples were immersed in iso-osmolar glutaraldehyde (see Appendix 1 and 2) and then dehydrated in a series of alcohols. The samples were cleared with a final wash in propylene oxide and then osmicated for four hours. The osmicated samples were embedded in Jembed 812 (J.B.EM services, Quebec) and then 0.5 μm transverse sections were cut using a glass knife. Great care was taken to ensure that the majority of axons were nearly circular in a given cross section. This precaution ensured that all axons were sectioned perpendicular to their orientation *in vivo*. The 0.5 μm sections were counterstained with a 2:1 mixture of Richardson's stain (Richardson et al., 1960; Appendix 1) and Toluidine blue. The stain was filtered just prior to its application to the samples. Sections were examined under a Leitz SM600 light microscope using an oil immersion objective (x100 magnification).

3.6 Selection of Samples to be Studied

Samples from nine cats were collected prior to the initiation of this study but all the samples were not utilized in the final morphometric analysis. As was mentioned above, the samples from NIH 9, 10, 11 and 13 were excluded from this study due to poor tissue preservation (Table 2). NIH 14 was not used because it would have been the only ulnar nerve to be included and, therefore, there would have been no other samples with which to compare it. The radial nerve samples from NIH 12-17 were excluded because the distally located radial nerve patch electrodes differed in construction from the circumferential nerve cuffs used in the rest of the experiment.

In light of the limitations of the aforementioned samples, this study focused on the median nerves from NIH 12, 15, 16 and 17. Tissue preservation was good in these samples and the neurophysiological CAP data showed a wide range of responses.

Subject	Median	Ulnar	Radial	FDP and EDL	Sample Quality
NIH-9	YES	YES			Poorly fixed
NIH-10	YES	YES			Poorly fixed
NIH-11	YES	YES			Poorly fixed
NIH-12	YES		YES		Good
NIH-13		YES	YES		Poorly fixed
NIH-14		YES	YES		Good
NIH 15	YES		YES	FDP YES EDL YES	Good
NIH 16	YES		YES		Good
NIH 17	YES		YES		Good

Table 2: Summary of 9 implants showing the nerve cuffs implanted in each case. Samples used for further morphometric analysis are shaded.

3.7 Data Collection

During all processing, the experimenter was blind to the identity of the nerve cross sections. The identity of the samples was revealed after all size related data had been collected.

3.7.a Hardware

A Javelin Chromachip II electronic camera (Javelin Electronics, Japan) was mounted to the ocular tube of a Leitz SM600 microscope to allow for binary imaging of the histological sections. The video image was fed directly into an Vision Plus-AT black and white frame grabber (Imaging Technology, Bedford, MA). The frame grabber was housed in a 90 mHz Pentium class IBM clone. Optimas 5.2 image analysis software (Optimas Corp, Seattle, WA) was installed in the computer to analyze the data coming from the frame grabber. A Wacom Art II graphics tablet (Wacom Industries, Vancouver, WA) was used for manual correction of any touching fibers. The live video image, combined with any on-line enhancements made by the Optimas software, were then displayed on another monitor (Sony Corp, Japan). Refer to Fig. 7 for a diagrammatic depiction of the data collection hardware.
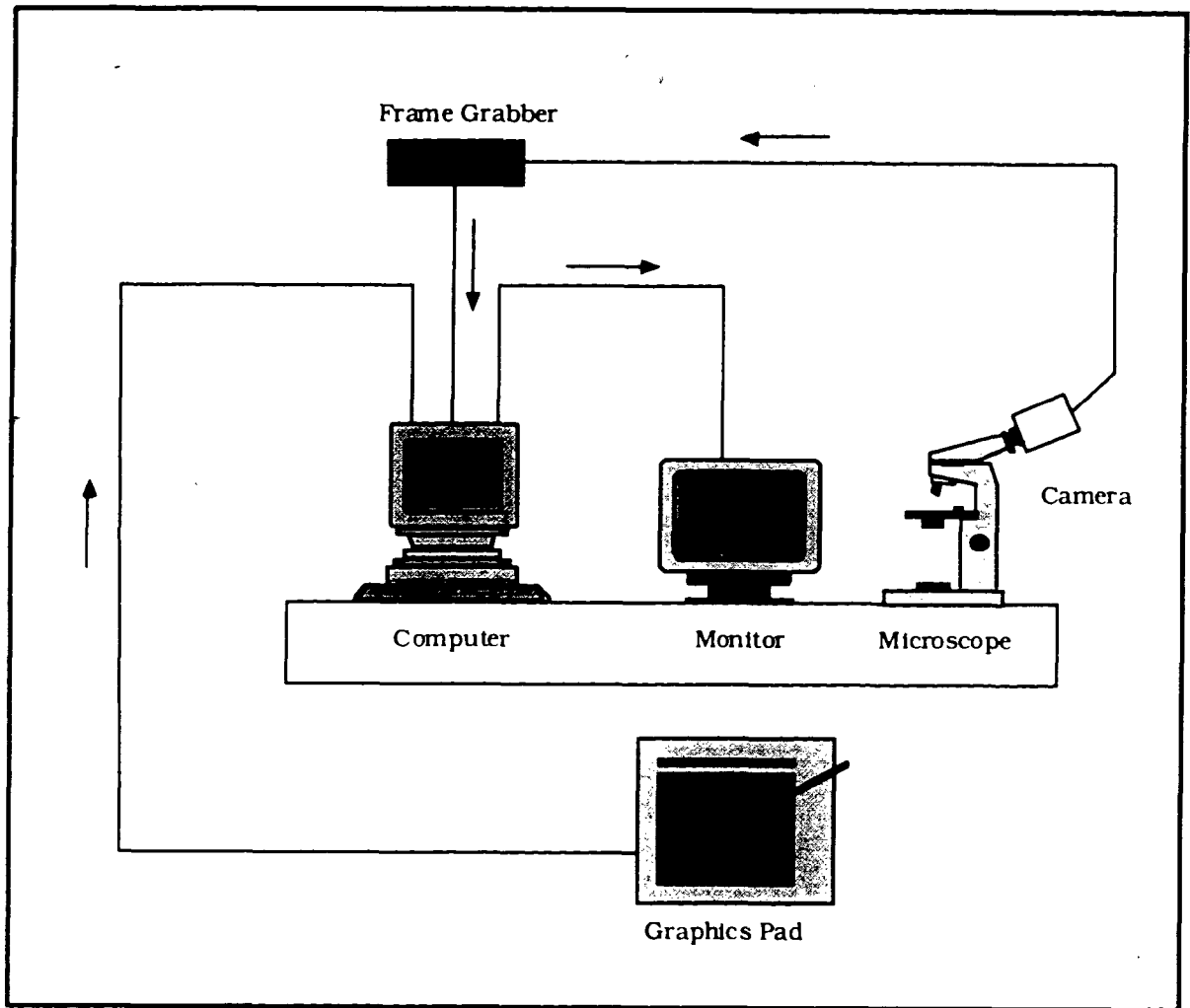
Figure 7: Computer setup. Note that the frame grabber is shown external to the computer only to facilitate description. It actually resided within the computer chassis.

3.7.b Resolution of Optical System

Resolution of the Microscope

The resolution of any microscope can be calculated by:

$$d = 1.22 \left(\frac{\lambda}{NA_{Objective} + NA_{Condenser}} \right)$$

Where: d= the minimum discernible distance between two points

λ= the wavelength of light used in the comparison

NA= the numerical aperture of the lenses

This experiment utilized white light for all measurements ($\lambda \approx$ 400-700 nm). The numerical apertures were 1.25 for the oil immersion lens and 0.9 for the condenser. Thus, the optical resolution of the system was approximately 0.4 μm.

Electronic Resolution

A calibrated graticle was used to determine the magnification and resolving ability of the entire optical system. Captured images were measured to be 50 μm by 60 μm. The camera resolution was 760 x 485 pixels ($\cong$ 0.1 μm /pixel) while the frame grabber had a 512 x 480 pixel resolution ($\cong$ 0.1 μm /pixel).

Overall Resolution and Significant Figures

The resolution of the microscope was the limiting factor in this experiment. Images obtained from the entire system were accurate to within $\approx$ 0.4 μm.

When large numbers of individual measurements were averaged together, the measurement uncertainty was partially cancelled out and, thus, the averaged values were expressed to the nearest 0.1 μm.

3.7.c Software and Macros

In order to determine whether differential changes occurred in cuffed nerves, this study examined the size distribution of the axons at the periphery of the nerve cross section (Perimeter Zone in this study) as compared to the size distribution of those fibers located closer to the interior (Interior Zone in this study). Fig. 8 provides a schematic representation of the two zones.

Perimeter Zone axons were those axons located in the last full microscope screen before the perineurium. Sometimes slightly more than 50 µm of axons were collected for this zone and sometimes slightly less. Most samples were very close to being exactly 50 µm. The data collection process is described in greater detail in the following sections.
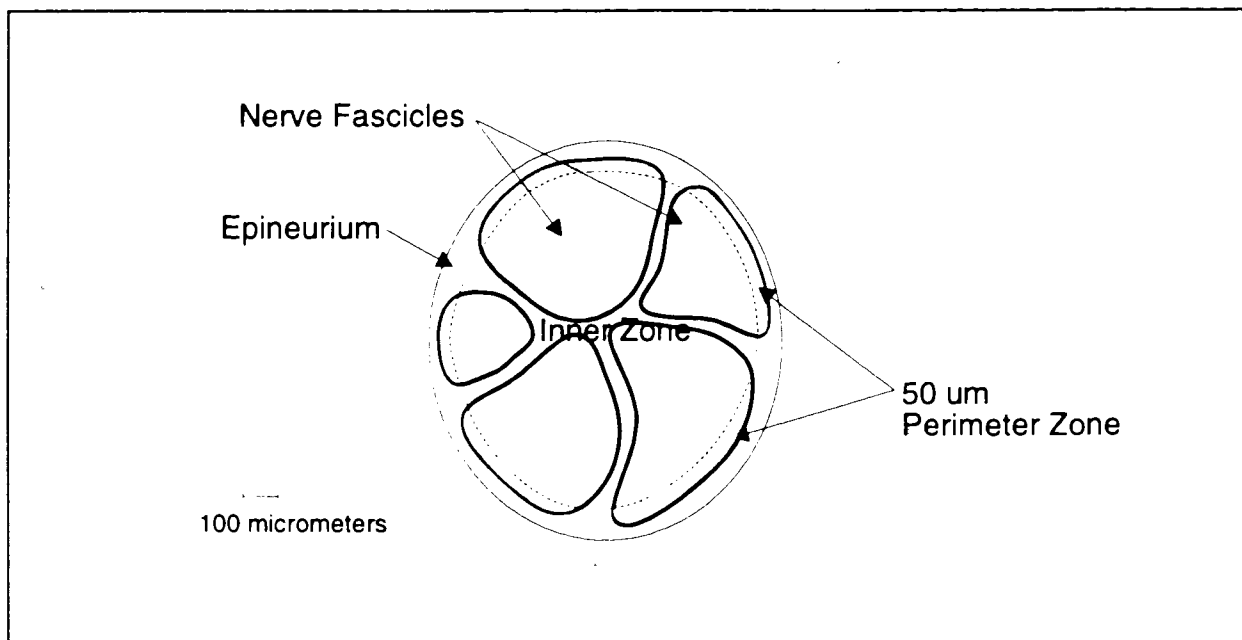

Figure 8: Cross section of a peripheral nerve showing the distribution of nerve fascicles within the epineurium. The Perimeter Zone encompasses the outer 50 µm of the nerve cross section.

Initial Sample Collection

In order to accurately measure all axons in a given nerve without duplicating or excluding any axons, it was necessary to establish criteria for the inclusion or exclusion of axons in a given image field. A schematic depiction of a typical nerve cross section microscope field is presented (Fig. 9) to facilitate discussion of these parameters. Sampling was initiated at the top of the nerve sample near the edge of the perineurium of that fascicle. Once the sampling of the axons in a given microscope field was complete, the microscope stage was moved such that the axons in the next adjacent horizontal field of view were sampled in a sequential fashion. Upon reaching the edge of the epineurium, the stage was adjusted vertically such that the field of view dropped down one field and then sampling resumed in the next row but in the reverse horizontal direction.

In order to sample all axons within a given cross section while avoiding duplication of the measurement of some of the axons, great attention had to be paid to the vertical distance moved during the transition from one row to the next. Large axons routinely crossed from one field to another (Fig. 9, part C; Fig. 10, parts a-d) such that, unless care was taken during field transition, these axons would not be included in any sample. A spuriously small fiber size distribution would have resulted if these typically larger fibers were excluded. During horizontal transitions, this effect was minimized by the operator's careful notation of the existence of fibers that crossed over from one screen to another. The stage was then moved far enough to just include these fibers in the next field of view (Fig. 10 parts a and b).

Axons that carry over vertically from one horizontal row to another (Row A to Row B in Fig. 9c; frame B to C or frame C to D in Fig. 10) were accounted for by affixing a strip of clear sticky tape to the screen just above the largest overhanging axon on a given screen. In this way, the tape serves as a clue to the operator as to the size of the axons that have been missed (see axons at the bottom of Fig. 10, part b and at the top of Fig. 10, part c). If subsequent screens had larger overhanging axons, then the tape is adjusted accordingly. At the end of each row, the microscope stage was adjusted only by the amount dictated by the clear sticky tape. The larger axons that were missed in the first pass were picked up in the next row's data. As with the horizontal transitions, any smaller axons included in both the adjacent horizontal rows were eliminated manually during later stages of the process. In this way,

31

axons that "hung over" from one row to another row were included and the smaller axons were not double counted.
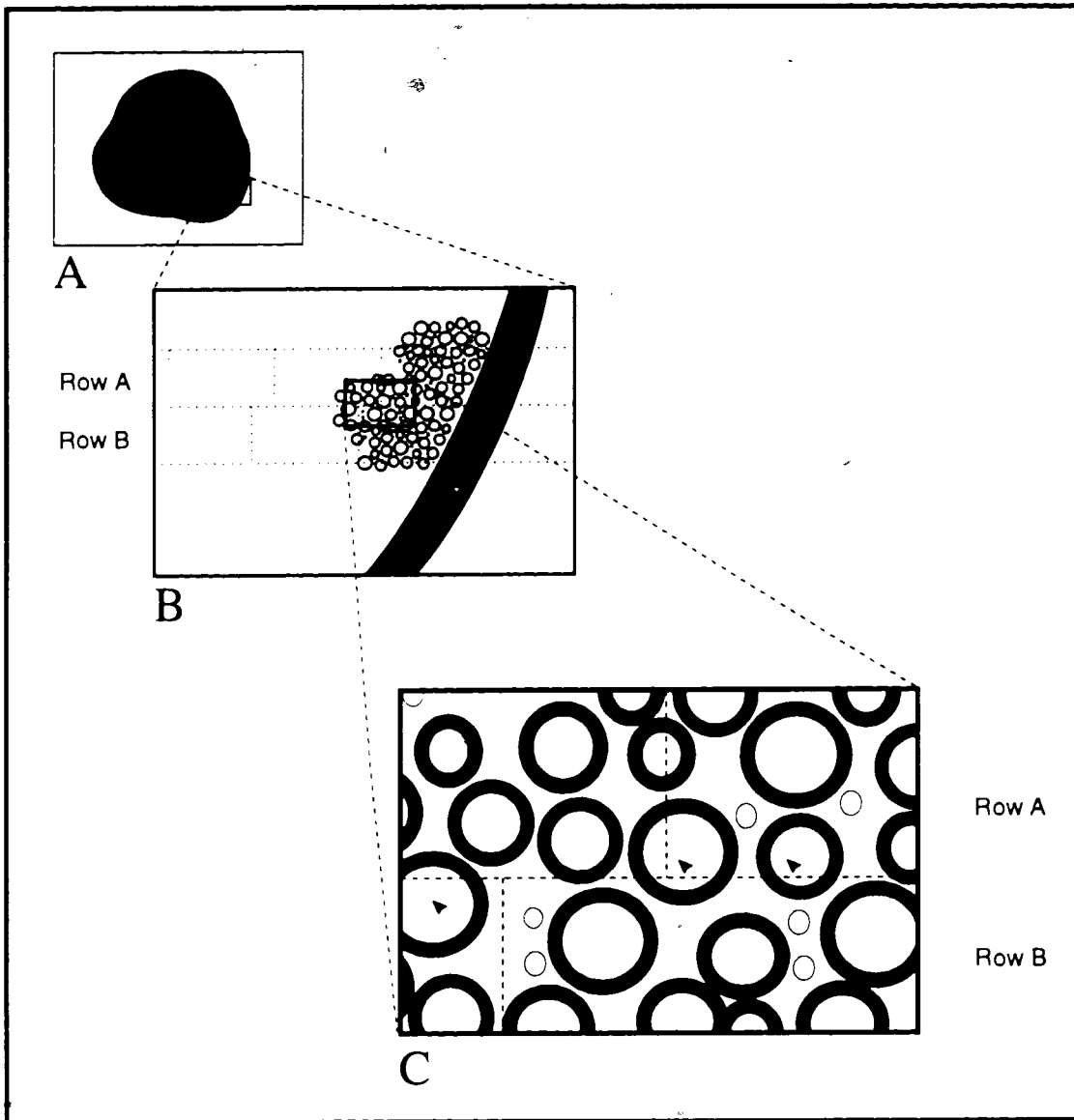
Figure 9: A: Schematic representation of a whole nerve cross section viewed under relatively low magnification. B: Enlarged portion of part A showing a group of axons (dark circles) near the edge of the perineurium. Dotted lines indicate the outer edges of consecutive microscope fields. C: Enlarged view of part B showing in greater detail how some axons "hang over" (arrowheads) from one field to another. Once again, the circles represent axons of different sizes. Dotted lines represent the divisions between consecutive fields of view. See text for a description of the technique used to account for these axons.
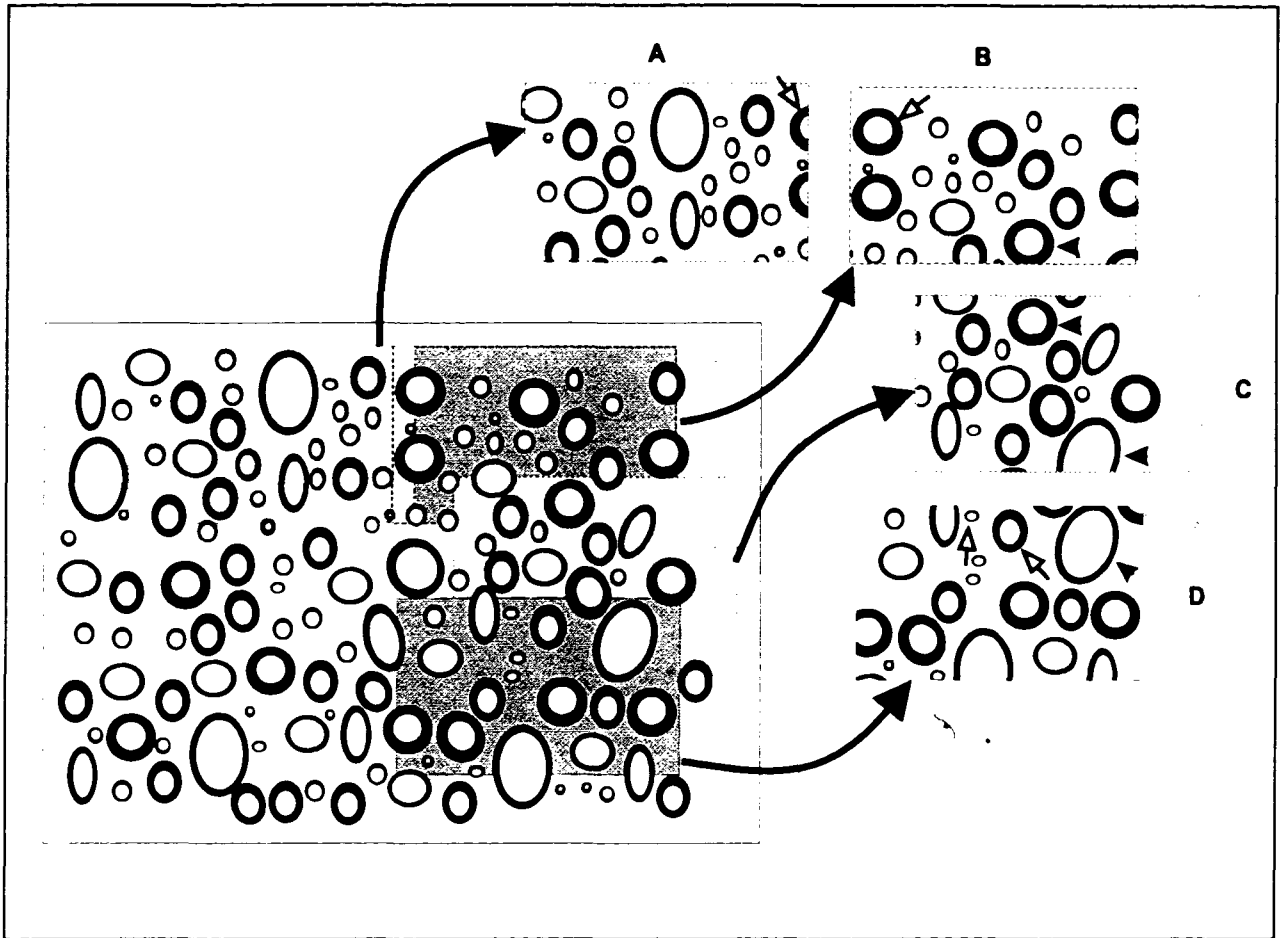
Figure 10: Schematic representation of images gathered during montage video sampling. Note the overlap of field A and field B and note that the rightmost axons of field A (black arrowheads) determined how far the microscope slide was moved over for field B. Also note that the largest axons at the bottom of fields C and D determined how much overlap occurred between adjacent horizontal rows.

Filtering and Montage Creation

Digital image collection was facilitated by the use of a macro developed by the author (Autosaving Macro, Appendix 6). The macro captured live images from the video camera, imprinted these images with a sample code for the nerve, printed the image to a laser printer (5cm by 8cm) and then saved the image in a raw data file. A bulk filtering macro was applied to the saved, raw data (Bulk Filtering macro, Appendix 6) to reduce the amount of background variation apparent in the pixel values of the saved images. The filtering process allowed for better, more consistent discrimination of the foreground/ background threshold. The filtered images were saved again in a filtered image file for future processing.

The 5cm by 8cm printed images mentioned above were sequentially affixed to a large sheet of newsprint such that a montage of the fascicle was created. Fibers located in more than one saved image were noted with a coloured marker for future removal.

Correction of Touching Fibers/ Elimination of Duplicate Axons

A macro was developed by the author (Retouching Macro, Appendix 6) that aided in both the separation of touching fibers and the removal of duplicate fibers. The macro loaded a filtered image to the computer screen. Manual corrections were applied to the image where fibers were touching or where duplicate fibers were located. A Wacom Art II graphics tablet provided the user interface for making the changes. Duplicate axons were removed (using the montage as a guide) and touching axons were separated with background colour. The macro re-saved the corrected image after each change was made.

Data Collection and Export

A final data collection macro was developed (Data Gathering Macro, Appendix 6) for collection of the morphometric variables. This macro opened a saved, filtered image and allowed the user to remove any non-neural objects from the image. The areas and perimeters of axons and fibers were computed through the Optimas software. The macro matched axon and fiber parameters to one another and this information was sent to an Excel spreadsheet (Microsoft, Redmond, WA). Axons touching the edge of the screen were ignored by the software as were any screen objects less than 2 μm. Axons located within 50 μm of the inner edge of the epineurium (Fig. 8) were binned separately from the remainder of the axons to allow for assessment of any possible edge effects.

Calculation of Variables

This study has assumed that axons and fibers can be approximated to be perfect circles *in vivo* (Auer, 1994). The theoretical circular axon diameter and circular fiber diameter were calculated from the perimeters of axon and fiber respectively (Appendix 5). Perimeter

measures were utilized rather than axon or fiber areas because perimeter measurements are less susceptible to errors associated with oblique cuts of the tissue (Fig. 11).

Average axon diameter was calculated by taking the average of all axon diameters in a given nerve cross section. This measurement was used as summary statistic of the overall axon size distribution of the nerve.

Average fiber diameter was calculated by taking the average of all fiber diameters in a given nerve cross section. Average fiber diameter represented a summary of the overall fiber size distribution of the nerve.

Myelin sheath thickness was calculated as half of the difference between the fiber diameter and the axon diameter for each axon. Average myelin sheath thickness was derived and utilized in the same manner as average axon diameter and average fiber diameter.

The degree of myelination per axon can also be assessed by calculating the G-ratio for each axon (Gillespie and Stein, 1983). G-ratio was calculated as the ratio of the axon circumference divided by the fiber circumference. G-ratio is scaled from 0 to 1.0 with values closer to 1.0 indicating lower relative myelination per axon and values closer to zero showing relatively thicker myelination.

A Circularity Index (C.I.) for both axons and fibers was calculated (Usson et al., 1987) as:

$$C.I. = \frac{4\pi(Area)}{(Perimeter)^2}$$

Where: Area = the measured area of the element (axon or fiber)
           Perimeter = the measured perimeter of the element

Axon and Fiber Circularity Indices allowed for the comparison of the deviation of each axon or fiber from a perfect circle. A value of 1.0 would be obtained for a perfectly circular structure. Values close to 1.0 indicate that little shrinkage occurred during processing and values less than 0.5 indicate low circularity.

Total conduction area was calculated as the total number of fibers in a cross section multiplied by the average axon area of that cross section (in mm^2).

35
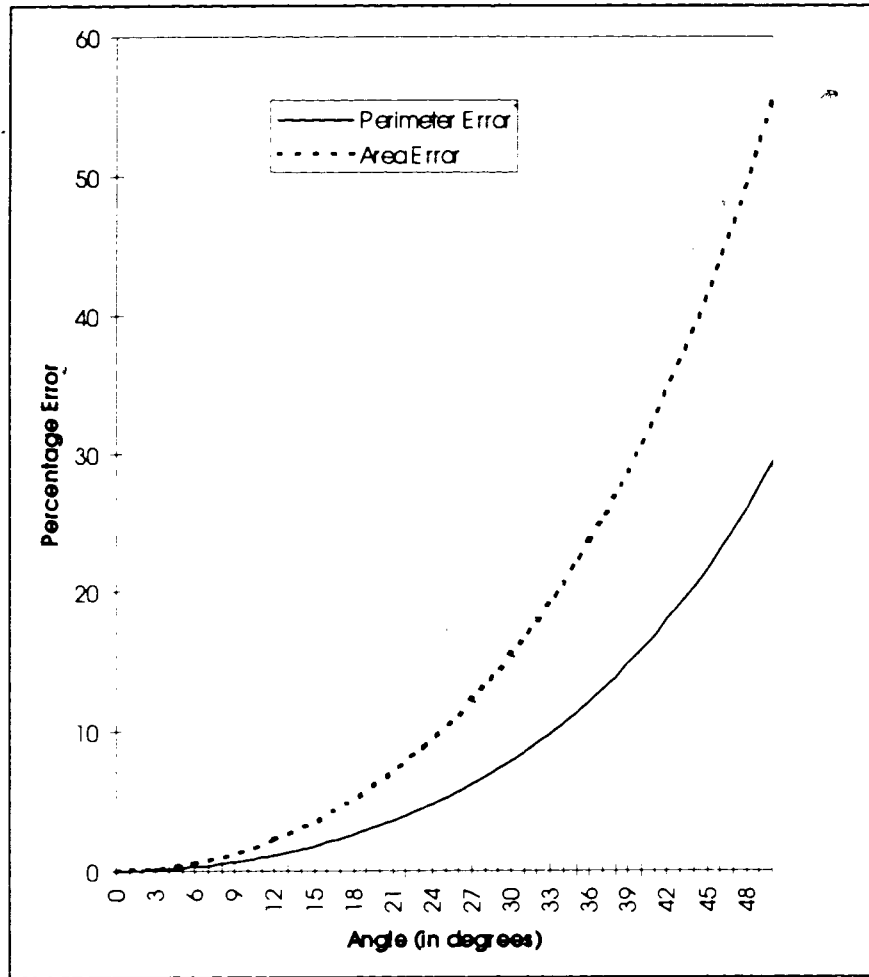
Figure 11: Error comparison of axon area calculations derived from the perimeter and the measured area as they relate to the angle that the cut is from perfectly perpendicular.

4. RESULTS

4.1 General

The ages of the cats on day 0 of implant ranged from 10 to 23 months (Table 3).

Subject Number	Age at Implant (months)	Months Implanted	Age at Explant (months)
NIH 12	10	10	20
NIH 15	13	12	25
NIH 16	15	10	25
NIH 17	23	6	29

Table 3: Age at implant, months implanted and age at explant for the four subjects used in this experiment.

Figure 12 shows a montage of individual images that were collected together into a fascicle. These results were typical for the majority of the fascicles examined. This raw data was filtered and then processed as described in the Methods section.

A total of 39,487 axons were sampled from the cuffed and control nerves of four subjects (Table 4). Control nerves averaged 5,008 axons while cuffed nerves averaged 4,864 axons. These totals were not found to be statistically different using a paired two tailed t-test at $\alpha=0.05$.

	NIH 12	NIH 15	NIH 16	NIH 17	Average
Cuffed					
Inner	4,976	4,476	3,810	3,992	
Perimeter	486	563	433	718	
Total	5,462	5,039	4,232	4,710	4,861
Control					
Inner	4,892	4,189	4,699	3,849	
Perimeter	627	413	567	797	
Total	5,519	4,602	5,266	4,646	5,008

Table 4: Number of axons per experimental subject. Note: average number of cuffed axons per nerve was not significantly different from the average number of control axons per nerve.

Nerve conduction areas (cross sectional area not including connective tissue) were relatively consistent between cuffed and control nerves (Table 4). This, along with the similarity in cuffed to control axon numbers mentioned above, suggests that the control nerves were well matched to experimental nerves.

Extensive connective tissue sheath development was observed around the nerves that had cuffs implanted on them. Total implanted nerve cross-sectional areas were, on average, 130 % of control nerves (Table 4). This value was calculated by dividing the area of the cuffed nerve by the area of the control nerve. The result was then expressed as a percentage.

The portion of the nerve devoted to nerve conduction (Conduction Area in Table 4) was reduced. This change is examined in greater detail in later sections.
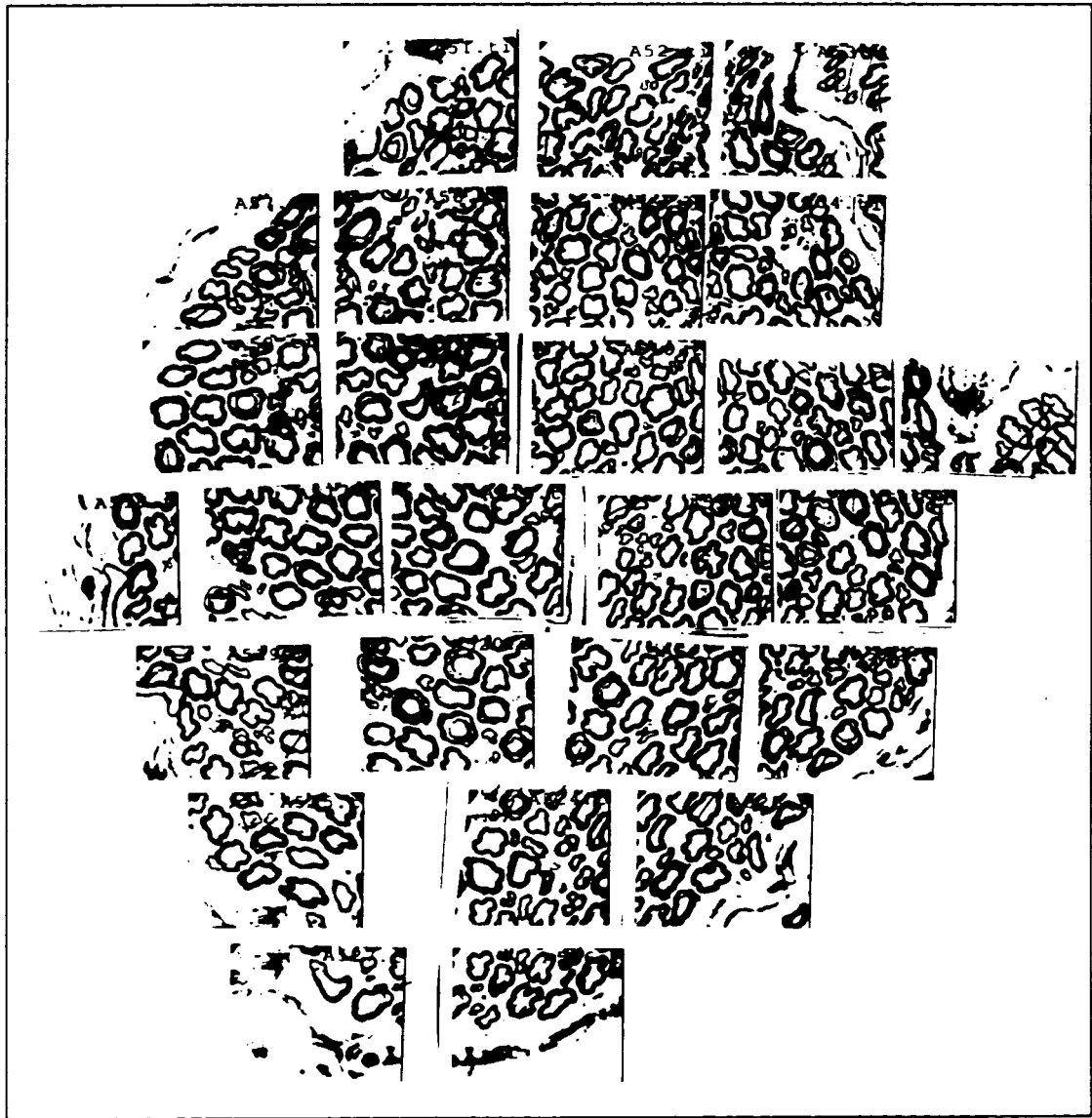
Figure 12: Montage of an entire nerve fascicle from NIH 17 control. Each square represents an individual 60 μm by 50 μm saved image. Three hundred and twenty one axons were counted in this fascicle.

		Control	Cuffed	% of control
Conduction Area	**N12**	0.10	0.09	89
	N15	0.11	0.08	72
	N16	0.11	0.08	74
	N17	0.10	0.11	102
Overall		0.11	0.09	84
Epineurial Area	**N12**	0.63	0.60	95
	N15	0.50	0.49	97
	N16	0.48	0.42	87
	N17	0.43	0.46	107
Overall		0.51	0.49	96
Total Nerve Area	**N12**	0.63	0.82	130
	N15	0.50	0.67	134
	N16	0.48	0.54	113
	N17	0.43	0.63	143
Overall		0.51	0.67	129

Table 5: Summary table of conduction area (sum of all axon areas, in mm^2), epineurial area (total area bordered by the epineurium, in mm^2) and total nerve area (connective tissue sheath and epineurial area combined, in mm^2). Note that nerve areas equal epineurial areas in control (uncuffed) nerves.

In general, a bimodal distribution was observed for axon diameter, fiber diameter and myelin thickness size histograms (e.g., Fig. 16 a, b; Fig. 17 a, b; Fig. 18 a, b) although there were some exceptions. Axon diameters for the Inner and Perimeter Zones of NIH 12 (Fig. 16 a, b) showed a highly bimodal distribution while the axon diameter distributions for NIH 15 (Fig. 22 a, b) were largely unimodal. Myelin Thickness distributions varied; NIH 15 (Fig. 24 a, b) showed highly bimodal distributions whereas NIH 17 (Fig. 30 a, b) exhibited nearly unimodal distributions. Fiber diameter histograms (Fig. 17 a, b; Fig. 22 a, b; Fig. 26 a, b; Fig. 29 a, b) tended to exhibit greater bimodality than either the axon diameter or myelin thickness distributions. The bimodality of a given morphometric distribution was not associated with whether or not the nerve had been cuffed. Cuffed samples with a highly bimodal structure tended to have control samples that were correspondingly bimodal (e.g., Fig. 26 a). Unimodal cuffed samples also tended to have unimodal control samples (e.g., Fig. 30 b).

Axon Circularity (Fig. 19 a, b), Fiber Circularity (Fig. 20 a, b) and G- ratio (Fig. 21 a, b) all tended to have Gaussian distributions. The variance associated with the axon circularity distributions was greater than either fiber circularity or G-ratio (Tables 10 and 11).

Some morphometric measures showed fascicle dependent variations while others did not. Average axon diameters, average fiber diameters and average myelin thicknesses varied depending on the fascicle of origin (Table 6) while values obtained for Axon Circularity, Fiber Circularity and G-ratio did not vary between fascicles (Table 7).

Axon diameter, fiber diameter and myelin thickness distributions also showed variations in the size and shape of the histogram features (Figs. 13, 14 and 15). Maximum values for each measure varied somewhat between fascicles as did the degree of bimodality observed per fascicle and the relative proportion of the distribution located under a given size range.

Fascicle 1	Axon Diameter (μm)	Fiber Diameter (μm)	Myelin Thickness (μm)
n= 971			
Average	7.2	12.9	2.9
StDev	3.0	4.8	1.4
Fascicle 2			
n= 448			
Average	6.7	11.6	2.4
StDev	3.0	4.6	1.2
Fascicle 3			
n= 1180			
Average	6.5	12.1	2.8
StDev	2.7	4.5	1.3
Fascicle 4			
n= 1311			
Average	6.7	12.0	2.6
StDev	2.8	4.2	1.2
Fascicle 5			
n= 279			
Average	7.1	12.1	2.5
StDev	3.0	4.6	1.2
Summary			
n= 4189			
Average	6.8	12.2	2.7
StDev	2.9	4.5	1.3

Table 6: Axon diameter, fiber diameter and myelin thickness averages detailed for each Inner Zone fascicle of NIH 15. Averages of all the fascicles are supplied at the bottom of the table.

Fascicle 1	Fiber Circularity Index	Axon Circularity Index	G-ratio
n= 971			
Average	0.73	0.60	0.56
StDev	0.09	0.14	0.11
Fascicle 2			
n= 448			
Average	0.73	0.58	0.58
StDev	0.08	0.14	0.10
Fascicle 3			
n= 1180			
Average	0.73	0.56	0.54
StDev	0.08	0.15	0.10
Fascicle 4			
n= 1311			
Average	0.73	0.57	0.57
StDev	0.07	0.14	0.11
Fascicle 5			
n= 279			
Average	0.72	0.61	0.59
StDev	0.08	0.12	0.10
Summary			
n= 4189			
Average	0.73	0.58	0.56
StDev	0.08	0.14	0.11

Table 7: Axon circularity, fiber circularity and G-ratio averages detailed for each Inner Zone fascicle of NIH 15. Averages of all the fascicles are supplied at the bottom of the table.
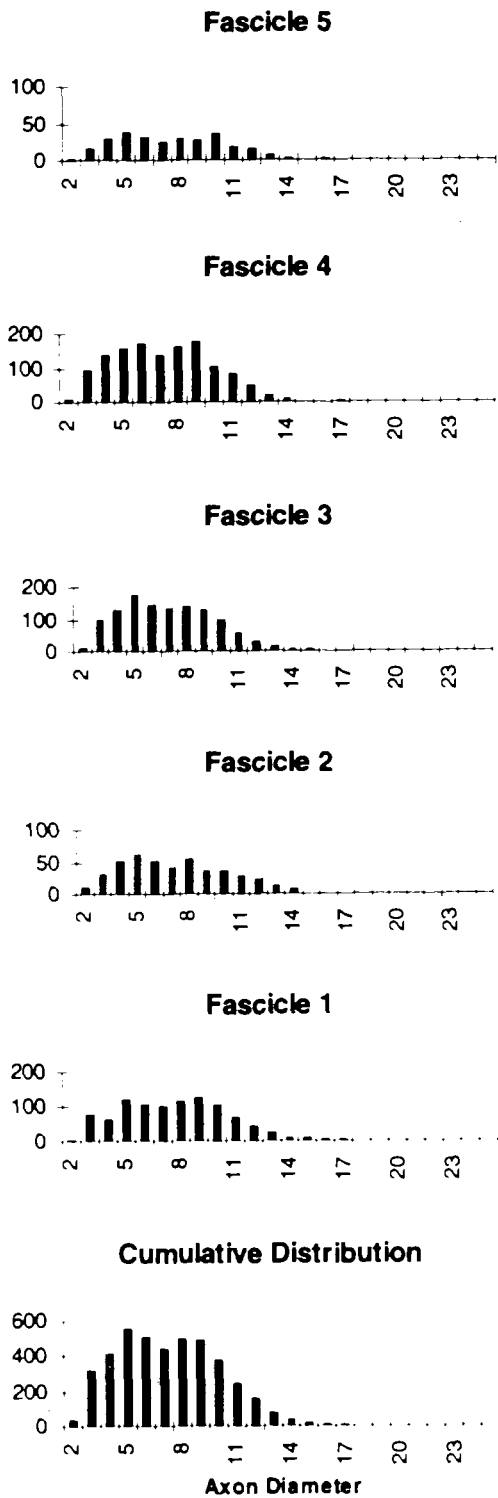
Figure 13: Comparison of axon diameter distributions in each of 5 nerve fascicles for the Inner Zone.of NIH 15. Axon Diameters are expressed in μm.
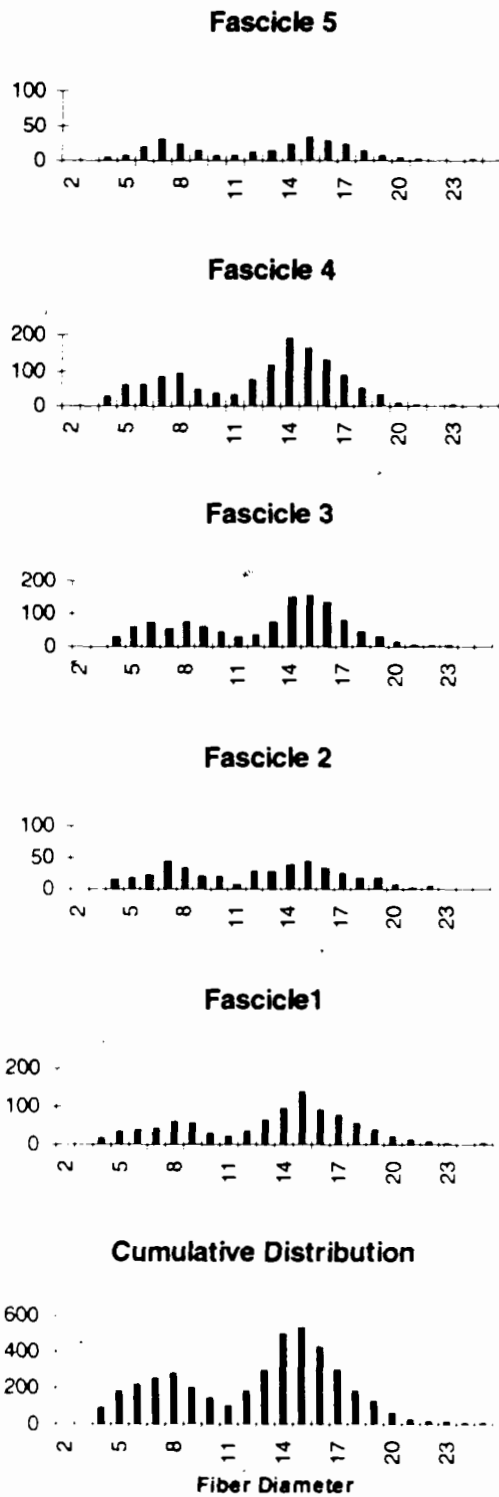
Figure 14: Comparison of fiber diameter distributions in each of 5 nerve fascicles for the Inner Zone of NIH 15. Fiber Diameters are expressed in μm.
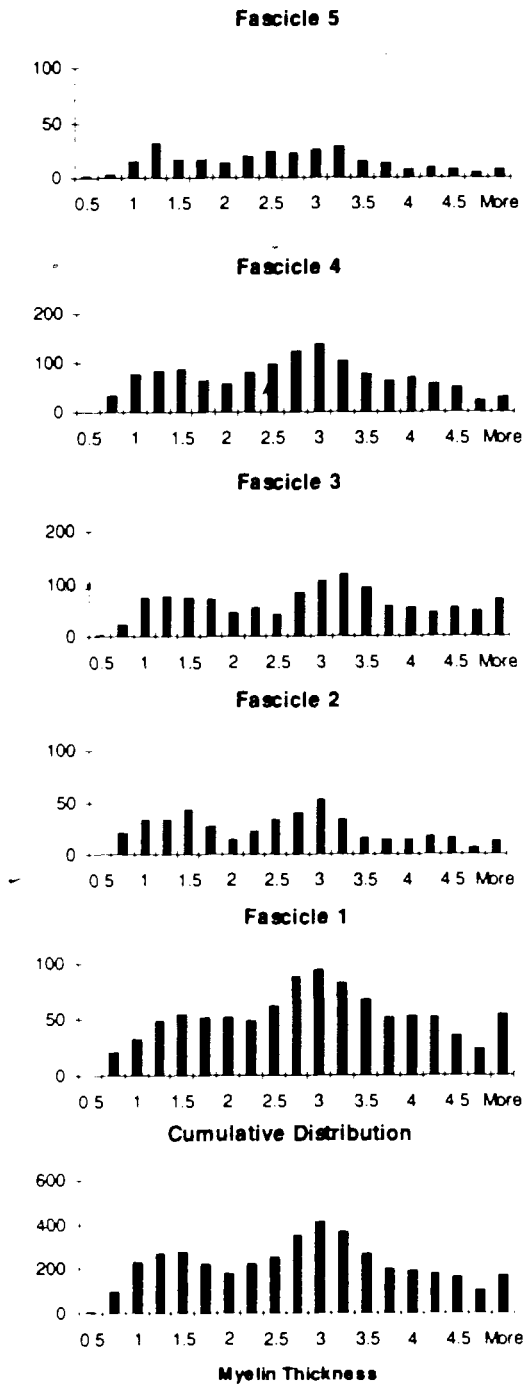
Figure 15: Comparison of myelin thickness distributions in each of 5 nerve fascicles for the Inner Zone of NIH 15. Myelin Thicknesses are expressed in μm.

4.2 Differences between cuffed and control nerves.

There were a number of morphometric differences between cuffed and control nerves (Refer to Tables 8 and 9 for a summary).

Axon Diameter

In 3 of 4 Perimeter Zones and in 3 of 4 Inner Zones, the mean axon diameters of the cuffed nerves were significantly smaller than control at $p<0.001$ (NIH 15, 16 and 17 in both cases).

Fiber Diameter

Average fiber diameters were significantly smaller than control ($p<0.001$) in 2 of 4 cuffed Perimeter Zones (NIH 15 and 16) and in 2 of 4 Inner Zones (NIH 15 and 16). All other fiber diameters were significantly lower than control at $p<0.05$.

Myelin Thickness

Three of four Perimeter Zone myelin thickness averages (NIH 12, 15 and 16) were significantly lower than control ($p<0.001$) while in the other nerve it was significantly increased (NIH 17). The same pattern was true for the Inner Zone myelin thickness averages.

Differences in Axon Circularity, Fiber Circularity and G-ratio were less consistent than the changes for axon diameter, fiber diameter and myelin thickness averages (Refer to Tables 10 and 11 for a summary).

Axon Circularity

One Perimeter Zone cuffed nerve showed significantly increased axon circularity with respect to control at $p<0.001$ (NIH 16), one showed significantly decreased circularity (NIH

47

17) and two showed no statistically significant change at p<0.001 (NIH 12 and 15). In the Inner Zone cuffed samples, 2 of 4 showed significantly lower axon circularity than the control nerve at p<0.001(NIH 12 and 17), one showed a significant increase (NIH 15) and one showed no difference (NIH 16).

Fiber Circularity

Fiber Circularity measures were equally mixed. In both the Perimeter and Inner Zones, one nerve showed significantly higher circularity than control (NIH 17), one exhibited significantly lower circularity (NIH 16 for Perimeter and NIH 12 for Inner) while the rest showed no statistically significant changes.

G-ratio

In the Perimeter Zone, 2 of 4 nerves had significantly (p<0.001) higher G-ratios than control (NIH 12 and 15) while one had a significantly lower G-ratio (NIH 17). In the Inner, two nerves had significantly higher G-ratios than control (NIH 12 and 16) while two had significantly lower G-ratios at p<0.001 (NIH 15 and 17).

Overall

Cuffed to control cross-section comparisons displayed some unique characteristics for each morphometric observation. These distributions are presented in Figs. 16 to 30.

Looking at overall averages across cats for all the data yields much the same message as above but the statistical power of these observations was weaker (refer to the bottom of Tables 8 and 9). Overall average changes in axon diameter showed that cuffed axons were 90.5% of control in the Perimeter Zone (p=0.07) and 93.7% of control in the Inner Zone (p=0.21). Fiber diameters were 90.9% of control in the perimeter (p=0.07) and 94.1% of control in the Inner (p=0.16). Myelin thickness measures in the cuffed nerves averaged 92.3% of control (p=0.29) in the perimeter and 94.9% of control (p=0.29) in the Inner.

In keeping with the inconsistent trends observed above for Axon Circularity, Fiber Circularity and G-ratio, there were virtually no differences between cuffed and control values for the overall averages of these morphometric measures (refer to bottom of Tables 10 and 11).

Due to the variable nature of the Axon Circularity, Fiber Circularity and G-ratio measurements, these measures were not useful indicators of cuffed to control differences. As such, they were not utilized in this study as primary indicators of damage. The frequency histograms and cumulative frequency histograms for these variables have been presented for NIH 12 (Figs. 19 to 21) only to give a feel for the character of these distributions.

Perimeter Zone	Control Total/ Avg. (µm)	S.D.	Cuffed Total/ Avg. (µm)	S.D.	Cuffed % of control	Significant Difference
Axon Diameter						
N12	6.3	±3.0	6.3	±3.1	100	ns
N15	6.8	±3.5	5.8	±2.7	86	⊗⊗⊗
N16	6.8	±2.9	6.1	±2.7	89	⊗⊗⊗
N17	6.6	±2.6	5.8	±2.4	87	⊗⊗⊗
Fiber Diameter						
N12	10.4	±4.3	10.1	±4.5	96	⊗⊗
N15	11.9	±5.3	10.0	±4.3	84	⊗⊗⊗
N16	11.3	±4.3	9.8	±3.9	87	⊗⊗⊗
N17	10.3	±3.5	9.9	±3.8	96	⊗
Myelin Thickness						
N12	2.1	±0.9	1.9	±0.1	90	⊗⊗⊗
N15	2.6	±1.2	2.1	±1.1	82	⊗⊗⊗
N16	2.2	±0.9	1.9	±0.9	84	⊗⊗⊗
N17	1.8	±0.1	2.1	±0.9	113	⊗⊗⊗

Overall Averages	Control	Cuffed	% of control	Paired 2 tailed p-value
Axon Diameter	6.6 ±0.3	6.0 ±0.3	90	0.07
Fiber Diameter	11.0 ±0.8	10.0 ±0.1	91	0.07
Myelin Thickness	2.2 ±0.3	2.0 ±0.1	92	0.29

Table 8: Summary of morphometric measures. All values shown are averages ± standard deviations. Significant differences were calculated using an unequal sample size technique for cuffed/ control comparisons and a paired t-test was performed to obtain the two tailed p-values for overall averages (⊗⊗⊗ = p<0.001, ⊗⊗ = p< 0.01, ⊗ = p<0.05, ns =not significant.

Inner Zone	Control	Cuffed		
	Total/ Avg. S.D. (μm)	Total/ Avg. S.D. (μm)	Cuffed % of control	Significant Difference
Axon Diameter				
N12	6.3 ±2.7	6.4 ±2.8	101	⊗
N15	6.8 ±2.9	5.7 ±2.4	83	⊗⊗⊗
N16	6.4 ±2.7	6.2 ±2.7	96	⊗⊗⊗
N17	6.6 ±2.7	6.2 ±2.6	94	⊗⊗⊗
Fiber Diameter				
N12	10.4 ±4.2	10.3 ±4.1	99	ns
N15	12.2 ±4.5	10.5 ±4.1	86	⊗⊗⊗
N16	11.1 ±4.1	10.2 ±4.2	92	⊗⊗⊗
N17	10.7 ±4.0	10.6 ±4.0	99	⊗⊗
Myelin Thickness				
N12	2.1 ±0.9	2.0 ±0.9	96	⊗⊗⊗
N15	2.7 ±1.3	2.5 ±1.2	91	⊗⊗⊗
N16	2.3 ±1.0	2.0 ±1.0	87	⊗⊗⊗
N17	2.1 ±1.2	2.2 ±0.9	107	⊗⊗⊗

| Overall Averages	Control	Cuffed	% of control	Paired 2 tailed p-value
Axon Diameter	6.5 ±0.2	6.1 ±0.3	94	0.21
Fiber Diameter	11.1 ±0.8	10.4 ±0.2	94	0.16
Myelin Thickness	2.3 ±0.3	2.2 ±0.2	95	0.29

Table 9: Summary of morphometric measures. All values shown are averages ± standard deviations. Significant differences were calculated using an unequal sample size technique for cuffed/ control comparisons and a paired t-test was performed to obtain the two tailed p-values for overall averages (⊗⊗⊗ = $p<0.001$, ⊗⊗ = $p< 0.01$, ⊗ = $p<0.05$, ns =not significant.

Perimeter Zone	Control		Cuffed			
	Total/ Avg. (μm)	S.D.	Total/ Avg. (μm)	S.D.	Cuffed % of control	Significant Difference
Axon C.I.						
N12	0.52	±0.15	0.50	±0.16	96.2	⊗
N15	0.55	±0.15	0.51	±0.17	92.7	⊗⊗⊗
N16	0.61	±0.13	0.60	±0.15	98.4	⊗
N17	0.55	±0.45	0.66	±0.11	120.0	⊗⊗⊗
Fiber C.I.						
N12	0.69	±0.09	0.67	±0.10	97.1	⊗
N15	0.71	±0.08	0.69	±0.10	97.2	⊗⊗⊗
N16	0.74	±0.07	0.75	±0.08	101.4	⊗⊗
N17	0.70	±0.28	0.78	±0.05	111.4	⊗⊗⊗
G-Ratio						
N12	0.60	±0.08	0.62	±0.09	103.3	⊗⊗⊗
N15	0.57	±0.10	0.59	±0.11	103.5	⊗⊗⊗
N16	0.60	±0.08	0.61	±0.09	101.7	⊗
N17	0.64	±0.10	0.58	±0.09	90.6	⊗⊗⊗

| Overall Averages	Control	Cuffed	% of control	Paired 2 tailed p-value
Axon C.I.	0.56 ±0.04	0.57 ±0.08	102	0.79
Fiber C.I.	0.71 ±0.02	0.72 ±0.05	102	0.63
G-Ratio	0.60 ±0.03	0.60 ±0.02	100	0.91

Table 10: Summary of morphometric measures. All values shown are averages ± standard deviations. Significant differences were calculated using an unequal sample size technique for cuffed/ control comparisons and a paired t-test was performed to obtain the two tailed p-values for overall averages (⊗⊗⊗ = p<0.001, ⊗⊗ = p< 0.01, ⊗ = p<0.05, ns =not significant.

Inner Zone	Control		Cuffed			
	Total/ Avg. (μm)	S.D.	Total/ Avg. (μm)	S.D.	Cuffed % of control	Significant Difference
Axon C.I.						
N12	0.49	±0.16	0.47	±0.14	95.9	⊗⊗⊗
N15	0.58	±0.14	0.52	±0.15	89.7	⊗⊗⊗
N16	0.55	±0.16	0.55	±0.16	100.0	⊗⊗
N17	0.56	±0.15	0.64	±0.12	114.3	⊗⊗⊗
Fiber C.I.						
N12	0.67	±0.09	0.66	±0.08	98.5	⊗⊗⊗
N15	0.73	±0.08	0.73	±0.07	100.0	ns
N16	0.71	±0.08	0.70	±0.09	98.6	ns
N17	0.70	±0.08	0.76	±0.06	108.6	⊗⊗⊗
G-Ratio						
N12	0.60	±0.08	0.62	±0.08	103.3	⊗⊗⊗
N15	0.56	±0.11	0.54	±0.10	96.4	⊗⊗⊗
N16	0.58	±0.09	0.61	±0.09	105.2	⊗⊗⊗
N17	0.62	±0.11	0.58	±0.08	93.5	⊗⊗⊗

Overall Averages	Control	Cuffed	% of control	Paired 2 tailed p-value
Axon C.I.	0.55 ±0.04	0.55 ±0.07	100	0.99
Fiber C.I.	0.70 ±0.03	0.71 ±0.04	101	0.59
G-Ratio	0.59 ±0.03	0.59 ±0.04	100	0.89

Table 11: Summary of morphometric measures. All values shown are averages ± standard deviations. Significant differences were calculated using an unequal sample size technique for cuffed/ control comparisons and a paired t-test was performed to obtain the two tailed p-values for overall averages (⊗⊗⊗ = p<0.001, ⊗⊗ = p< 0.01, ⊗ = p<0.05, ns =not significant.

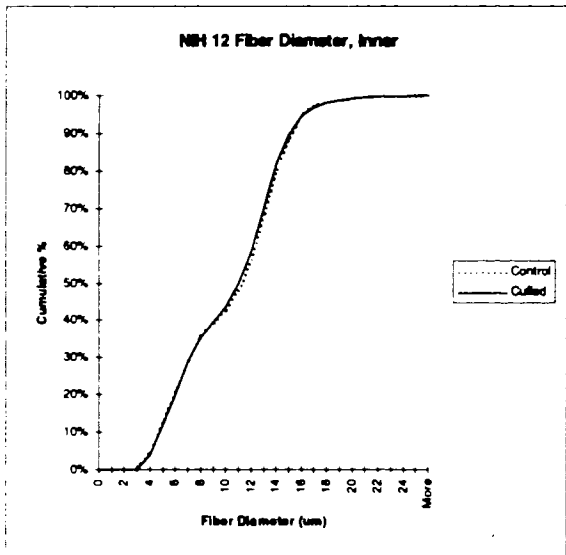## 4.2.a Detailed Examination of NIH 12
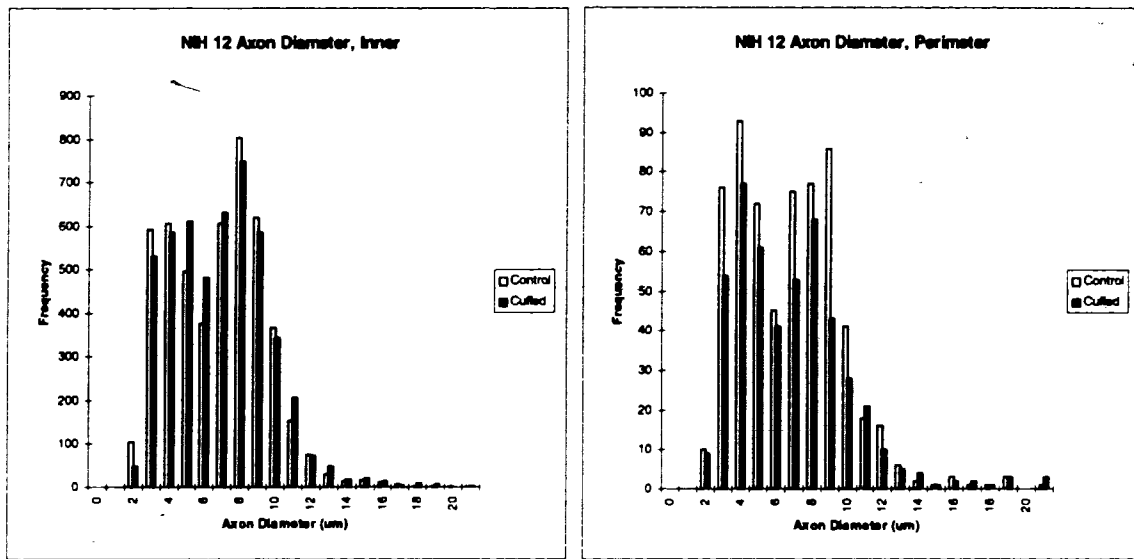
a)

b)
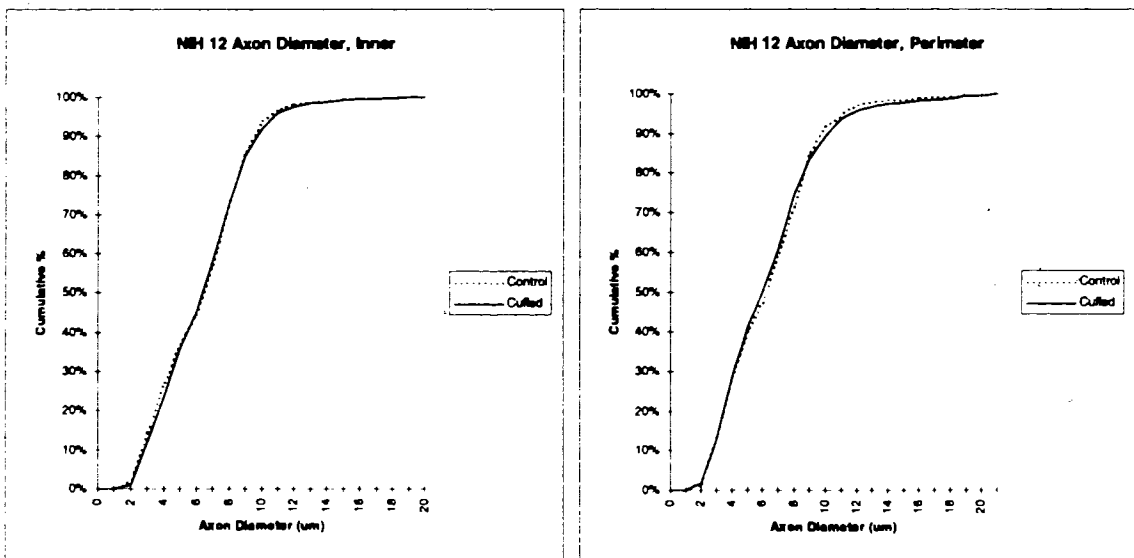
c)

d)

Figure 16: a) Frequency histogram for NIH 12 Inner Zone axon diameter in both the cuffed and control nerves; b) Frequency histogram for axon diameters in the Perimeter Zone of NIH 12; c) Cumulative frequency histogram corresponding to frame a); d) Cumulative frequency histogram corresponding to frame b).
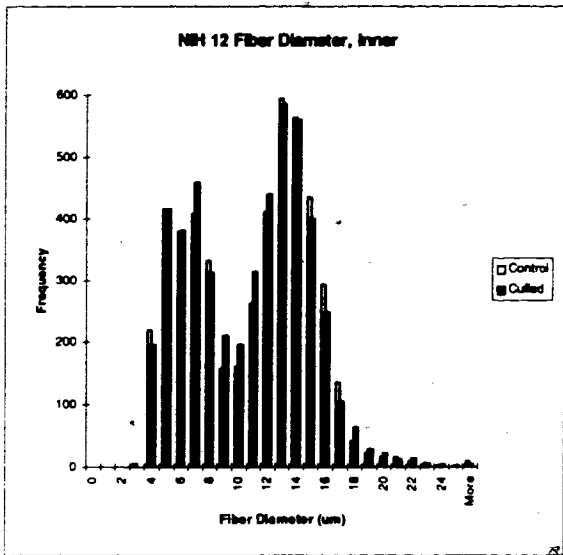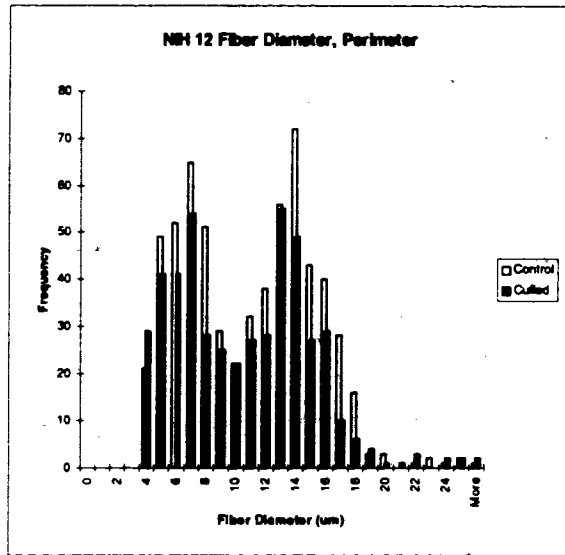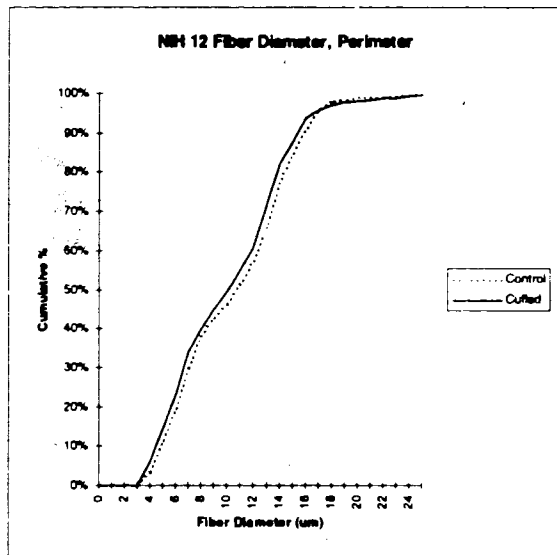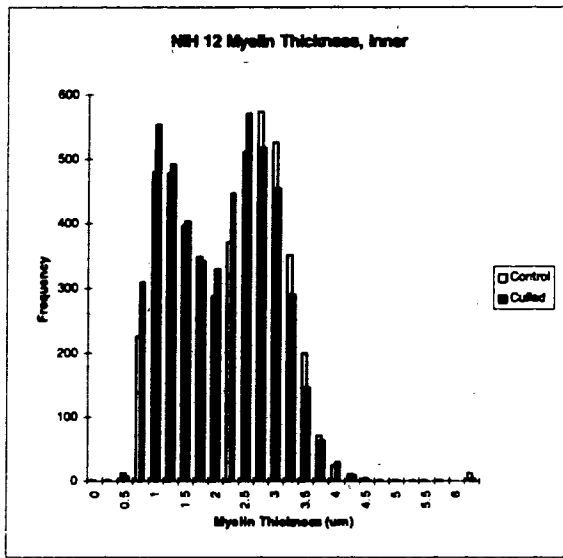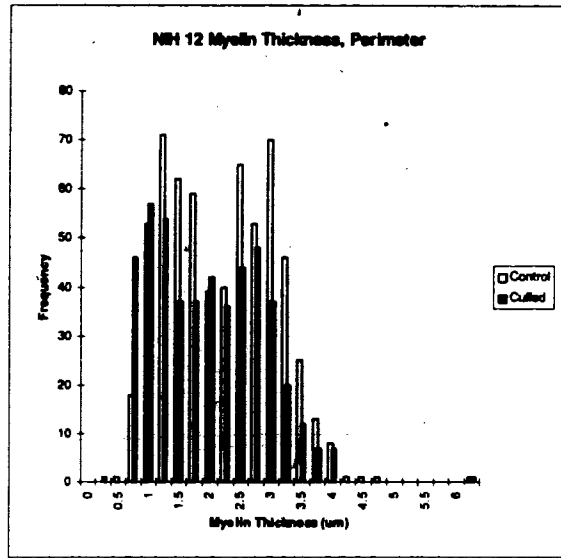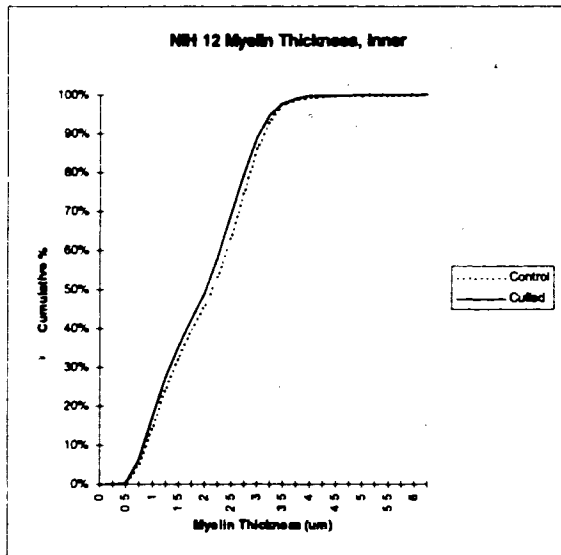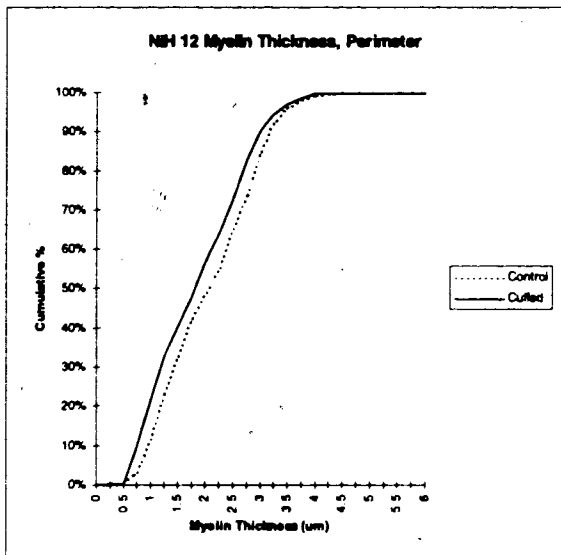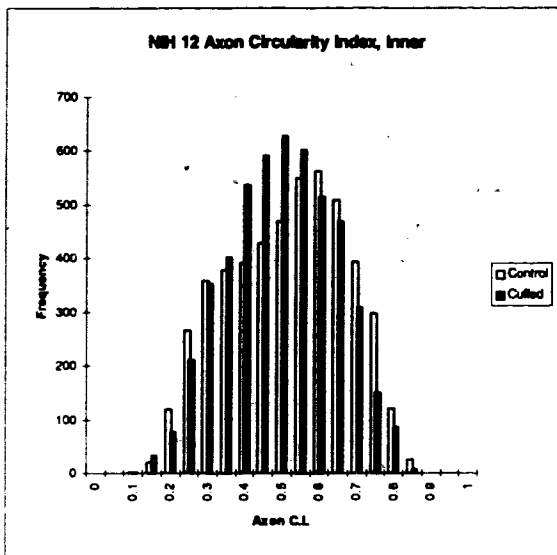
Figure 17: a) Frequency histogram for NIH 12 Inner Zone fiber diameter in both the cuffed and control nerves; b) Frequency histogram for fiber diameters in the Perimeter Zone of NIH 12; c) Cumulative frequency histogram corresponding to frame a); d) Cumulative frequency histogram corresponding to frame b).
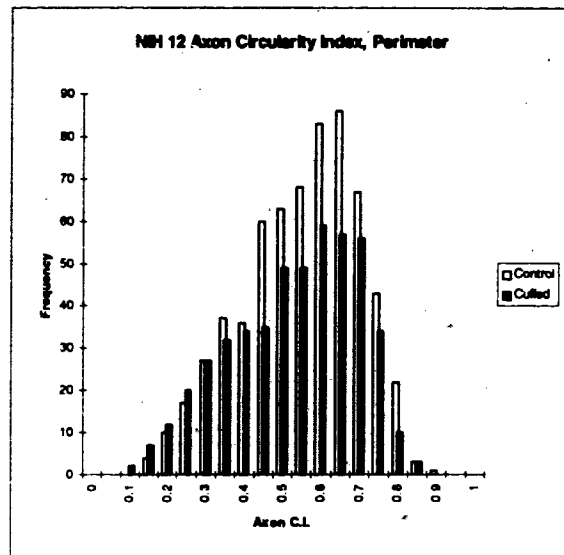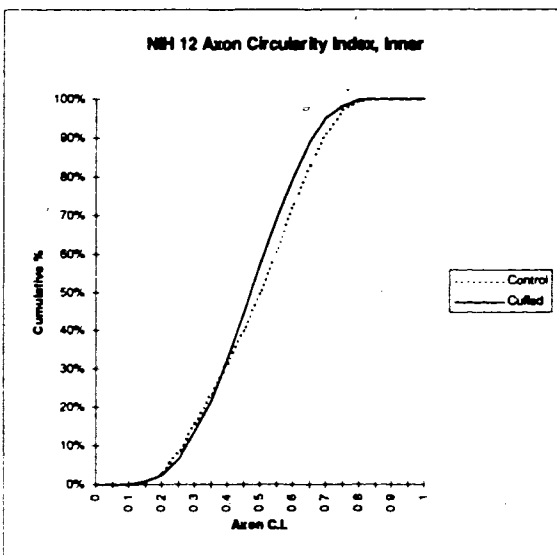
Figure 18: a) Frequency histogram for NIH 12 Inner Zone myelin thickness in both the cuffed and control nerves; b) Frequency histogram for myelin thickness in the Perimeter Zone of NIH 12; c) Cumulative frequency histogram corresponding to frame a); d) Cumulative frequency histogram corresponding to frame b).
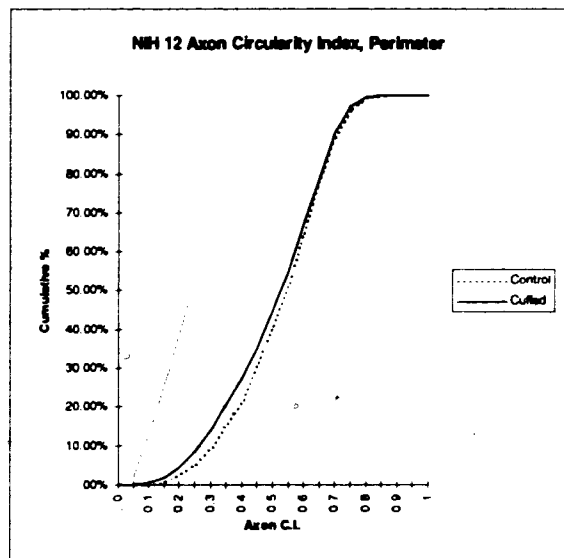
Figure 19: a) Frequency histogram for NIH 12 Inner Zone Axon Circularity Index in both the cuffed and control nerves; b) Frequency histogram for axon circularity in the Perimeter Zone of NIH 12; c) Cumulative frequency histogram corresponding to frame a); d) Cumulative frequency histogram corresponding to frame b). Axon C.I. = Axon Circularity Index.
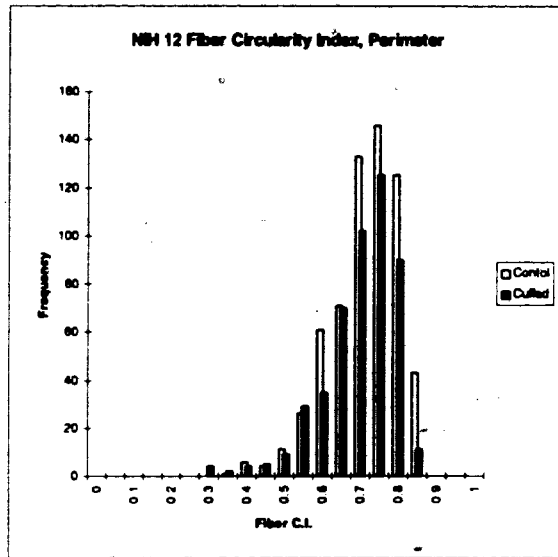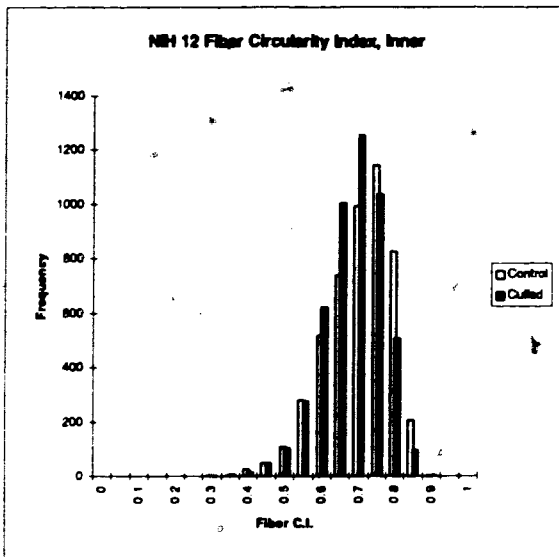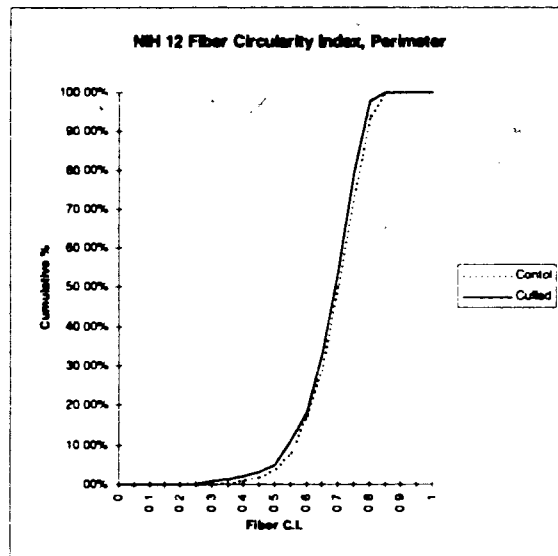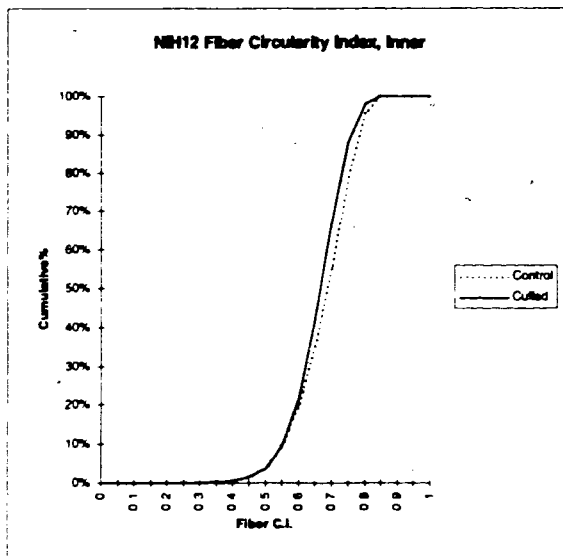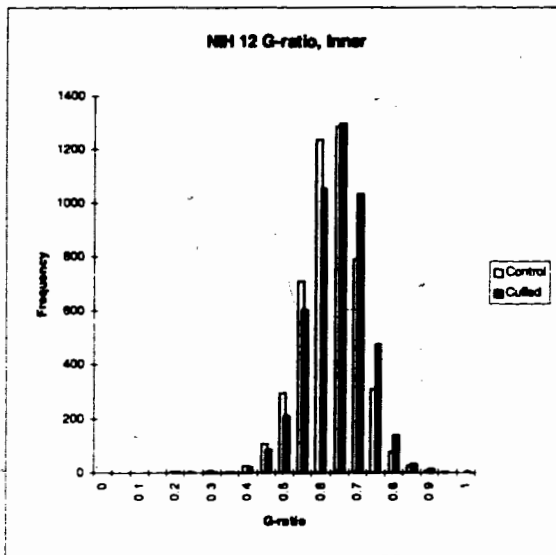
Figure 20: a) Frequency histogram for NIH 12 Inner Zone Fiber Circularity Index in both the cuffed and control nerves; b) Frequency histogram for fiber circularity in the Perimeter Zone of NIH 12; c) Cumulative frequency histogram corresponding to frame a); d) Cumulative frequency histogram corresponding to frame b). Fiber C.I. = Fiber Circularity Index.

Figure 21: a) Frequency histogram for NIH 12 Inner Zone G-ratio in both the cuffed and control nerves; b) Frequency histogram for G-ratio in the Perimeter Zone of NIH 12; c) Cumulative frequency histogram corresponding to frame a); d) Cumulative frequency histogram corresponding to frame b).

4.2.b Detailed Examination of NIH 15

a)

b)
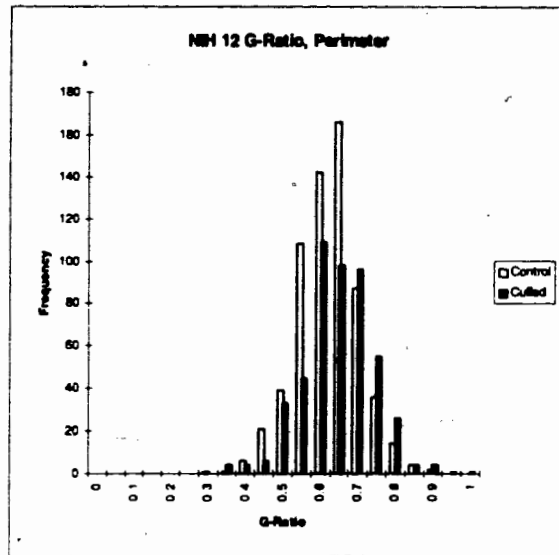

c)

d)

Figure 22: a) Frequency histogram for NIH 15 Inner Zone axon diameter in both the cuffed and control nerves; b) Frequency histogram for axon diameters in the Perimeter Zone of NIH 15; c) Cumulative frequency histogram corresponding to frame a); d) Cumulative frequency histogram corresponding to frame b).
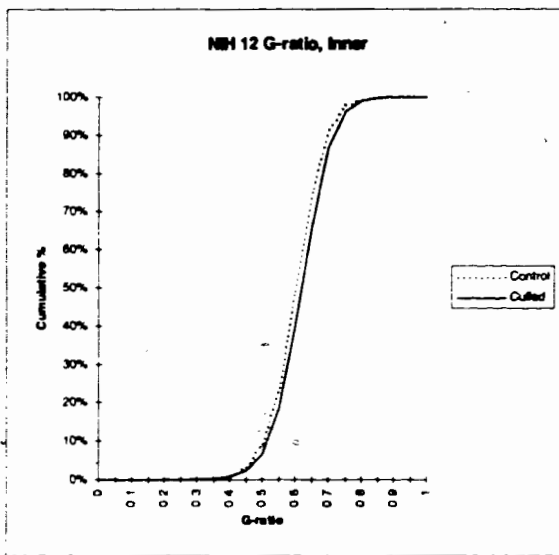
Figure 23 a) Frequency histogram for NIH 15 Inner Zone fiber diameter in both the cuffed and control nerves; b) Frequency histogram for fiber diameters in the Perimeter Zone of NIH 15; c) Cumulative frequency histogram corresponding to frame a); d) Cumulative frequency histogram corresponding to frame b).

a)

b)

c)
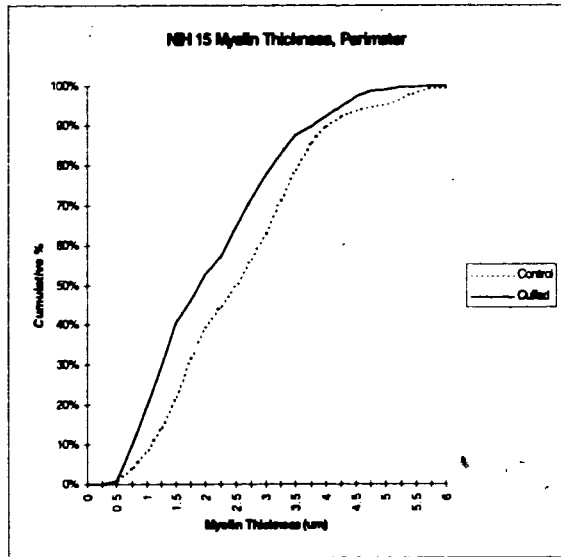
d)

Figure 24 a) Frequency histogram for NIH 15 Inner Zone myelin thickness in both the cuffed and control nerves; b) Frequency histogram for myelin thickness in the Perimeter Zone of NIH 15; c) Cumulative frequency histogram corresponding to frame a); d) Cumulative frequency histogram corresponding to frame b).
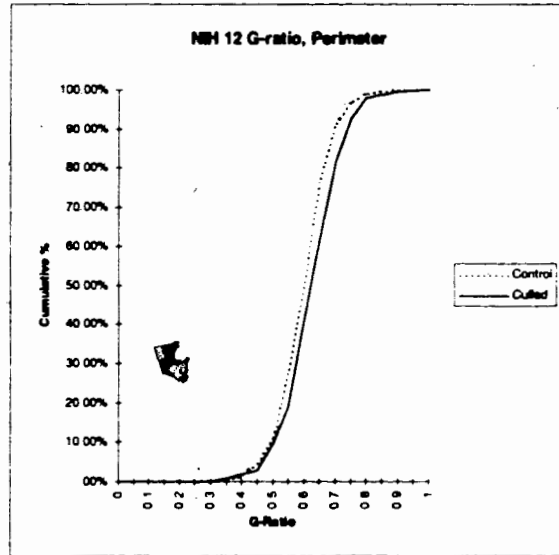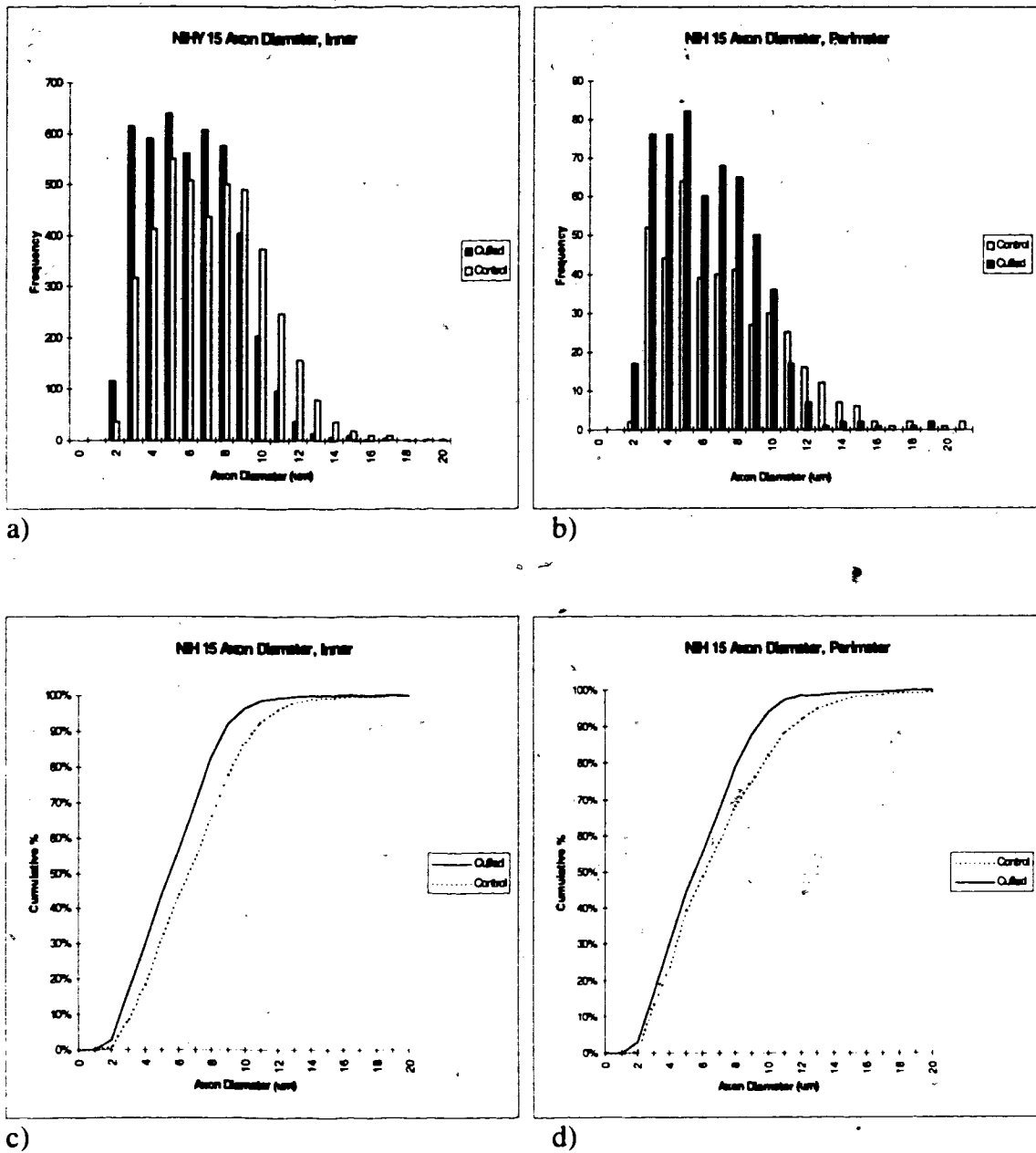
4.2.c Detailed Examination of NIH 16
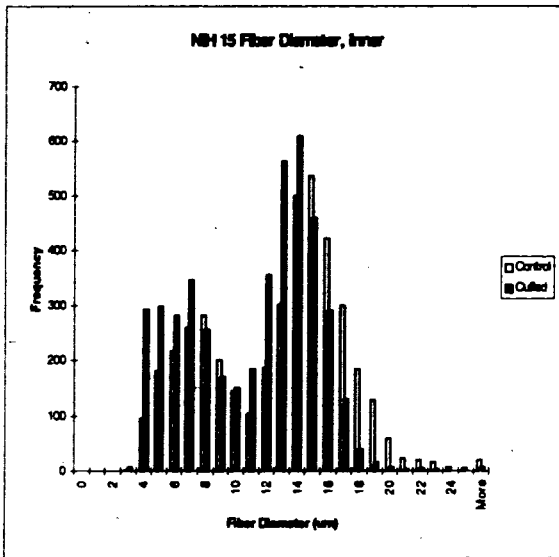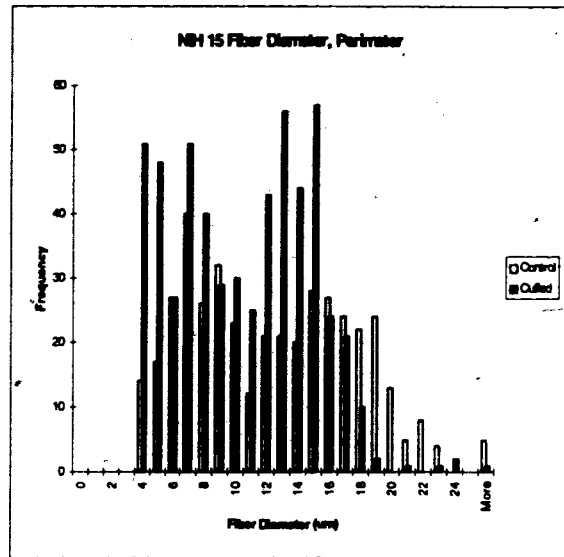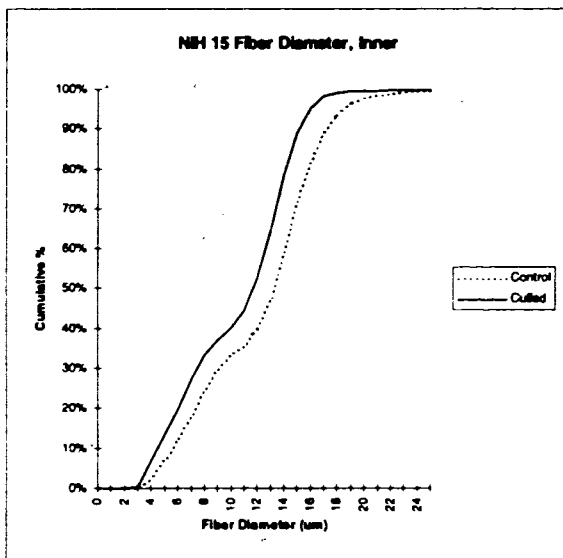

a)

b)

c)

d)
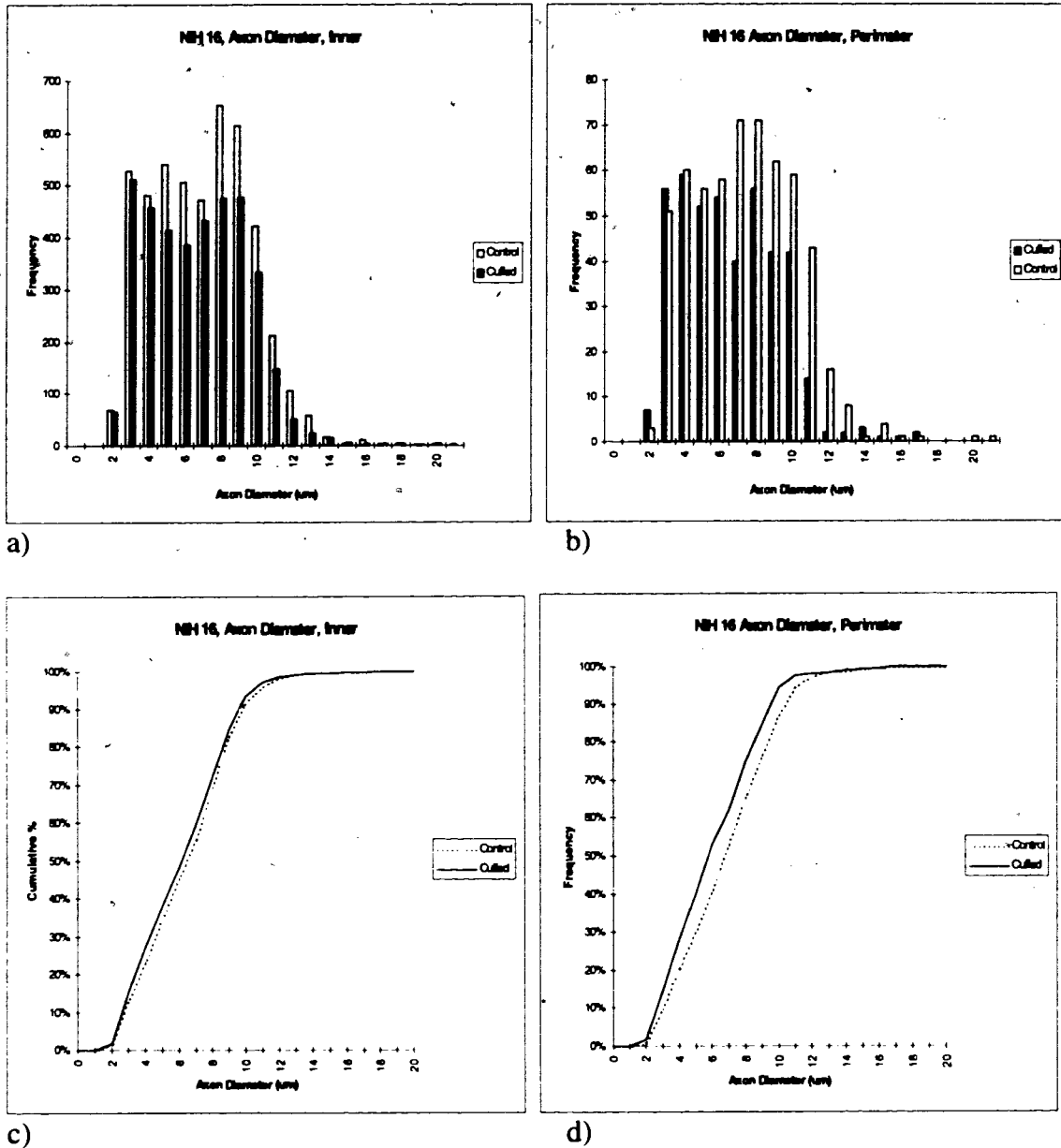
Figure 25 a) Frequency histogram for NIH 16 Inner Zone axon diameter in both the cuffed and control nerves; b) Frequency histogram for axon diameters in the Perimeter Zone of NIH 16; c) Cumulative frequency histogram corresponding to frame a); d) Cumulative frequency histogram corresponding to frame b).
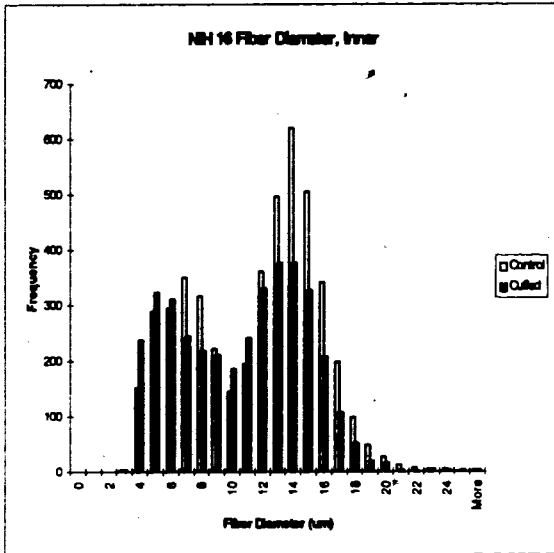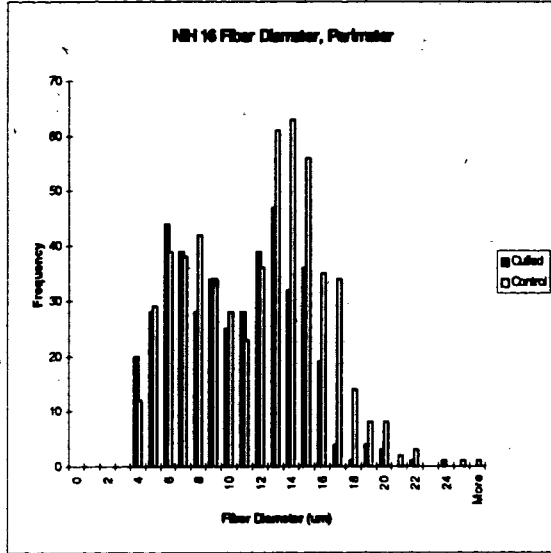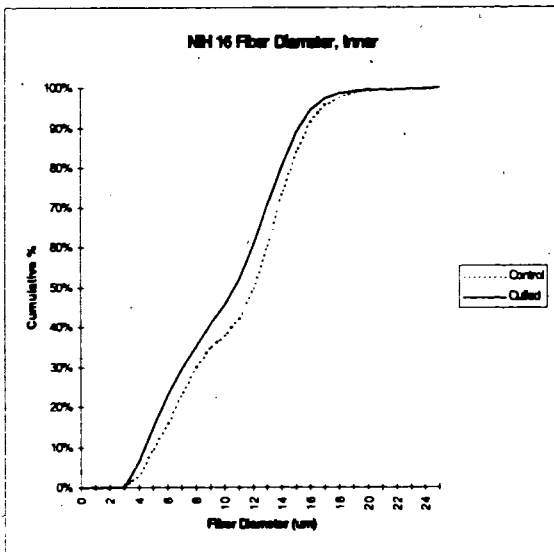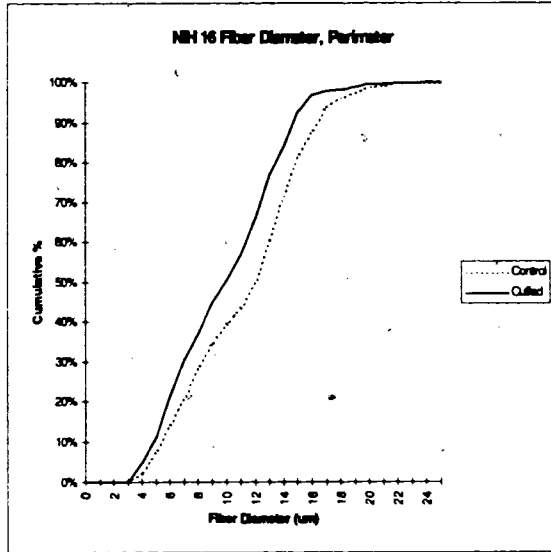
Figure 26 a) Frequency histogram for NIH 16 Inner Zone fiber diameter in both the cuffed and control nerves; b) Frequency histogram for fiber diameters in the Perimeter Zone of NIH 16; c) Cumulative frequency histogram corresponding to frame a); d) Cumulative frequeney histogram corresponding to frame b).
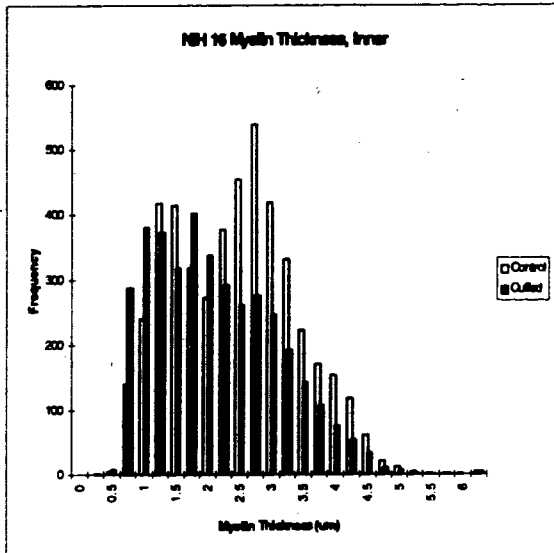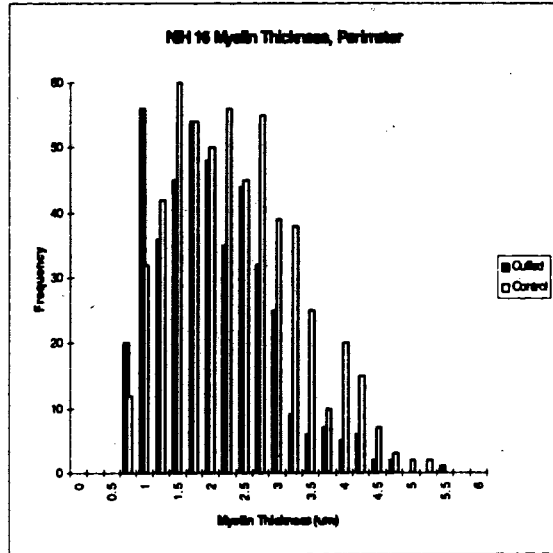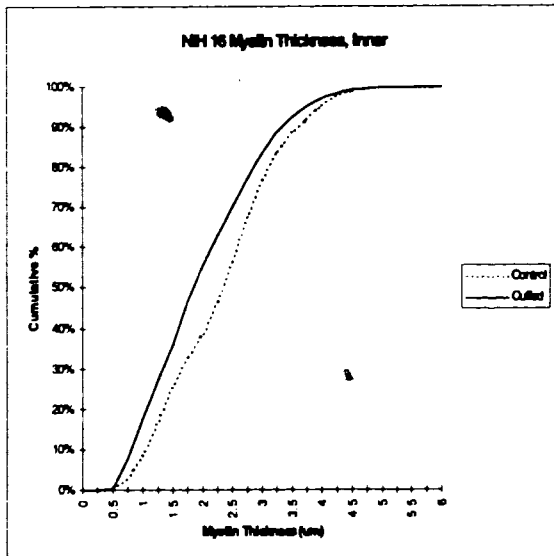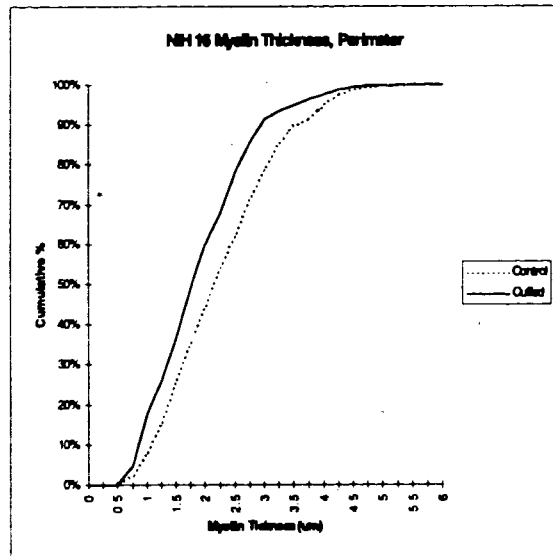
Figure 27 a) Frequency histogram for NIH 16 Inner Zone myelin thickness in both the cuffed and control nerves; b) Frequency histogram for myelin thickness in the Perimeter Zone of NIH 16; c) Cumulative frequency histogram corresponding to frame a); d) Cumulative frequency histogram corresponding to frame b).

4.2.d Detailed Examination of NIH 17

a)

b)

c)

d)
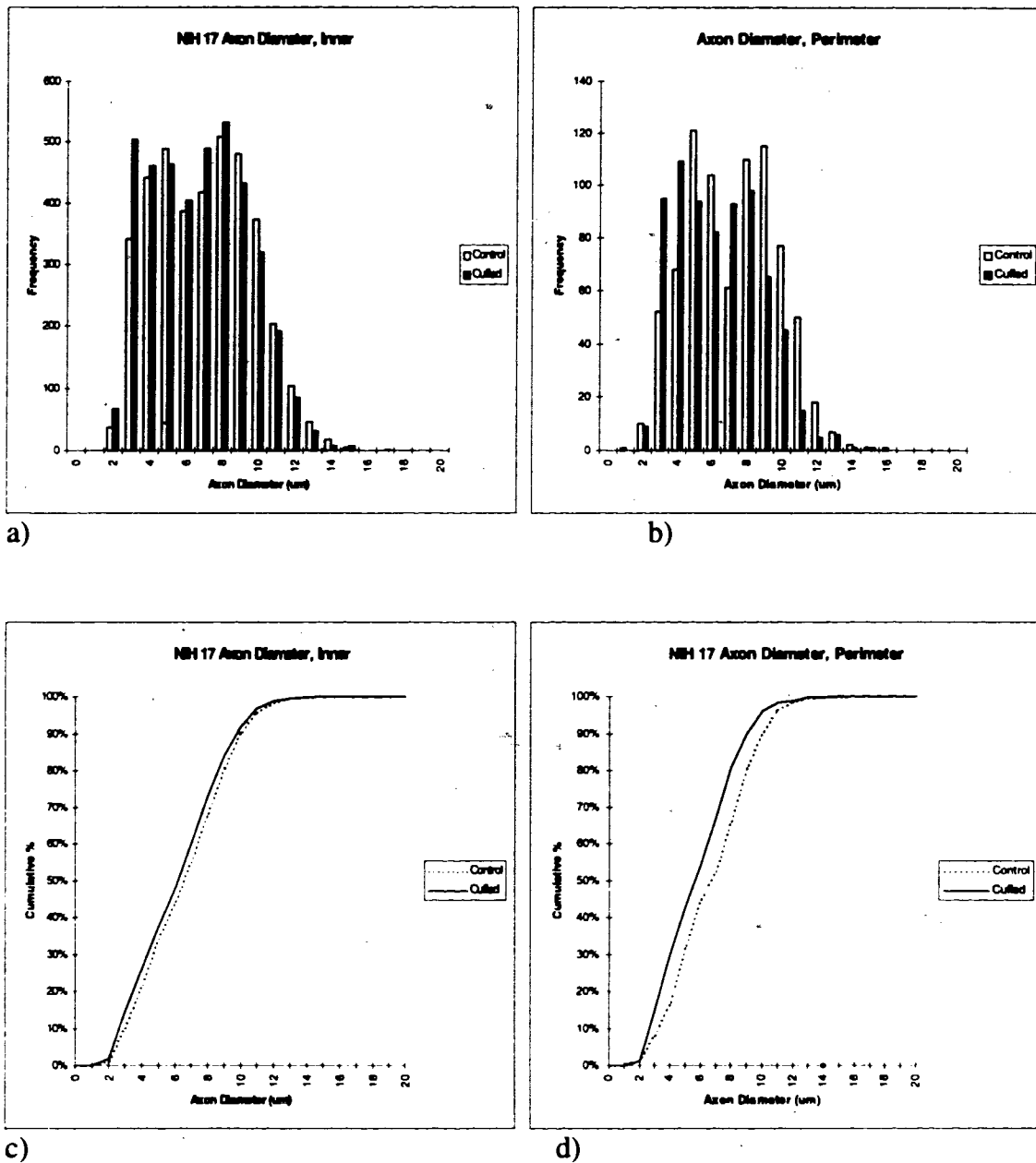
Figure 28 a) Frequency histogram for NIH 17 Inner Zone axon diameter in both the cuffed and control nerves; b) Frequency histogram for axon diameters in the Perimeter Zone of NIH 17; c) Cumulative frequency histogram corresponding to frame a); d) Cumulative frequency histogram corresponding to frame b).
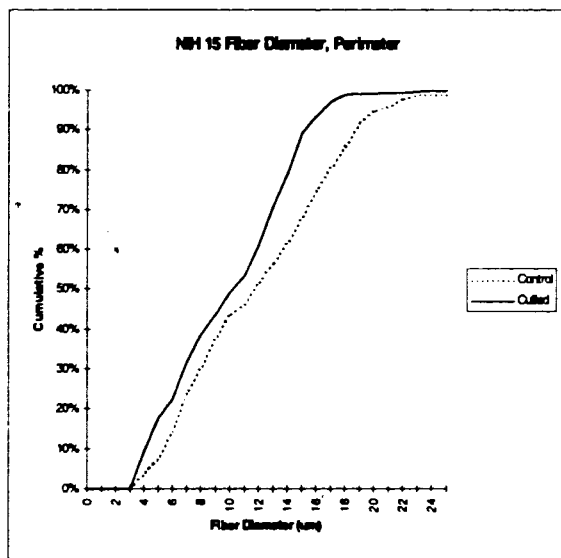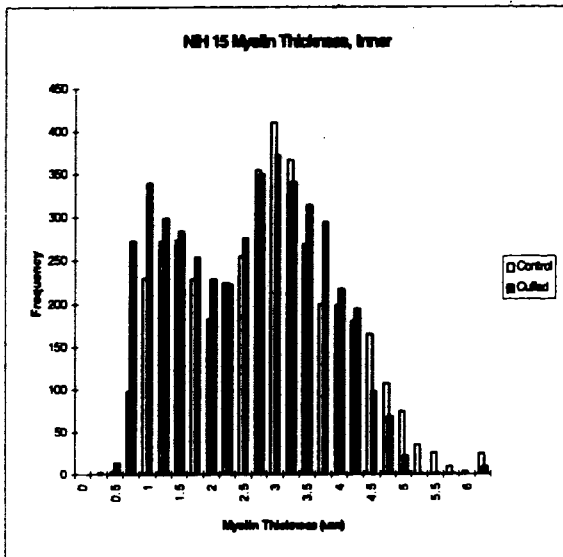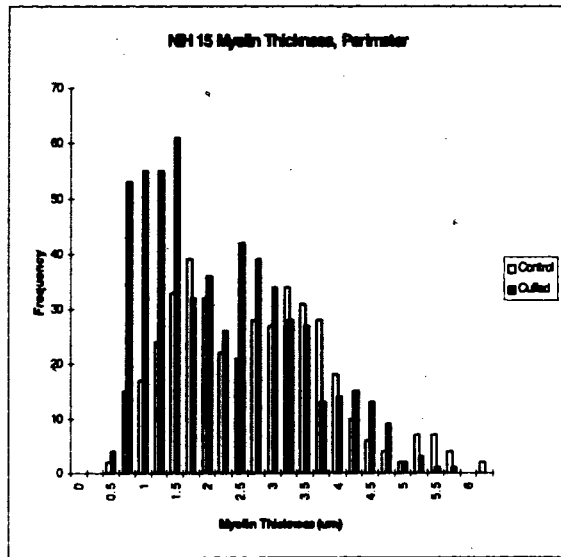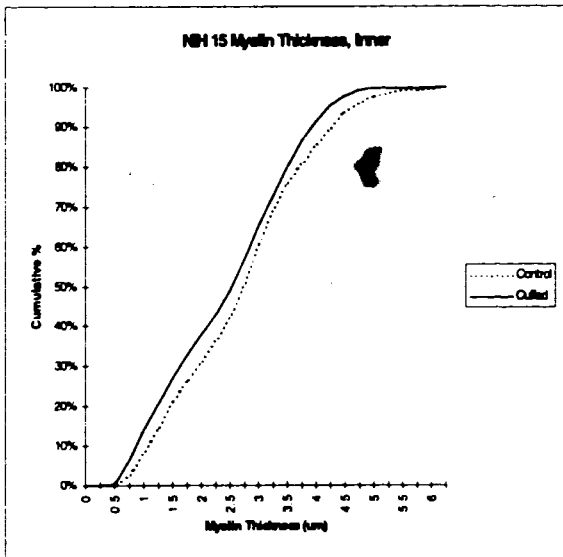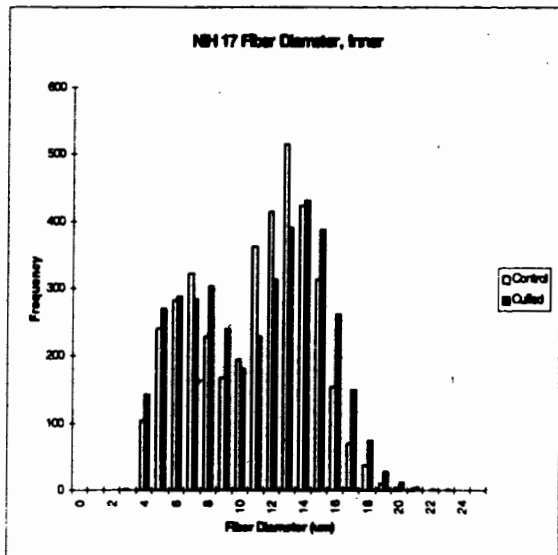
a)
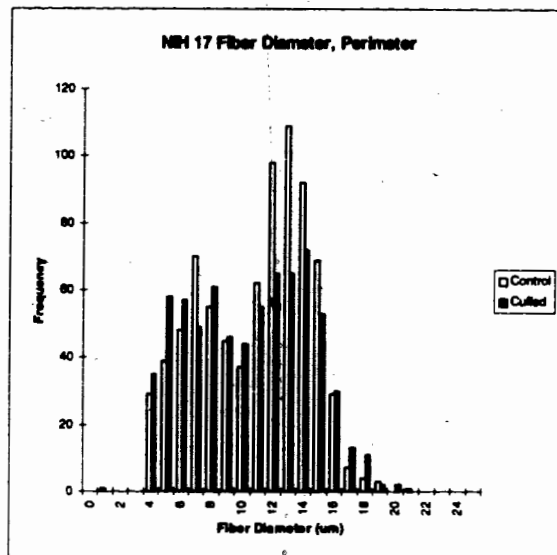
b)
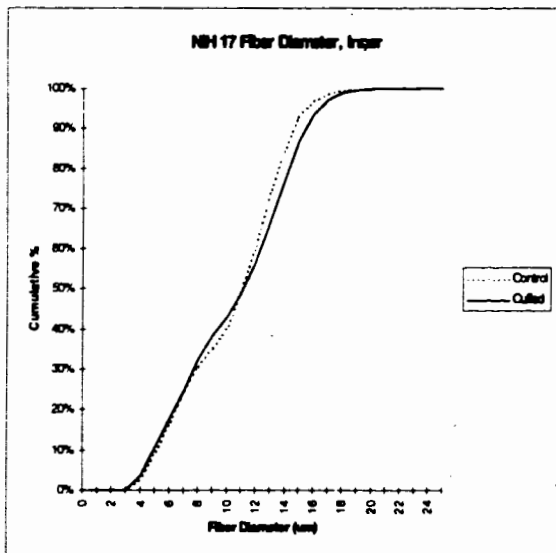
c)
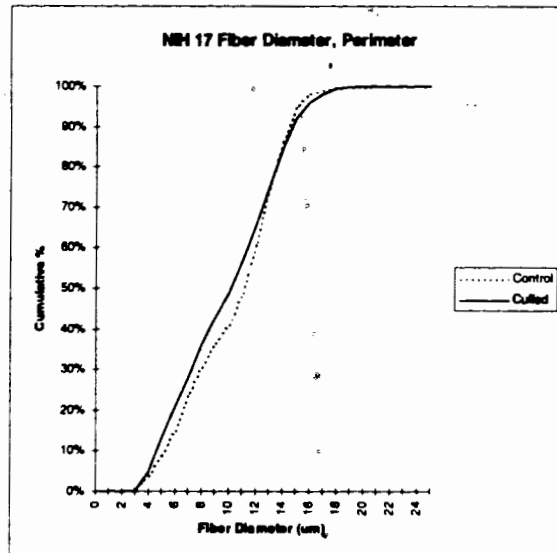
d)

Figure 29 a) Frequency histogram for NIH 17 Inner Zone fiber diameter in both the cuffed and control nerves; b) Frequency histogram for fiber diameters in the Perimeter Zone of NIH 17; c) Cumulative frequency histogram corresponding to frame a); d) Cumulative frequency histogram corresponding to frame b).
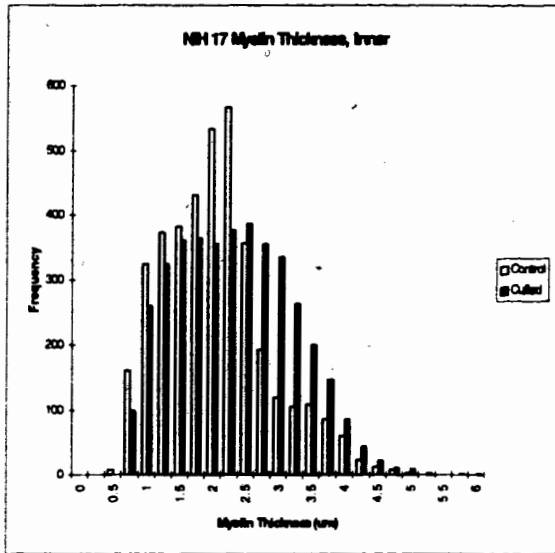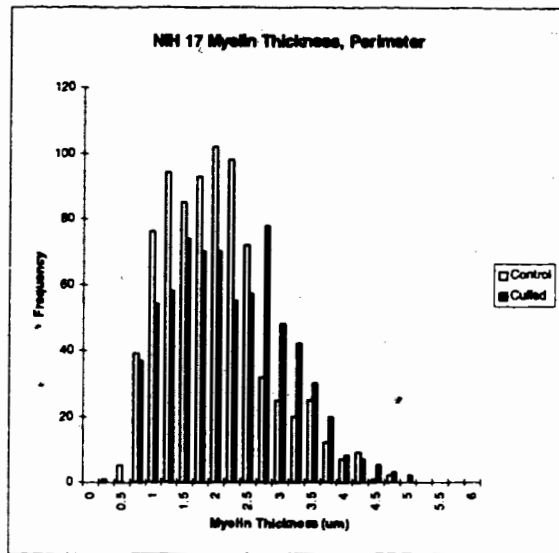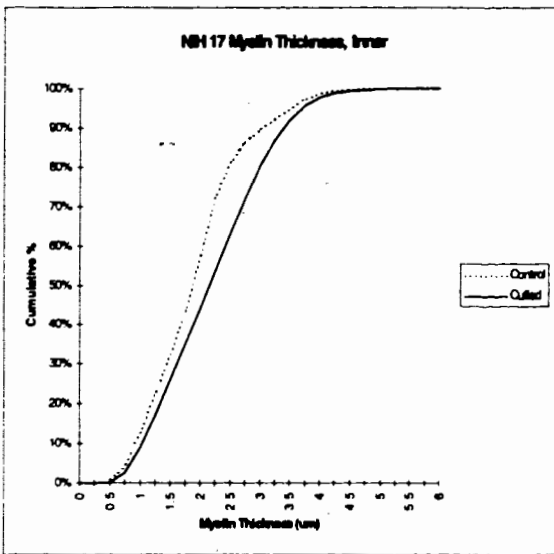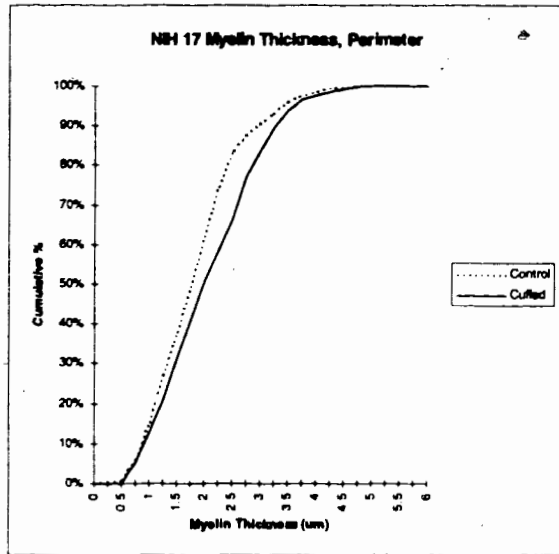
Figure 30 a) Frequency histogram for NIH 17 Inner Zone myelin thickness in both the cuffed and control nerves; b) Frequency histogram for myelin thickness in the Perimeter Zone of NIH 17; c) Cumulative frequency histogram corresponding to frame a); d) Cumulative frequency histogram corresponding to frame b).

4.3 Perimeter Zone compared to Inner Zone.

Comparison of the cumulative histograms for axon diameter, fiber diameter and myelin thickness in the Perimeter Zone with the same measures in the Inner Zone provides evidence that Perimeter axons were affected to a greater extent than Inner axons. Control fiber diameter cumulative histograms in the Perimeter Zones of NIH 12, NIH 15 and NIH 16 (Fig. 17d, Fig. 22d and Fig. 26d respectively) showed a greater difference between cuffed and control than did the Inner Zone distributions (Fig. 17c, Fig. 22c and Fig. 26c respectively). The same was true for cuffed to control comparisons for myelin thickness in NIH 12, NIH 15 and NIH 16 (Fig. 18c, d; Fig. 24 c, d and Fig. 27 c, d respectively).

Axon diameter comparisons between Inner and Perimeter were less consistent. A greater difference was observed in the Perimeter Zone distributions of NIH 15 and NIH 16 as compared to their respective Inner Zone distributions (Fig. 22 c, d and Fig. 25 c, d). In contrast, the distributions for NIH 12 axon diameter were virtually identical between cuffed and control in both the Inner and Perimeter Zones (Fig. 16 c, d) and the distributions for NIH 17 suggest that the Inner Zone axon diameters were reduced slightly more than the Perimeter Zone axon diameters.

Consideration of the quartile comparisons for Inner and Perimeter Zones yielded the same conclusion. Inner Zone mean axon diameter differences between cuffed and control ranged between 0.26 μm to 0.5 μm while the Perimeter differences were 0.7 μm and 1.0 μm. Thus, Perimeter Zone axon diameters showed an almost twofold greater difference in average than did the Inner axons (Fig. 31 a, b).

The trend was observed with fiber diameter quartile averages and myelin thickness quartile averages. Fiber diameter quartile means dropped, on average, 0.5 μm across all size ranges in the Inner Zone while the Perimeter Zone fiber diameters were 1.4 μm lower in cuffed as compared to control (Fig. 32 a, b). Myelin thickness quartile averages showed a 0.09 μm decline in the Inner Zone while a 0.25 μm drop was observed in the Perimeter (Fig. 33 a, b).
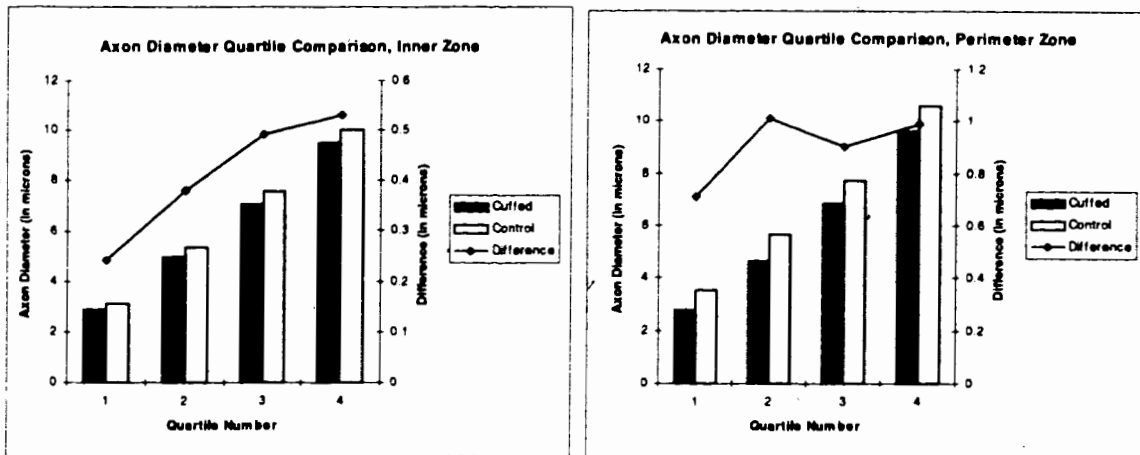
Figure 31: Comparison of the average axon diameter per quartile for the Inner Zone and the Perimeter Zone. Note: none of the differences were statistically significant at $\alpha=0.05$.
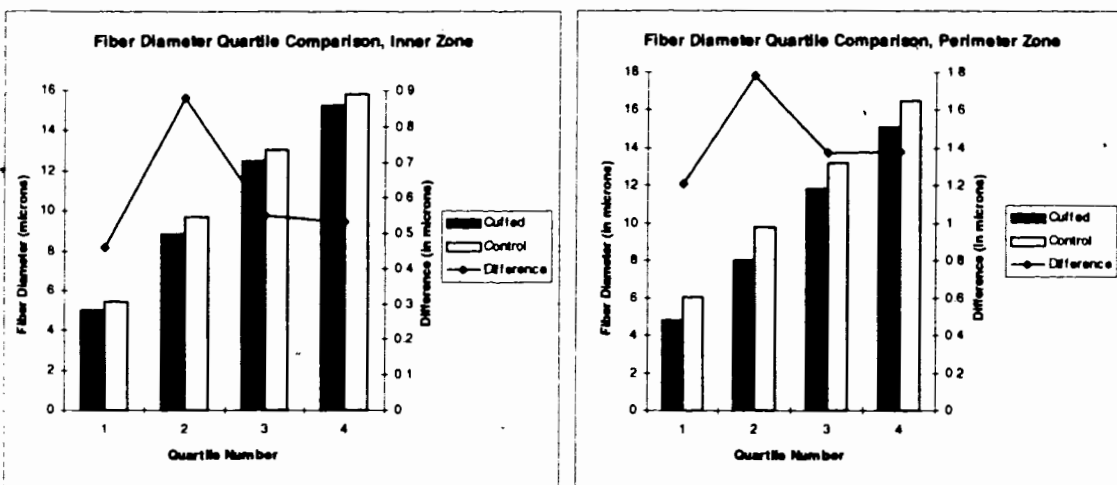
Figure 32: Comparison of the average fiber diameter per quartile for the Inner Zone and the Perimeter Zone. Note: none of the differences were statistically significant at $\alpha=0.05$.
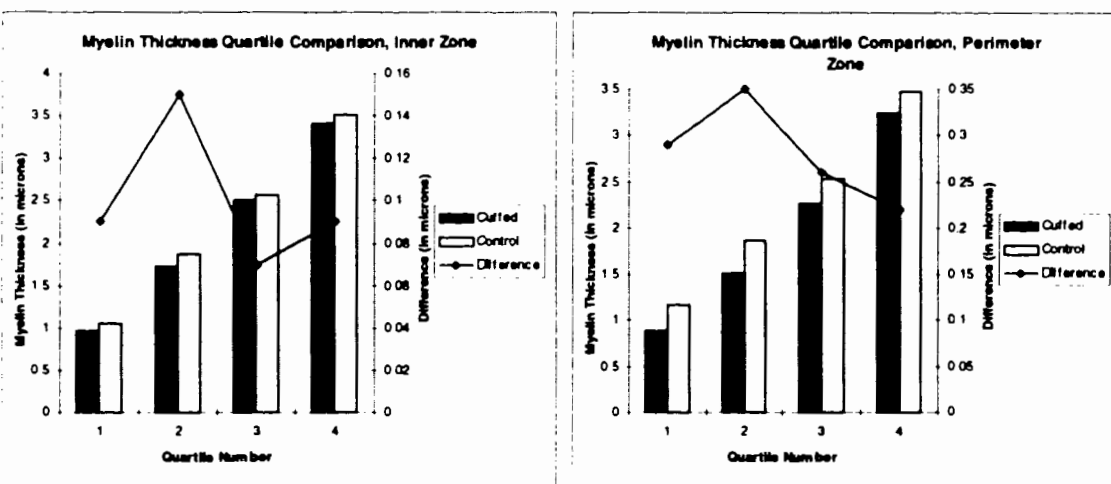
Figure 33: Comparison of the average myelin thickness per quartile for the Inner Zone and the Perimeter Zone. Note: none of the differences were statistically significant at $\alpha=0.05$.

70

4.4 Larger axon changes compared to smaller axon changes

Morphometric measures of axon diameter, fiber diameter and myelin thickness suggest that axons become smaller axons following cuff implant. There tended to be more control axons than cuffed axons in the 8 to 12 μm, 12 to 16 μm and >16 μm regions of the size spectrum while the reverse was true in the 0 to 4 μm and 4 to 8 μm regions (Fig. 34). This finding suggests that axons in the cuffed nerves were generally reduced in diameter.

Fiber diameters show a similar pattern. There tended to be a higher percentage of control fibers in regions greater than 10 μm as compared to the cuffed samples with the most marked differences were observed in the 15 to 20 μm size range. The converse was true in the regions less than 10 μm (Fig. 35).

Myelin thickness also showed a trend toward reduced values at larger thicknesses. A higher percentage of total fibers tended to have myelin thicknesses in the 2-3 μm, 3-4 μm and 4-5 μm ranges in control samples as compared to cuffed. The myelin thickness ranges from 0-1 μm and from 1-2 μm tended to show the opposite (Fig. 36).

While the aforementioned data indicate that it is likely that axon diameters, fiber diameters and myelin thickness values were reduced in cuffed nerves during the implant period, we have still not addressed the issue of whether these changes are shown to a greater extent in the larger axons as compared to smaller axons. Comparison of the inter-quartile size changes from Figs. 31, 32 and 33 showed that, using a paired t-test, no statistically significant (α=0.05) differences were observed between size decreases in larger axons with respect to smaller axons. Changes in size were relatively constant across all size ranges in terms of total μm change with respect to control.

Inner Zone

Perimeter Zone
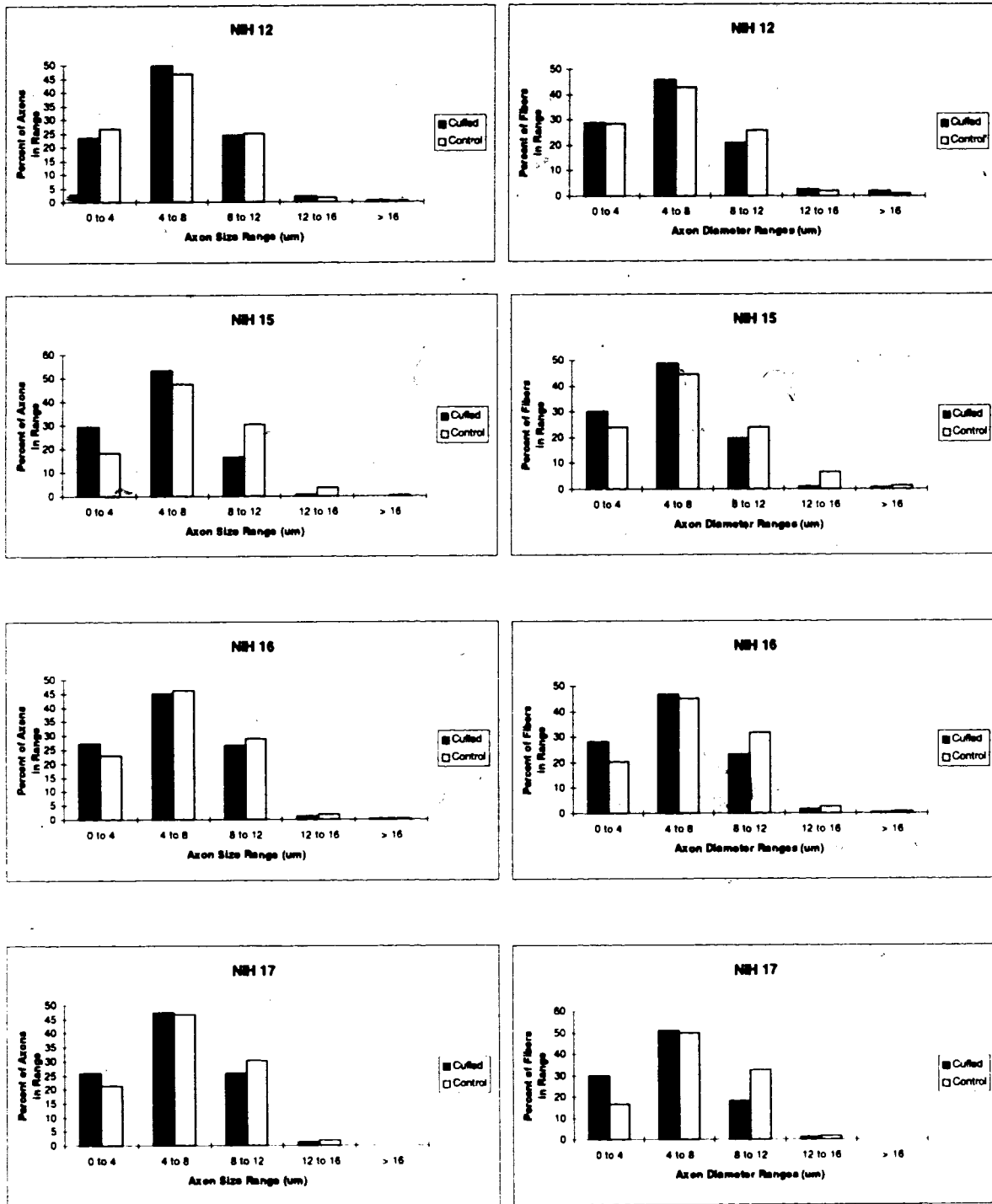
Figure 34: Inner Zone and Perimeter Zone axon size distributions for all 4 experimental subjects based on the percentage of fibers located in a given size range.

Figure 35: Inner Zone and Perimeter Zone fiber diameter size distributions for all 4 experimental subjects based on the percentage of fibers located in a given size range.

Inner Zone   Perimeter Zone
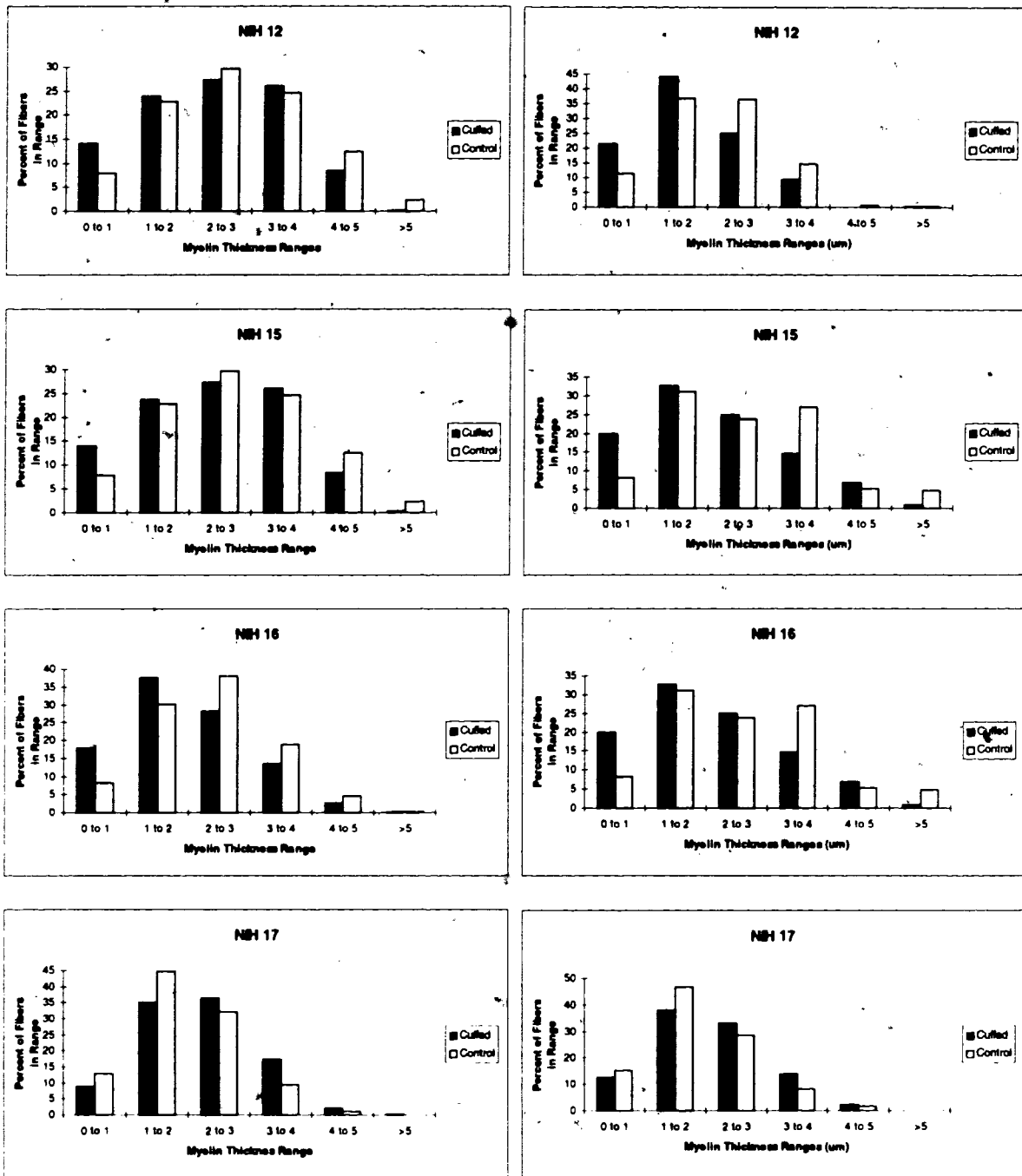
Figure 36: Inner Zone and Perimeter Zone myelin thickness size distributions for all 4 experimental subjects based on the percentage of fibers located in a given size range.

4.5 Morphometric changes related to CAP changes.

The findings that cuffed axon diameter, fiber diameter and myelin thickness were lower than control were taken as indicators of presumed damage within the cuffed nerves. The differences observed in each cat were correlated to their own set of neurophysiological data. Correlations with other morphometric measures are included in Appendix 7.

In this study, the neurophysiological measurements showed wide variations (Table 12). Compound action potentials showed decreases to as little as 31% of day 0 for NIH 12 and went as high as 129% of day 0 for NIH 16. Time to ENG onset increased to 150% of day 0 for NIH 17 and decreased to 89% of day 0 for NIH 15. Time to ENG 1st positive peak showed similar variations as time to ENG onset. Cuff impedance measures varied from 85% of day 0 for NIH 15 to 239% of day 0 for NIH 16. Overall, two amplitudes increased with respect to day 0 and two decreased, three samples showed increased time to ENG onset, three nerves showed increased time to 1st positive peak and 3 samples showed increased impedance with respect to day 0.

Assuming that morphometry and neurophysiology can be correlated, one would expect to observe several situations during an injury scenario. Decreased axon and fiber diameters should be associated with decreased CAP amplitude, increased time to ENG onset and increased time to ENG 1st positive peak. Decreased myelin thickness should also be correlated with these same changes in neurophysiological measures. Generally, the observed results were opposite to those that were expected.

Subject	Total Implant Days	Parameters	Value (day 0)	Value (final)	% of Day 0
NIH-12	289	Amplitude	0.624 mV	0.194 mV	31.1%
		t_{onset}	1.048 ms	1.212 ms	115.7%
		$t_{1st\ +ve\ peak}$	1.228 ms	1.328 ms	108.1%
		Impedance	1.6 kΩ	3.3 kΩ	206.3%
NIH 15	372	Amplitude	0.344 mV	0.440 mV	127.9%
		t_{onset}	1.124 ms	1.004 ms	89.32%
		$t_{1st\ +ve\ peak}$	1.304 ms	1.160 ms	88.7%
		Impedance	2.0 kΩ	1.7 kΩ	85.0%
NIH 16	298	Amplitude	0.472 mV	0.608 mV	128.8%
		t_{onset}	1.088 ms	1.420 ms	130.5%
		$t_{1st\ +ve\ peak}$	1.236 ms	1.590 ms	128.6%
		Impedance	1.8 kΩ	4.3 kΩ	238.9%
NIH 17	183	Amplitude	0.256 mV	0.150 mV	58.6%
		t_{onset}	1.224 ms	1.830 ms	149.5%
		$t_{1st\ +ve\ peak}$	1.380 ms	2.070 ms	150.0%
		Impedance	1.6 kΩ	2.7 kΩ	168.8%

Table 12: Summary of 4 subjects, showing total days implanted, %ENG amplitude with respect to day zero, time to ENG onset (t_{onset}) with respect to day zero and time to first positive peak ($t_{1st\ +ve\ peak}$) with respect to day zero.

Comparing axon diameter differences to changes in CAP amplitude (Fig. 37a,b) yielded a slightly negative correlation (r= -0.7128 Inner Zone, r= -0.6925 Perimeter Zone). Fiber diameter changes (Fig. 37 c, d) exhibited highly negative correlations with changes in CAP amplitude (r= -0.8723 Inner Zone, r= -0.9815 Perimeter Zone). Myelin thickness (Fig. 37 e, f) also exhibited a strong negative correlation with changes in CAP amplitude (r= -0.8373 Inner Zone, r= -0.9537).

Inner Zone   Perimeter Zone
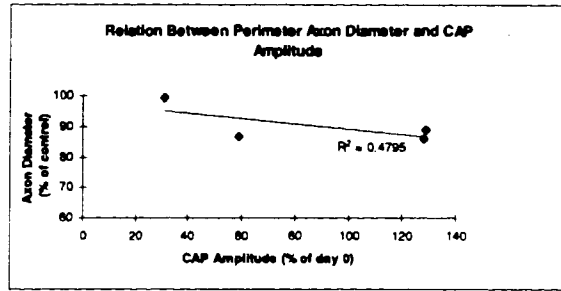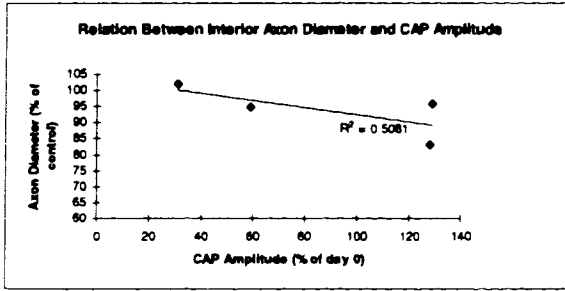
A)   B)
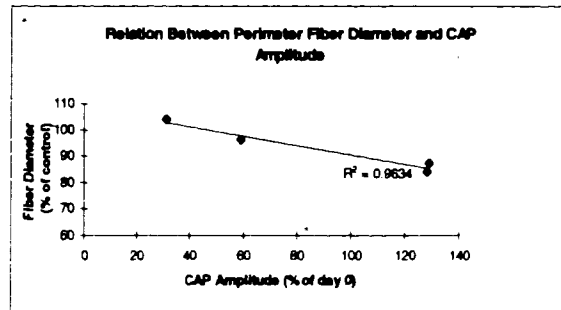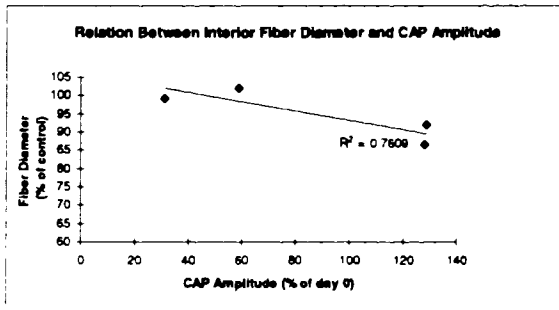
C)   D)
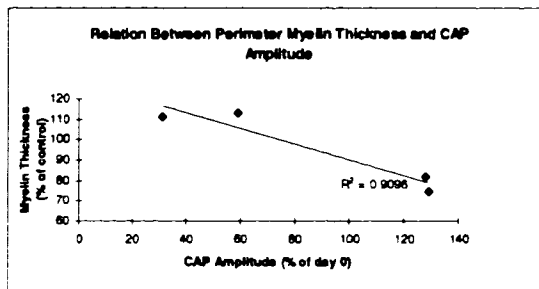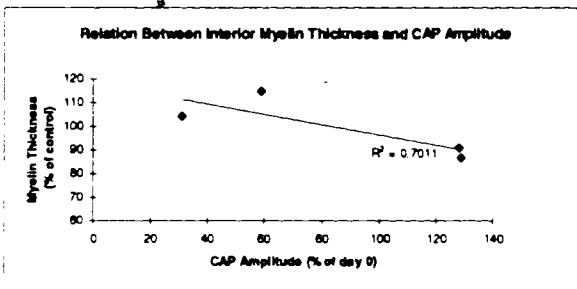
E).   F)

Figure 37: **A)** Correlation of all 4 cats' Inner Zone axon diameter measures (% of control) with changes in CAP amplitude (% of day 0). **B)** Correlation of all 4 cats' Perimeter Zone axon diameter measures (% of control) with changes in CAP amplitude (% of day 0). **C)** Correlation of all 4 cats' Inner Zone fiber diameter measures (% of control) with changes in CAP amplitude (% of day 0). **D)** Correlation of all 4 cats' Perimeter Zone fiber diameter measures (% of control) with changes in CAP amplitude (% of day 0). **E)** Correlation of all 4 cats' Inner Zone myelin thickness measures (% of control) with changes in CAP amplitude (% of day 0). **F)** Correlation of all 4 cats' Perimeter Zone myelin thickness measures (% of control) with changes in CAP amplitude (% of day 0).

Changes in time to ENG onset were also associated with morphometric changes that were opposite to what might have been expected following axonal injury. Inner axon diameter changes (with respect to control) were weakly correlated (r= 0.3013) with changes in time to ENG onset (Fig. 38a). The same was true in the Perimeter Zone (r= 0.1054) (Fig. 38b). Inner Zone fiber diameter changes (Fig. 38c) were more strongly correlated to ENG changes (r= 0.5928) but Perimeter Zone changes (Fig. 38d) were not (r= 0.1136). Myelin thickness differences showed the same generally weak positive correlations (r= 0.4608, Inner; r=0.2516, perimeter) (Fig. 38 e and f respectively).

Morphometric changes showed weak positive correlations to time to 1st ENG positive peak. Axon diameter differences were weakly correlated with changes in time to ENG 1st positive peak (Fig. 39 a, b) in both the Inner and Perimeter Zones (r= 0.2814 and 0.3824 respectively). Fiber diameter measures showed similar trends (r= 0.5600, Inner Zone; r= 0.0678, Perimeter Zone) (Fig. 39 c, d). Inner Zone myelin thickness changes (Fig. 39 e, f) were weakly correlated with time to ENG 1st positive peak (r= 0.4323) and Perimeter Zone differences demonstrated an even weaker relationship (r= 0.2100).

Inner Zone   Perimeter Zones
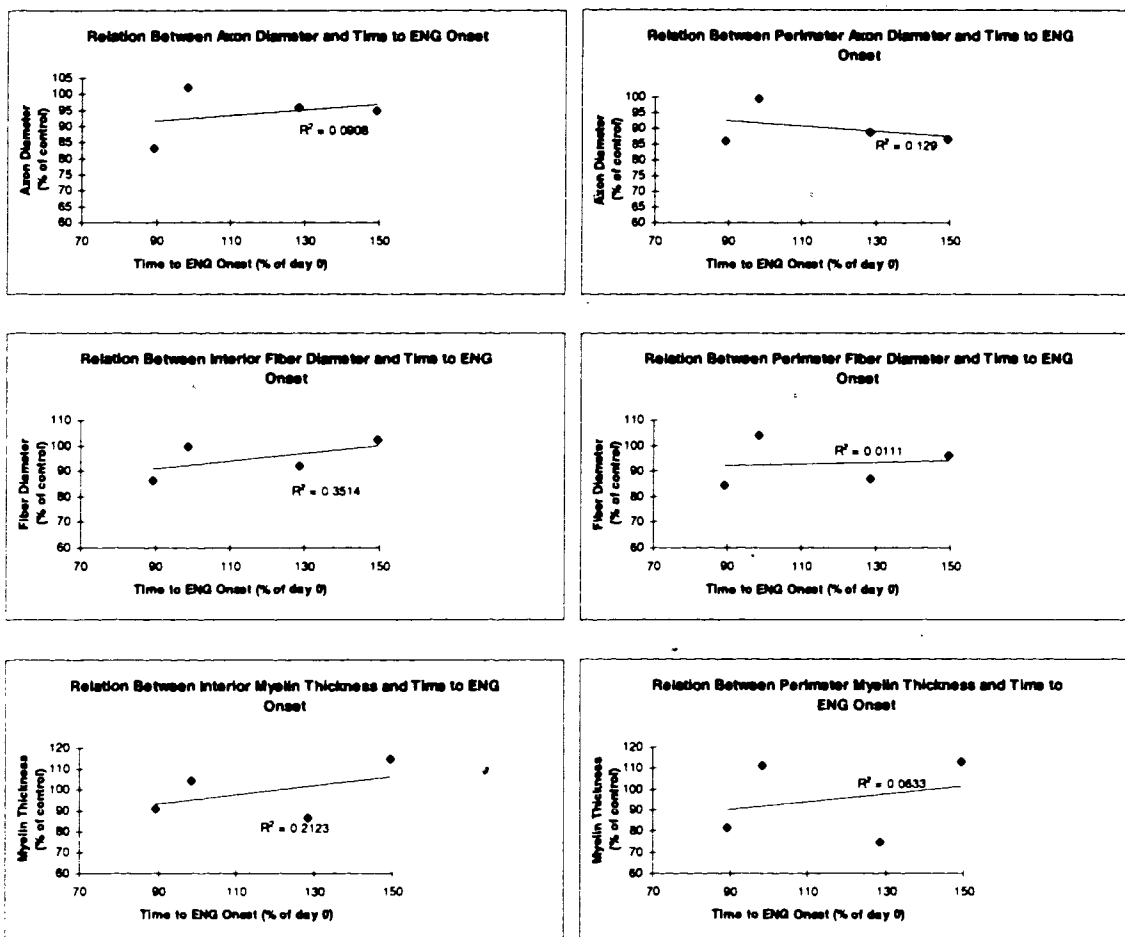
Figure 38: A) Correlation of all 4 cats' Inner Zone axon diameter measures (% of control) with changes in Time to ENG onset (% of day 0). **B)** Correlation of all 4 cats' Perimeter Zone axon diameter measures (% of control) with changes in Time to ENG onset (% of day 0). **C)** Correlation of all 4 cats' Inner Zone fiber diameter measures (% of control) with changes in Time to ENG onset (% of day 0). **D)** Correlation of all 4 cats' Perimeter Zone fiber diameter measures (% of control) with changes in Time to ENG onset (% of day 0). **E)** Correlation of all 4 cats' Inner Zone myelin thickness measures (% of control) with changes in Time to ENG onset (% of day 0). **F)** Correlation of all 4 cats' Perimeter Zone myelin thickness measures (% of control) with changes in Time to ENG onset (% of day 0).

Inner Zone

Perimeter Zone
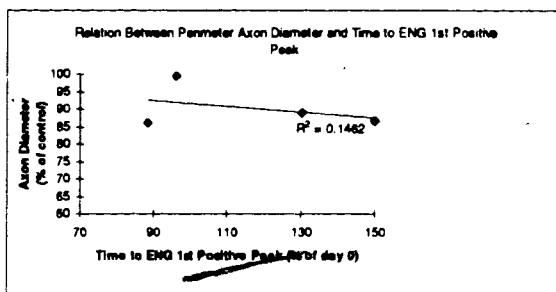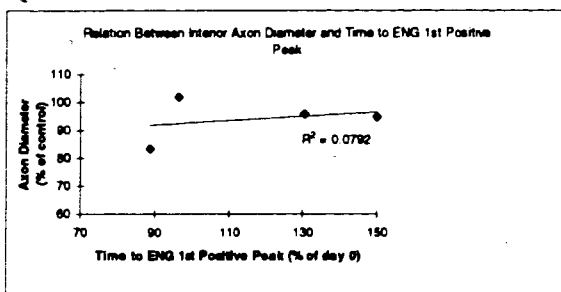
A)

B)
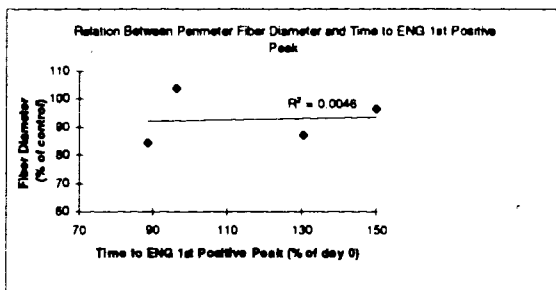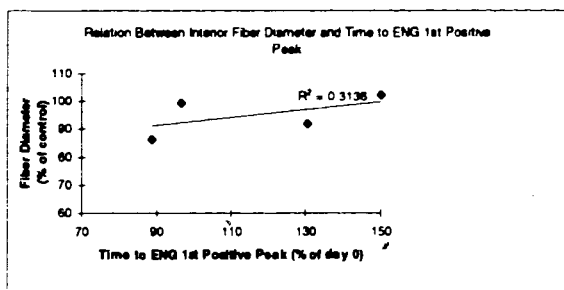
C)

D)
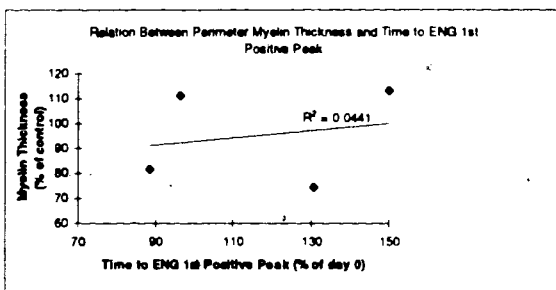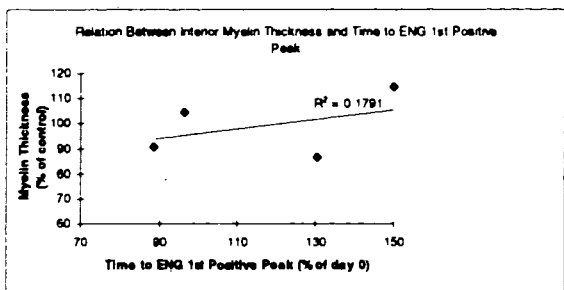
E)

F)

Figure 39: A) Correlation of all 4 cats' Inner Zone axon diameter measures (% of control) with changes in Time to ENG 1st positive peak (% of day 0). **B)** Correlation of all 4 cats' Perimeter Zone axon diameter measures (% of control) with changes in Time to ENG 1st positive peak (% of day 0). **C)** Correlation of all 4 cats' Inner Zone fiber diameter measures (% of control) with changes in Time to ENG 1st positive peak (% of day 0). **D)** Correlation of all 4 cats' Perimeter Zone fiber diameter measures (% of control) with changes in Time to ENG 1st positive peak (% of day 0). **E)** Correlation of all 4 cats' Inner Zone myelin thickness measures (% of control) with changes in Time to ENG 1st positive peak (% of day 0). **F)** Correlation of all 4 cats' Perimeter Zone myelin thickness measures (% of control) with changes in Time to ENG 1st positive peak (% of day 0).

5. DISCUSSION

5.1 Are cuffed nerves different from control?

Cat median nerves implanted with our circumferential nerve cuff electrodes were found to exhibit a number of differences compared to the uncuffed, contralateral control nerves. Cuffed to control comparisons, within-cats, tended to show significantly lower mean axon diameters, mean fiber diameters and mean myelin thicknesses. These morphometric measures have been used as indicators of nerve health in the past and this study reinforces their usefulness as indicators in morphometric analyses.

Cuffed nerves were not systematically different from control using Axon Circularity, Fiber Circularity and G-ratio measures. This result can be interpreted in two ways. First, it could be said that these variables were not useful for differentiating cuffed nerves from control nerves. If quantifying such differences is our goal, then these morphometric measures cannot be used. On the other hand, it could also be said that this lack of a difference tends to emphasize the subtle nature of the effects of cuffs on nerves. Axon Circularity, Fiber Circularity and G-ratio have been used in the past to quantify dramatic changes in nerve morphology and it is possible that the differences observed in this study were too mild to be measured.

In this study, among-cat differences were less striking than were the within-cat comparisons. Overall mean axon diameter, overall mean fiber diameter and overall mean myelin thickness were not significantly different from control at $p < 0.05$. There are two possible explanations for the discrepancy between the within-cat comparisons and the across cat comparisons.

First, within-cat comparisons preserved the individual idiosyncrasies of a given cat while the among-cat comparisons tended wash out the individual differences.

Second, the number of cats used in this experiment may have been too low to allow for the detection of these differences. In order to address this question, we must calculate the statistical power of the current experiment. Statistical power refers to a statistic's ability to detect a difference given the assumption that a difference actually exists. The power score can

be manipulated depending on the experimenter's willingness to accept the probability of making either a type I error (α) or a type II error (β).

For this experiment, the power statistic was calculated as follows (Howell, 1989; Colton, 1974):

$$\gamma = \frac{\mu_1 - \mu_2}{\sigma}$$

and

$$\delta = \gamma\sqrt{N}$$

Where:

γ=   a measure of the degree of separation between the means
μ_1=   mean of sample 1
μ_2=   mean of sample 2
σ =   estimate of the population standard deviation
δ=   power (as a z statistic)
N=   the number of subjects

Power values of 0.97 at α=0.05 and 0.92 at α=0.01 were calculated for the differences in average axon diameter and average fiber diameter. The power values for myelin thickness were lower due, mostly, to a proportionately larger among-cat variance (Tables 8 and 9). Power for myelin thickness differences across cats was 0.72 at α=0.05 and 0.58 at α=0.01. A score of 0.01 indicates very low power and a score of 0.99 is considered very high. A power score of 0.80 is often considered necessary before proceeding with an experiment.

Based on these calculations, we can say with some certainty that our test is powerful enough to detect actual differences between cuffed and control overall average axon diameter and overall fiber diameter (at α=0.01 and N=4). We can be less certain that our test can reliably detect differences in overall myelin thickness.

While a larger sample size would increase the power of the among-cat myelin thickness comparison, the high power values obtained for axon diameter and fiber diameter tend to suggest that we should have detected a difference in these variables if one existed. Since this was not the case, we can conclude that there was no among-cat difference for mean axon diameter and mean fiber diameter. This finding further brings into question the usefulness and appropriateness of performing among-cat comparisons for morphometric studies.

In conclusion, it can be said that there were differences between cuffed and control nerves. Cuffed nerves tended to exhibit lower values in three important morphometric measures (axon diameter, fiber diameter and myelin thickness). Within-cat comparisons yielded stronger differences than did among-cat comparisons. The appropriateness of performing among-cat pooling was called into question.

5.2 Did these cuffs cause damage?

Before we begin a discussion of whether or not damage was observed, we must first define it. In this study, the term damage referred to negative differences in any of the morphometric measures utilized (i.e. lower axon diameter, fiber diameter or myelin thickness as compared to control). Damage also referred to negative changes in any of the neurophysiological measures. These included decreased CAP amplitude, increased time to ENG onset and increased time to ENG first positive peak. Damage, in this sense, was not meant to imply the instance of any functional deficit. In fact, no obvious functional deficiencies were observed in the cats during the experimental period.

It was clear that, despite any statistical concerns regarding the overall averages, there was a general trend toward cuffed axons showing fewer larger axons and more smaller axons (Figs. 35 to 37). These data suggest that some or all of the axons shrunk to become smaller axons during the implant period.

These findings are consistent with two established models of nerve damage: low level chronic nerve compression and low level anoxia/ ischemia.

Low Level Compression

Low level nerve compression could have occurred in our cuffs in one of two ways.

First, the cuffs could have applied direct pressure to the nerve and, thus, the integrity of the axons could have been interrupted (Aguayo et al, 1971). While specific precautions were taken to prevent this occurrence, we cannot eliminate it as a possible factor.

Second, the cuffs could have caused a slight damming up of the endoneurial fluid through compression of the venules. Rydevik et al. (1981) have shown that pressures as low as 30 mmHg can impair venular blood flow. Due to a lack of lymph vessels, any decrease in nerve fluid outflow (without a concomitant decrease in inflow) leads to a build up of fluid within the endoneurial space and a consequent increase in endoneurial fluid pressure. Four possible mechanisms have been proposed to explain how an endoneurial edema can cause axonal damage (Lundborg et al., 1983):

- the increased pressure acts as a direct insult to the axons
- the change in electrolytic composition due to the influx of fluid destroys the internal milieu necessary for proper neuronal function
- the increased fluid pressure interferes with capillary flow and capillary nutrient exchange
- the increase in endoneurial pressure may serve to occlude the epineurial vessels as they pass obliquely through the perineurium into the endoneurial space.

The cuffed nerves in this study showed a decrease in the proportion of the nerve devoted to signal conduction (Conduction Area in Table 5). In contrast, the cuffed nerves demonstrated no change in the size of the nerve that was bounded by the epineurium (Epineurial Area in Table 5). This discrepancy indicates that something other than neural tissue has taken up the space forfeited by the shrunken axons. In all likelihood, the space was filled either by edemateous fluid or by fibroblasts. Long standing edemas can often lead to, fibrotic scarring of peripheral nerves (Myers and Powell, 1984).

Low Level Anoxia/ Ischemia

Prolonged oxygen deprivation leads to a decrease in both fast and slow axonal transport within peripheral nerves (Dahlin et al, 1984, Dahlin and McLean, 1986). Since axonal transport is responsible for the delivery of subcellular building blocks along the length of the nerve, any reduction in axonal transport will compromise the integrity of the axon. Reduced delivery of neurofilament and microtubule proteins to the axon have been associated with decreased axon calibers. The results observed in this study were consistent with this kind of change.

5.2.a Can causal relationships be established?

Discussion or conclusions regarding the incidence of shrinkage or damage during the implant period must be tempered with caution. The control nerves in this experiment do not allow definitive statements to be made about changes in morphology. Before and after snapshots of the experimental nerve could not be taken and, thus, we cannot say exactly what the experimental nerves looked like on day 0 of the experiment. Since morphometric sampling required the excision of the nerve from the subject, these kinds of comparisons were impossible. The contralateral control nerve provided the closest approximation possible.

While no before and after comparisons were possible, we can say that the differences observed in this experiment were generally consistent with changes observed in experimental models of nerve damage (as mentioned above). We are able to extrapolate our findings to suggest that the cuffed nerves in this study may have experienced similar, less severe types of injury. We cannot, however, say with perfect certainty that damage took place.

The level of confidence that can be placed on making statements of damage depends very much on the closeness of the match between cuffed and control nerve. In this experiment, these matches were quite close. Nerve sizes (not including connective tissue) were similar between cuffed and control nerves (Table 4), the number of fascicles per nerve sample were comparable, the total numbers of axons were not statistically different and the degree of bimodality observed in the control distributions was similar to that of the cuffed distributions. Taken together, these findings suggest that the control nerves did provide a good match for the cuffed nerves in this experiment.

In conclusion, cuffed nerves showed changes in axonal morphology that were consistent with both low level chronic compression injuries and with low level anoxia/ ischemia injuries. Given the complex interplay of these two types of injury, it is not surprising that the cuffed nerves showed indications of both. Statements of causation were impossible to make in this experiment due to the nature of the control situation but the close matches observed between cuffed and control nerves lent credence to the conclusion that cuffed nerves were mildly affected in this experiment.

5.3 Were Perimeter Zone axons affected more than Inner Zone axons?

Axons located in the Perimeter Zones of cuffed nerves experienced greater changes with respect to the Inner Zone axons of the same cuffed nerve. In most cases, the absolute difference (in μm) with respect to control for axon diameter, fiber diameter and myelin thickness was twice as great in the Perimeter Zone as compared to the Inner Zone.

These findings suggest that axons located around the outer perimeter of cuffed nerves were affected to a greater extent during the cuff implant than were the axons that were located nearer to the core of the nerve. These findings are consistent with those observed during compression neuropathy studies (Aguayo et al, 1971; Lundborg, 1987; Lundborg, 1988; Myers and Powell, 1984; Powell and Myers, 1986).

The difference between the Inner and Perimeter zones has exciting implications for future workers in this field. Since the axons in the outer 50 μm were affected the most during chronic nerve cuff implantation, it stands to reason that these axons are the most sensitive indicators of damage. The number of axons located in the outer 50 μm was typically about 10% of the total number of axons found in the whole nerve. Thus, opportunities exist for sampling to take place only in the outer perimeter of the nerve. In this way, the processing time for each nerve sample would be greatly reduced with no cost to the accuracy or validity of the results.

Perimeter Zone axons showed twice the absolute change with respect to control as did the Inner axons. These results suggest that, while our cuffs are relatively safe, we may need to continue refining the cuff design to try to maximize its safety. In addition, the greater effect observed in the Perimeter Zone, combined with the fact that there were fewer axons in this zone, opens up the possibility for future researchers to simply sample the Perimeter Zone axons for signs of nerve damage.

5.4 Were larger axons affected more than smaller axons?

The results observed in this study suggest that most or all axons became somewhat smaller during the cuff implant period. Contrary to what was expected from the literature

(Ochoa et al., 1972; Stein et al., 1977; Stein and Oguztöreli, 1978; Lundborg, 1987), our results suggest that there was a general shift to smaller axon dimensions across the entire size spectrum (Fig. 40).

This finding is difficult to explain. Our results are quite clear and very consistent across all morphometric variables and, yet, there are decades of nerve compression research which suggest that the larger axons should have been differentially more affected. One possible explanation of this result could be that the compressive component of the cuff implant (See Section 5.2) was reduced in importance as compared to the anoxic element. Anoxia would have affected all axons equally regardless of size since all axons rely on oxygen to the same extent for axonal transport.

Another possible explanation might be that the morphometric measures employed in this experiment were much more powerful than those used in past studies. In this study, all axons were examined from entire nerve cross sections such that large samples of axons from each size range were able to be compared. In addition, previous research did not break the data down into quartiles as was done in this study. This comparison was critical for elucidating the nature of the changes in our data set. Other workers may have missed these details.
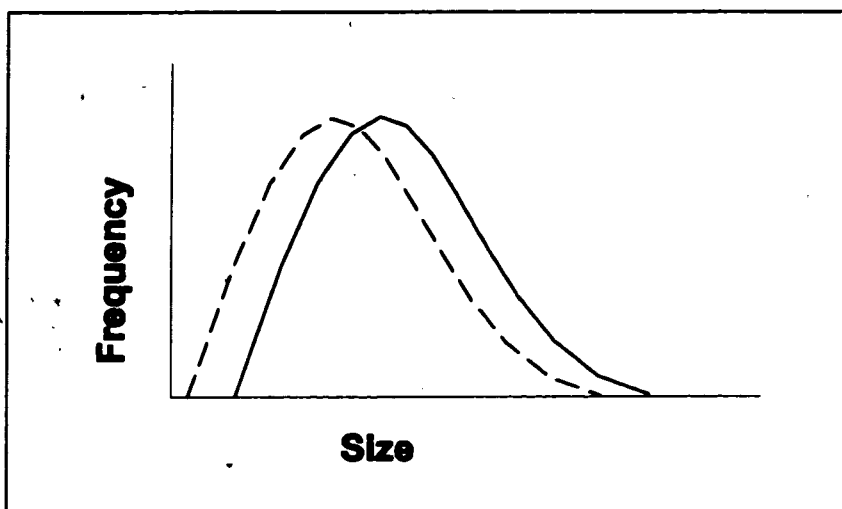
Figure 40: Schematic illustration of the size changes observed for axon diameter, fiber diameter and myelin thickness. The solid line represents the control distribution and the dashed line represents the cuffed distribution. A unimodal distribution is illustrated but the same changes would be true for a bimodal distribution.

5.5 Were Morphometric Changes Correlated with Neurophysiological Changes?

5.5.a CAP Amplitude was negatively related to morphometric measures

When axon diameter, fiber diameter and myelin thickness measures (expressed as a percentage of control) were correlated to changes in neurophysiological data (with respect to day 0) the results were opposite to what was expected. All three measures showed negative correlations with CAP amplitude changes. Based on known relations between axon sizes and extracellular potential amplitudes (Marks and Loeb, 1976; Hoffer et al, 1979; Milner et al., 1981), it was expected that a decrease in axon diameter would have been associated with a concomitant decrease in the amplitude of the CAP. This study showed the opposite trend.

5.5.b Time to ENG onset and time to ENG first positive peak showed weak positive correlations with morphometric measures.

Correlations of either axon diameter, fiber diameter or myelin thickness changes with time to ENG onset or time to ENG positive peak changes showed almost no relationship with CAP amplitude. The sign of these weak relationships, however, was opposite to what was expected. The data showed that, as average axon or fiber diameter decreased and the degree of axon myelination decreased, the conduction velocity of the experimental nerves increased.

5.5.c Possible explanations for these paradoxical correlations

1. There is uncertainty with respect to the reliability of the day 0 CAP data.

As mentioned previously, we were unable to state categorically that nerve cuffs actually cause damage because we were unable to take a before and after snapshot of the morphology. A similar shortcoming exists for the neurophysiological measurements. We did not gather neurophysiology data from the control nerve at any time during the experiment, rather, we made the assumption that the signals from the two nerves would have been the same.

Of greater concern, is the finding that CAP Amplitudes can be transiently reduced by as much as 1/3 simply due to the manipulation of the nerve during the implant surgery (Hoffer, personal communication). In spite of the great care that was taken during surgery, there is no way to predict to what extent the CAP data were affected on day 0 of the experiment. The introduction of potential day 0 errors of the order of 30% makes it very difficult to interpret the neurophysiological data. All neurophysiological data were expressed as a percent of day 0 so any errors in the day 0 measurements were translated directly into the denominator of the final assessment of CAP signal amplitude.

2. The sample size may have been too small.

Another possible explanation for the paradoxical relationship observed between the morphometry and the neurophysiology could be the fact that we can place only limited faith in

a correlation derived from only four data points. Clearly, the simple fact that a non-zero relationship existed between one variable and another does not guarantee that this correlation was valid. Chance correlations can occur with regularity when the number of data points is less than five (Howell, 1989).

Applying a test of significance (Howell, 1989) to the correlations obtained, we see that only the correlations of CAP amplitude with the Perimeter Zone fiber diameter ($\alpha=0.02$) and Perimeter Zone myelin thickness ($\alpha=0.05$) reached statistical significance (Table 13).

	Perimeter				Inner	
	N	r	t statistic		r	t statistic
CAP Amplitude						
Axon Diameter	4	-0.69	-1.35		-0.71	-1.43
Fiber Diameter	4	-0.98	-7.24	**	-0.87	-2.52
Myelin Thickness	4	-0.95	-4.48	⊗⊗	-0.83	-2.16
ENG onset						
Axon Diameter	4	0.10	0.14		0.30	0.44
Fiber Diameter	4	0.11	0.16		0.59	1.04
Myelin Thickness	4	0.25	0.36		0.46	0.73
ENG 1st +ve peak						
Axon Diameter	4	0.38	0.58		0.28	0.41
Fiber Diameter	4	0.06	0.09		0.56	0.95
Myelin Thickness	4	0.21	0.30		0.43	0.67

Table 13: Summary of the r values obtained for each neurophysiological to morphometric correlation. Values with ** are significant at $\alpha=0.02$ and values with ⊗⊗ are significant at $\alpha=0.05$.

3. Cuffs which damaged nerves may, in fact, have yielded larger amplitude signals.

Despite any of the aforementioned uncertainty about the day 0 CAP measurements or the appropriateness of the sample size, we still observed significant negative relationships between CAP amplitude and both fiber diameter and myelin thickness changes of the Perimeter Zone. This paradox must be addressed.

The method in which the electrodes were sewn into the silicone cuff wall (Fig. 41) may have caused the electrodes to impinge on the nerve to a greater extent than the internal cuff diameter might have indicated. In addition, disturbance of the cuff could have moved the wire

electrodes into a position where they could have acted as nooses around the nerve (Fig. 41).
Potential sources of the torque presented in Fig. 41 might include muscular activity around the
cuff or connective tissue adhesion of either the cuff or the backpack leads to surrounding
tissue. The benefit of this situation, from a neurophysiological perspective, would be that the
electrode and nerve would be introduced into more intimate contact and the nerve signals
would be improved. The degree to which the signals might be improved is difficult to assess.

In situ fixation of the nerves inside the cuffs would be necessary as a first step for
assessing differences in electrode to nerve proximity. The data presented in this thesis did not
allow for this sort of comparison.

Modeling of each axon's contribution to the total CAP signal would shed some light on
the shape of the signal that we should have expected (Milner et al., 1981). If we make the
assumption that the Perimeter Zone axons would contribute the most to the overall signal
(Marks and Loeb, 1976), then this process could be very much simplified.

In conclusion, changes in CAP amplitude (with respect to day 0) were significantly
correlated with cuffed fiber diameter and myelin thickness differences (with respect to
control). These correlations were negative. This finding was opposite to what was expected.
There are a number of possible explanations for this apparent paradox but further research will
be required to provide a satisfactory explanation.
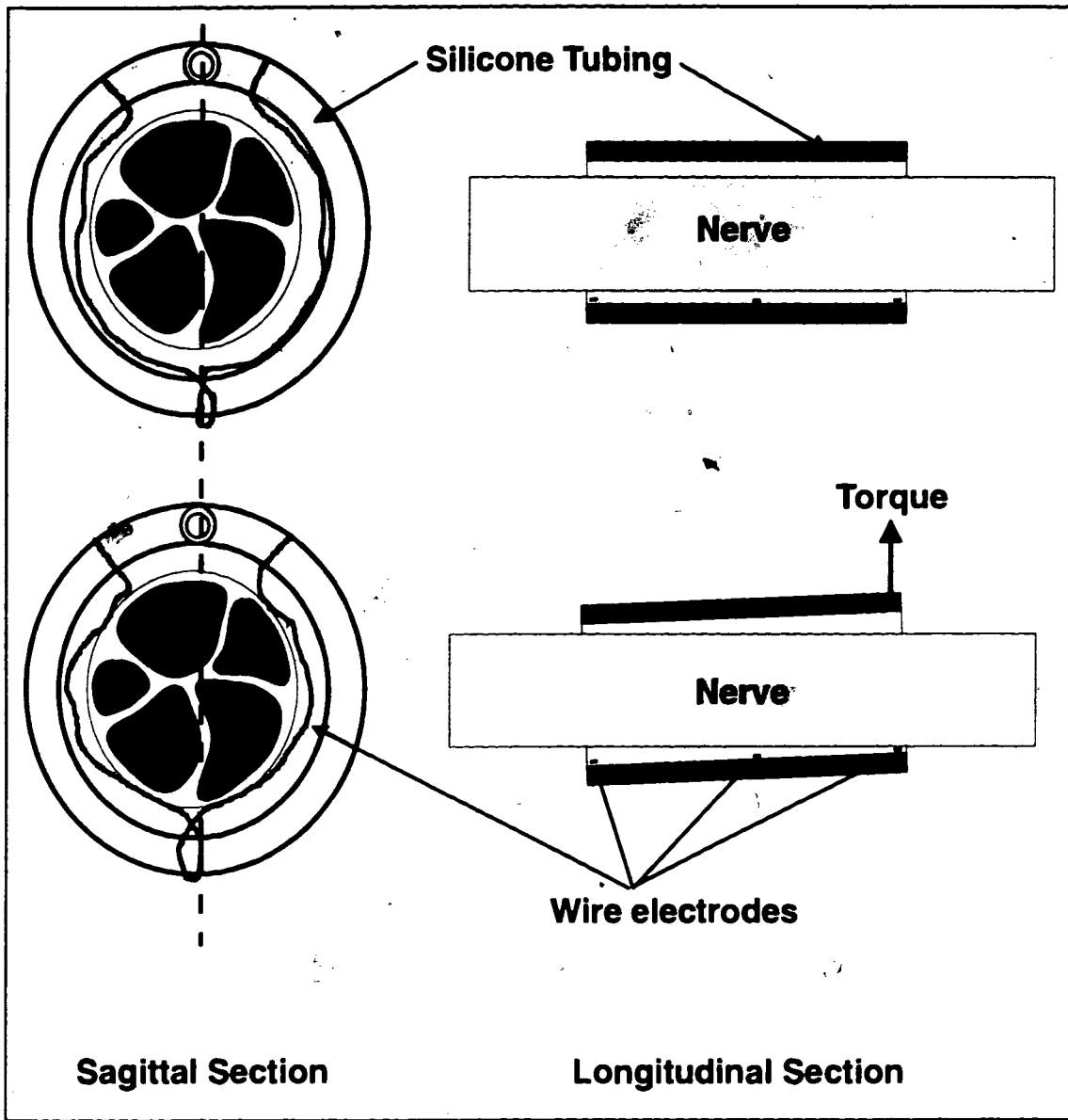
Figure 41: Left: Cross section of a peripheral nerve implanted with a circumferential recording electrode. In the top picture, the electrode wire is located near the inner circumference of the cuff as it should be. The bottom picture shows how the electrode wire oould act as a noose around the nerve even though the cuff diameter is appropriately sized. The dotted line represents the location of the longitudinal section presented on the right. **Right:** Note how the application of torque to the cuff brings the electrodes into closer contact with the nerve.

6. FUTURE DIRECTIONS

This thesis opens many interesting avenues of future exploration.

1. While the tissue fixation techniques utilized in this experiment were adequate for our purposes, the process could be improved. Perfusion of the nerve samples would have provided better fixation. In perfusion, the fixative is injected into the bloodstream and, as a result, works from the inside of the nerve to the outside. This is the opposite of the immersion fixation techniques utilized in this experiment. Perfusion typically allows for a wider separation of the axons within a cross section as compared to immersion. Increased separation would have dramatically increased axon classification speed and would have reduced the operator fatigue associated with this process.

2. Better examination of the nerve cuffs could be performed *in situ*. Nerve cuffs could be explanted with the nerves inside them and then the cuff and nerve could be embedded together. Sectioning of the nerves and nerve cuff together would allow us to check for the noose effect hypothesized in the discussion.

3. Electrophysiological measures of the control nerve could be taken on the initial day of implant. Not only would this allow for the comparison of day 0 CAP measurements between cuffed and control nerves but it would provide us with a more appropriate control situation. As it stands now, we cannot say with complete certainty whether or not the observed differences were a result of the chronic implantation of the cuffs or whether it was due to the original surgical intervention. This suggestion may be unrealistic since the implant surgeries currently take approximately 14 hours and any extension of this time frame would be very challenging for the surgeons.

4. Mathematical modeling could be used to examine in greater detail the nature of the CAP signals that should have been expected given the axon and fiber size distributions observed in this experiment. Such an exercise might provide insight into this study's lack of an observed CAP to morphometry correlation.

5. New cuff designs should be tested that decrease the potential for creating the noose effect. These new designs could be compared to current designs such that we might be able to confirm or disprove the noose hypothesis.

6. Ideally, sample analysis could become more automated. Numerous macro programs were written for this study but there are a number of other improvements that would dramatically increase the speed of processing. One example might be that the initial photographic sampling of the nerve could be put under the control of a computer. The stage could be moved by a servo motor and the coordinates of each frame could be recorded by the computer. The computer could then automatically apply the filtering macro developed in this thesis and it could use the coordinates of the frames to automatically remove any duplicate axons. These changes would make the entire morphometric process significantly less arduous and would permit the analysis of a greater number of nerves than were possible in this study.

7: CONCLUSIONS

A new morphometric analysis technique was developed for this thesis. Unlike other studies that only sampled axons from an entire nerve cross section, this study examined all the axons (approximately 5,000 per nerve) from whole median nerves. This extra effort was undertaken to minimize any potential sampling errors. This study was also unique in its attempt to correlate morphometric findings with neurophysiological data obtained from the same chronically implanted recording cuffs.

This study observed that implanted nerves had slight but statistically significant reductions in average axon diameter, fiber diameter and myelin thickness measures as compared to contralateral, unoperated control limbs. Overall, these morphometric measures were approximately 10% lower than in controls. There were no statistical differences in axon numbers and there appeared to be no obvious functional changes for the implant subject as a consequence of these changes.

Axons located in the outer 50 μm edge of the nerve (the Perimeter Zone) were affected almost twice as much as the rest of the nerve. This edge effect suggests that the Perimeter axons experienced greater mechanical damage due to cuff implant than did the Inner axons.

The percentage of axons with axon diameters greater than 8 μm was higher in control nerves than in cuffed nerves. Cuffed nerves had a higher percentage of axons with smaller axon diameters. The same pattern held true for fiber diameters greater than 10 μm and myelin thicknesses greater than 2μm. If we accept that the cuffed nerves once resembled the control nerves, then we can say that the fibers appeared to generally become smaller during the course of the implant period.

The size changes observed were consistent across the entire size spectrum. This meant that large and small cuffed axons were equally affected. This size change is consistent with a general shift to smaller axon sizes across the entire size distribution.

CAP amplitudes were found to be negatively correlated with fiber diameter and myelin thickness differences (with respect to control) in the perimeter zone. These data were opposite

95

to the results expected and may indicate that the circumferential wire electrodes inside the cuffs constricted the nerves to a greater extent than was expected from the cuff diameter alone.

References

Agnew WF, McCreery, DB Yuen TGH and Bullara LA. (1989). Histologic and physiologic evaluation of electrically stimulated nerve: considerations for the selection of parameters. *Annals of Biomedical Engineering*. 17(1): 39-60.

Aguayo A, Nair CPV and Midgeley R. (1971). **Experimental progressive compression** neuropathy in the rabbit. *Archives of Neurology.*24: 358-364

Auer R. (1994). Automated nerve fibre size and myelin sheath measurements using microcomputer-based digital image analysis: theory, methods and·results. *Journal of Neuroscience Methods*. 51: 229-238.

Bancroft J.D and Stevens A. (1990). In *The Theory and Practice of Histological Techniques:3rd edition* . Churchill-Livingstone, Edinburgh; N.Y.

Buckett JR, Peckham PH and Strother RB. (1980). Shoulder position conrtol: An alternative control technique for motion impaired individuals. *Proceedings of the International Conference on Rehabilitative Engineering*. Toronto, pp. 244-247.

Christensen PR. (1997). Sensory source identification from nerve recordings with multi-channel electrpdes arrays. *MASc Thesis*. School of Engineering Science, Simon Fraser University.

Dahlin LB and McLean WG. (1986). Effects of graded experimerital compression on slow and fast axonal transport in rabbit vagus nerve. *Journal of Neurological Sciences*. 72: 19-30·;

Dahlin LB, Nordborg C and Lundborg G. (1987). Morphological changes in nerve cell bodies induced by experimental nerve compression. *Experimental Neurology*. 95: 611-621

Dahlin LB, Rydevik B, WG McLean and Sjostrand J. (1984). Changes in fast axonal transport during experimental nerve compression at low pressures. *Experimental Neurology*. 84: 29-36.

Davis LA, Gordon T, Hoffer JA, Jhamandas J and Stein RB. (1978). Compound action potentials recorded from mammalian peripheral nerves following ligation or resuturing. *J. Physiol.* 285: 543-559,. ·

Droz B. (1969) Protein metabolism in nerve cells. *International Review of Cytology*. 25: 363-390.

Dyck PJ, Low PA, Sparks MF, Hexum LA and Karnes JL. (1980). Effect of serum hyperosmolarity on morphometry of healthy human sural nerve. *Journal of Neuropathology and Experimental Neurology*. 39: 285-295.

Franken, HM, Veltink PH and Boom HK. (1994) Restoring gait in paraplegics by functional electrical stimulation. *IEEE Eng. Med. Biol.* 3: 564-570.

Gillespie MJ and Stein RB. (1983). The relationship between axon diameter, myelin thickness and conduction velocity during atrophy of mammalian peripheral nerves. *Brain Res.* 259: 41-56.

Glenn WWL and Phelps ML. (1985). Diaphragm pacing by electrical stimulation of the phrenic nerve. *Neurosurgery.* 17: 974-984.

Grafstein B. (1975). The nerve cell body response to axotomy. *Experimental Neurology.* 48(3): 32-51.

Hambrecht FT. (1990). A brief history of neural prostheses for the motor control of paralyed extremeties. In *Neural Prostheses: Replacing Motor Function after Disease or Disability.* R.B. Stein, F. Hunter Peckham and D.P. Popovic (eds), Oxford University Press, New York, pp. 3-14.

Haugland M, Lickel A, Riso R, Adaniczyk MM, Keith M, Jensen IJ, Haase J and Sinkjaer T. (1995). Restoration of lateral hand grasp using natural sensors, in *Proc. of 5th Vienna Int. Workshop of FES*, Vienna, AS.

Haugland MK and Hoffer JA. (1994a). Slip information provided by nerve cuff signals: application in closed-loop control of functional electrical stimulation. *IEEE Trans. Rehab. Eng.*, Vol. 2, pp. 29-36.

Haugland MK and Hoffer JA. (1994b) Artifact-free sensory nerve signals obtained from cuff electrodes during functional electrical stimulation of nearby muscles. *IEEE Trans. Rehab. Eng.* 2: 37- 40.

Haugland MK, Hoffer JA and Sinkjaer T. (1994). Skin contact force information in sensory nerve signals recorded by implanted cuff electrodes. *IEEE Trans. Rehab. Eng.*, 2: 18-28.

Hoffer JA and Haugland M. (1992). Signals from tactile sensors in glabrous skin suitable for restoring motor functions in paralyzed humans. In *Neural Prostheses: Replacing Motor Function after Disease or Disability*, R.B. Stein, P.H. Peckham, and D. Popovic, editors. Oxford Univ. Press, pp. 99-125.

Hoffer JA. (1975). Long-term peripheral nerve activity during behaviour in the rabbit: The control of locomotion. *PhD. Thesis, Johns Hopkins Univ. Nov. 1975. Publication No. 76-8530, University Microfilms, Ann Arbour, Michigan; 124 pp.*

Hoffer JA. (1990). Techniques to record spinal cord, peripheral nerve and muscle activity in freely moving animals. In *Neurophysiological Techniques: Applications to neural systems. Neuromethods 15*, A.A. Boulton, B.B. Baker and C.H. Vanderwolf, Eds., Humana Press, Clinton, N.J., pp.65-145.

Howell DC. (1989) *Fundamental Statistics for the Behavioral Sciences: 2nd Edition.* PWS-Kent Publishing Company, Boston, MA

Kallesøe K, Hoffer JA, Strange K, Valenzuela I. (1996). Implantable cuff having improved

closure. U.S. Patent 5,487,756, awarded Jan. 30, 1996.

Kim JH, Manuelidis EE, Glenn WWL and Kaneyuki T. (1976). Histopathological changes in the phrenic nerve following long-term electrical stimulation. *The Journal of Thoracic and Cardiovascular Surgery.* 72(4): 602-608.

Kim JH, Manuelidis EE, Glenn WWL, Fakuda Y, Cole DS and Hogan JF. (1983). Light and electron microscopic studies of phrenic nerve after long-term electrical stimulation. *Journal of Neurosurgery.* 58: 84-91.

Krarup C and Loeb GE. (1988). Conduction studies in peripheral cat nerve using implanted electrodes: I. Methods and findings in controls. *Muscle and Nerve.* 11: 922-932.

Lundborg G and Rydevik B. (1973). Effects of stretching the tibial nerve of the rabbit: A preliminary study of the intraneural circulation and the barrier function of the perineurium. *The Journal of Bone and Joint Surgery.* 57B (2): 390-401.

Lundborg G, Gelberman RH, Minteer-Convery M, Lee YF and Hargens AR. (1982). Median nerve compression in the carpal tunnel- Functional response to experimentally induced controlled pressure. *The Journal of Hand Surgery.* 7(3): 252-259

Lundborg G, Myers R and Powell H. (1983). Nerve compression injury and increased endoneurial fluid pressure: a "miniature compartment syndrome". *Journal of Neurology, Neurosurgery and Psychiatry.* 46: 1119-1124

Lundborg G. (1975). Structure and function of the intraneural microvessels as related to trauma, edema formation, and nerve formation. *The Journal of Bone and Joint Surgery.* 57A: 938-948

Lundborg GR. (1987). *Nerve Injury and Repair.* Churchill-Livingstone, London; Edinburgh.

Marks WB and Loeb GE. (1976). Action currents, internodal potentials and extracellular records of myelinated mammalian nerve potentials derived from node potentials. *Biophysics Journal.* 16: 655-658

Martin JH and Jessell TM. (1991). Modality coding in the somatic sensory system. In *Principles of Neural Science: 3rd edition.* E.R. Kandel, J.H. Schwartz and T.M. Jessell eds. Appleton and Lange, Norwalk, Connecticut, pp: 342-352.

Mezin P, Tenaud C, Bosson JL and Stoebner P. (1994). Morphometric analysis of the peripheral nerve: advantages of the semi automated interactive method. *Journal of Neuroscience Methods.* 51: 163-169.

Milner TE, Stein RB, Gillespie J and Hanley B. (1981). Improved estimates of conduction velocity distributions using single unit action potentials. *Journal of Neurology, Neurosurgery, and Psychiatry.* 44(6): 476-484.

Mize RR. (1983). A microcomputer system for measuring neuron properties from digitized

images. *Journal of Neuroscience Methods*. 9: 105-113.

Myers RR and Powell HC. (1984). Galactose Neuropathy: Impact of chronic endoneurial edema on nerve blood flow. *Annals of Neurology*. 16: 587-594

Naples GG, Mortimer JT and Yuen TGH. (1990). Overview of peripheral nerve electrode design and implantation. In *Neural Prostheses Fundamental Studies* W.F. Agnew and D.B. McCreery Eds. Prentice Hall, Englewood Cliffs, N.J., p.108-145.

Naples GG, Mortimer JT, Scheiner A and Sweeney JD. (1988). A spiral nerve cuff electrode for peripheral nerve stimulation. *IEEE Transactions in Biomedical Engineering*. 35(11): 90-915.

Nathan RH. (1993). Control strategies in FNS systems for the upper extremities. *Critical Reviews in Biomedical Engineering*. 2(6): 485-568.

Ochoa J, and Marotte L. (1973). The nature of nerve lesion caused by chronic entrapment in the guinea-pig. *Journal of the Neurological Sciences*. 19: 491-495

Ochoa J, Fowler TJ and Gillat RW. (1972). Anatomical changes in peripheral nerves compressed by a pneumatic tourniquet. *Journal of Anatomy*. 113: 433-455.

Peckham P and Keith MW. (1992). Motor prostheses for restoration of upper extremity function. In *Neural Prostheses: Replacing Motor Function after Disease or Disability*. R.B. Stein, F. Hunter Peckham and D.P. Popovic (eds), Oxford University Press, New York, pp. 162-187.

Popovic DP. (1992). Functional electrical stimulation for lower extremties. In *Neural Prostheses: Replacing Motor Function after Disease or Disability*. R.B. Stein, F. Hunter Peckham and D.P. Popovic (eds), Oxford University Press, New York, pp. 233-251.

Powell HC and Myers RR. (1986). Pathology of experimental nerve compression. *Laboratory Investigation*. 55(1): 91-100

Prochazka A, Wieler M. and Gauthier M. (1996) The Bionic Glove. Abstract of the First Annual Conference of the International Functional Electrical Stimulation Society, Cleveland Ohio, May 14-16.

Richardson KC, Jarett L and Finke EH. (1960). Embedding in epoxy resins for ultrathin sectioning in electron microscopy. *Stain Technology*. 35: 313-323

Rydevik B, Lundborg G and Bagge U. Effects of graded compression on intraneural blood flow. *The Journal of Hand Surgery*. 1981: 6(1): 3-12

Rydevik B, Lundborg G. Permeability of intraneural microvessels and perineurium following acute, graded experimental nerve compression. *Scandanavian Journal of Plastic and Reconstructive Surgery*. 1977: 11: 179-187.

Rydevik B, McLean WG, Sjostrand J and Lundborg G. (1980). Blockage of axonal transport induced by acute, graded compression of the rabbit vagus nerve. *Journal of Neurology, Neurosurgery and Psychiatry.* 43: 690-698

Sinkjaer T, Haugland M and Haase J. (1994). Natural neural sensing and artificial muscle control in man. *Experimental Brain Research.* 98(3): 542-545.

Sinkjær T, Haugland M and Haase J. (1992). The use of natural sensory nerve signals as an advanced heel-switch in drop-foot patients. in *Proc. of the 4th Vienna Workshop on FES*, pp. 134-137.

Stein RB and Oguztöreli MN. The radial decline of nerve impulses in a restricted cylindrical extracellular space. *Biological Cybernetics.* 1978: 28: 159-165.

Stein RB, Charles D, Davis L, Jhamandas J, Mannard A and Nichols TR. (1975). Principles underlying new methods of chronic neural recording. *Canadian Journal of Neurological Sciences.* 2: 235-244.

Stein RB, Charles D, Hoffer JA, Arsenault J, Davis LA, Moorman S and Moss B. (1980) New approaches for the control of powered prostheses particularly by high-level amputees. *Bulletin of Prosthetics Research.* 17:1: 51-62.

Stein RB, Gordon T, Hoffer JA, Davis LA and Charles D. (1979). Long-term recordings from cat peripheral nerves during degeneration and regeneration: Implications for human nerve repair and prosthetics. In *Nerve Repair: its Clinical and Experimental Basis*, D.L. Jewett and H.R. McCarroll, Eds. C.V. Mosby: St. Louis; Ch. 17, pp. 166-176.

Stein RB, Nichols TR, , Jhamandas J, Davis L and Charles D. (1977). Stable long-term recordings from cat peripheral nerves. *Brain Research.* 128: 21-38.

Strange KD and Hoffer JA. (1995b). Using cutaneous neural signals to predict cat forelimb muscle activity during walking, in *Proc. of IEEE SMC*, Vancouver, Canada, Oct. 1995, vol.2, pp. 1199-1204.

Strange KD and Hoffer JA. (1996). Sensory signals from cat paw cutaneous receptors during walking: applicability for closed-loop control of FES, in preparation.

Strange KD, Hoffer JA, Kallesøe K, Schindler SM and Crouch DA. (1995a). Long term stability of nerve cuffs implanted in the cat forelimb, in *Proc. of RESNA '95*, Vancouver, Canada, June 1995, pp. 372-374.

Sunderland, S., (1968), *Nerves and Nerve Injuries.* London: Livingstone.

Tashman S and Zajac FE. (1992). Control of multijoint lower limb motor tasks with Functional Neuromuscular Stimulation. In *Neural Prostheses: Replacing Motor Function after Disease or Disability.* R.B. Stein, F., P.H. Peckham and D.P. Popovic (eds), Oxford University Press, New York, pp. 252-278.

Torch S, Stoebner P, Usson Y, Drouet D'Aubigny G and Saxod R. (1989). There is no simple adequate sampling scheme for estimating the myelinated fiber size distribution in human peripheral nerve: a statistical ultrastructural study. *Journal of Neuroscience Methods.* 27: 149-164

Usson Y, Torch S, Drouet d'Aubigny G. (1987). A method for automatic classification of large and small myelinated fibre populations in peripheral nerves. *Journal of Neuroscience Methods.* 20: 237-248.

Vallee RB and Bloom GS. (1991). Mechanisms of fast and slow axonal transport. *Annual Review of the Neurosciences.* 14:59-92.

Waters RL, McNeal DR, Faloon W and Clifford B. (1985). Functional Electrical Stimulation of the peroneal nerve for hemiplegia: Long term clinical follow-up. *Journal of Bone and Joint Surgery.* 67-A: 792-793.

Weiss P and Hiscoe HB. (1948). Experiments in the mechanisms of nerve growth. *Journal of Experimental Zoology.* 107: 315-395.

Appendices

Appendix 1: Fixation, Embedding and Staining Recipes

Fixative (as per Karnovsky, 1965)

Take 168 ml of concentrated Schultz's phosphate buffer (13.24 g Monobasic Sodium Phosphate, 135 g Dibasic Sodium Phosphate, 1 L double distilled water) and add 108 ml of 18.5 % paraformaldehyde. Heat solution to 60°C and add concentrated NaOH until the solution clears. Add 60 ml of 50% glutaraldehyde. Add 662 ml of double distilled H_2O. Stir for 10 minutes. Adjust pH to 7.2 with HCl.

Fixative (as per Dyck et al, 1980)

An iso-osmolar glutaraldehyde solution is produced by creating a 2.5% glutaraldehyde solution in 0.025 M cacodylic buffer (sodium cacodylate in distilled H_2O) . The temperature should be held at 10°C and the pH should be adjusted to 7.38.

Embedding Medium

For medium hardness blocks, combine:

1. 22.8 ml Jembed 812 Resin (J.B. EM Services, Dorval, Quebec)
2. 15.4 ml Dodecenyl Succinic Anhydride (DDSA)
3. 11.8 ml of Nadic Methyl Anhydride (NMA).

*Add 50 drops (1.5%) of tri (dimethylaminomethyl) phenol (DMP 30) as a catalyst for hardening.

Stains

Osmium Tetroxide:

A 2% Osmium tetroxide solution is created by combining 0.5 g of Osmium Tetroxide crystals in 25 ml of water.

Richardson's Stain (Richardson et al, 1960):

A: 1% Azure II in distilled H_2O.
B: 2% Methylene Blue in distilled H_2O.
C: 2% Borax in distilled H_2O.

Mix equal parts B and C. Mix equal parts A and the B/C combination.

Appendix 2: Histological processing

1. Plastic embedding was carried out as follows:

2. Fresh tissue samples were immersed in an iso-osmolar solution of glutaraldehyde (see Appendix 1) at room temperature for a period of one week.

3. The tissue samples were then rinsed in 2 changes of 0.1 M cacodylic buffer, 20 minutes total time.

4. Post fixation in a 2% Osmium Tetroxide solution (see Appendix 1) was carried out for 4 hours.

5. The samples were then received another rinse of 0.1 M cacodylic buffer.

6. The samples underwent gradient dehydration in ethyl alcohol (50,70,85,95 and 100%, 20 minutes for each alcohol grade).

7. The alcohol was displaced by two 7 minute washes in propylene oxide.

8. The samples were then placed in 2:1 mixture of epoxy resin and propylene oxide overnight.

9. The 2:1 mixture was removed and replaced with 100% resin for 4 hours.

10. Samples and resin were placed in a 60°C oven for 48 hours.

11. Plastic sections 0.5 μm thick were cut and a 2:1 mixture of Richardson's stain and Toluidine Blue was applied to the sections as a counter stain.

Appendix 3: Section Cutting Protocol

1. Secure the plastic block in the microtome clamp.

2. Warm a hotplate to approximately 60-90°C.

3. Trim away any excess plastic from the edges of the nerve using a razor blade. Note: this is done to ensure that sample will lay flat on the slide.

4. Rough cut the block face using a glass knife until a relatively smooth surface is obtained.

5. Using a fresh, sharp knife cut approximately a dozen 0.5 μm sections. Every 2-3 sections, transfer the samples to a water covered microscope slide using a thin metal wire. Ensure that the knife is free of any nicks that might mar the surface of the block. The knife will start to become dull after about 15-20 sections so a new knife will be required if further sections are desired.

6. Dry the microscope slide containing the dozen samples on the hotplate. For best results, dry away most of the water using a Kimwipe or some other sort of tissue paper. Be careful not to touch the tissue to the samples otherwise they will adhere to the tissue. Once the majority of the water has been removed, the samples will only need to remain on the hotplate for approximately 30 seconds. Excessive drying will produce tiny cracks in the sections and it is desirable to avoid this consequence.

7. Apply the 2:1 Richardson's stain: Toluidine Blue mixture to the dried samples for about 75 seconds. It is absolutely critical to apply the stain while the slide is still on the hotplate!. Rinse the stain off by running the slide under a gently running faucet. Be sure that the side with the sections is facing down, away from the water stream so that they are not washed off.

8. Dry the slide on the hotplate. Once again, remove any excess water from the slide by gently patting a fresh tissue to the sample side of the slide. The sections will be sufficiently affixed to the surface of the slide that they will be able to withstand gentle application of a tissue. Dry the slide for 30 seconds after the majority of the water has been removed using the tissue.

9. View the sections under a microscope. If they are of sufficient quality, apply a couple of drops of Permount to the slide and then affix a coverslip to the slide.

Appendix 4: Nerve Cuff Technical Drawings*

*All cuff drawings used by the kind permission of Klaus Kallesoe.
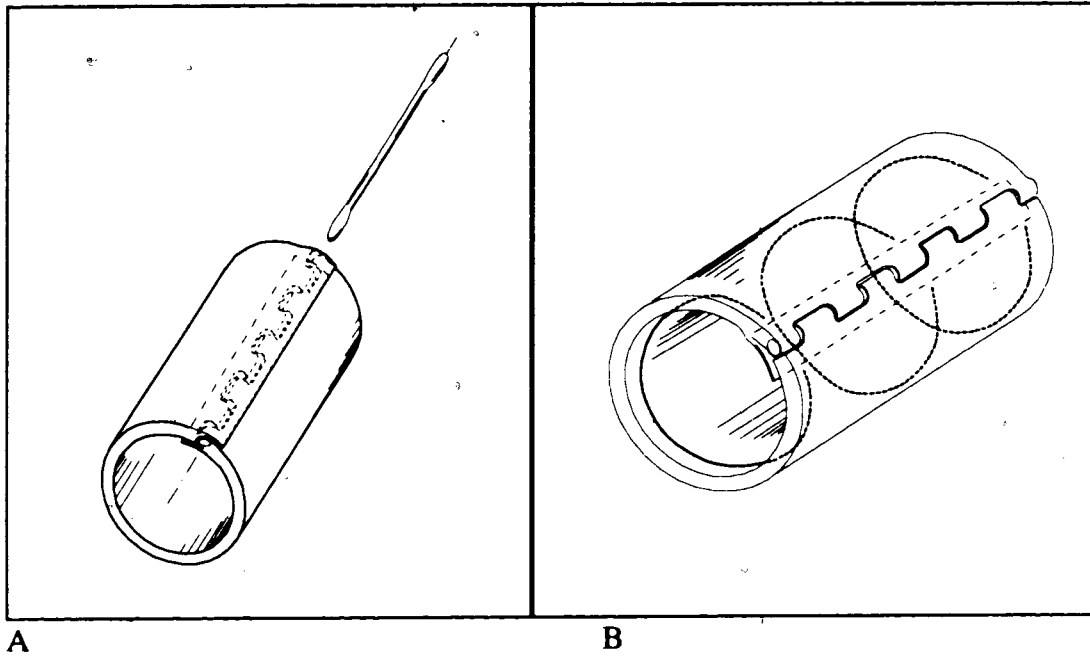

Fig. A4.1: A. Nerve cuff showing the insertion of the baton closing device. B. Nerve cuff showing the location of the circumferential electrodes (dotted lines).
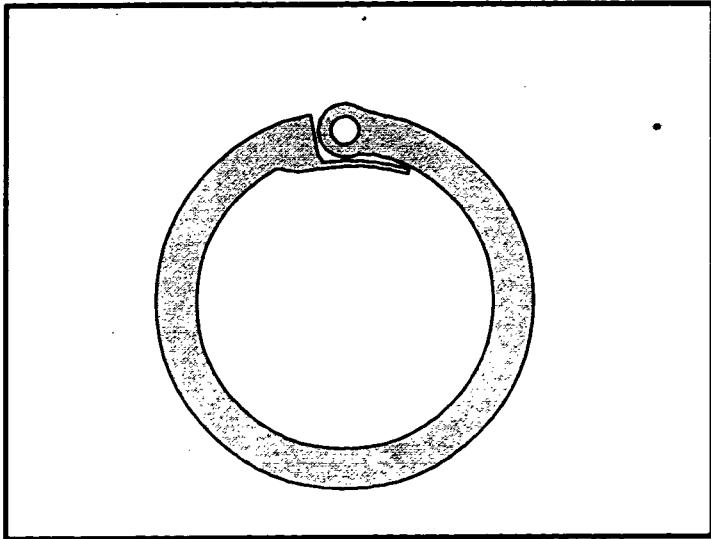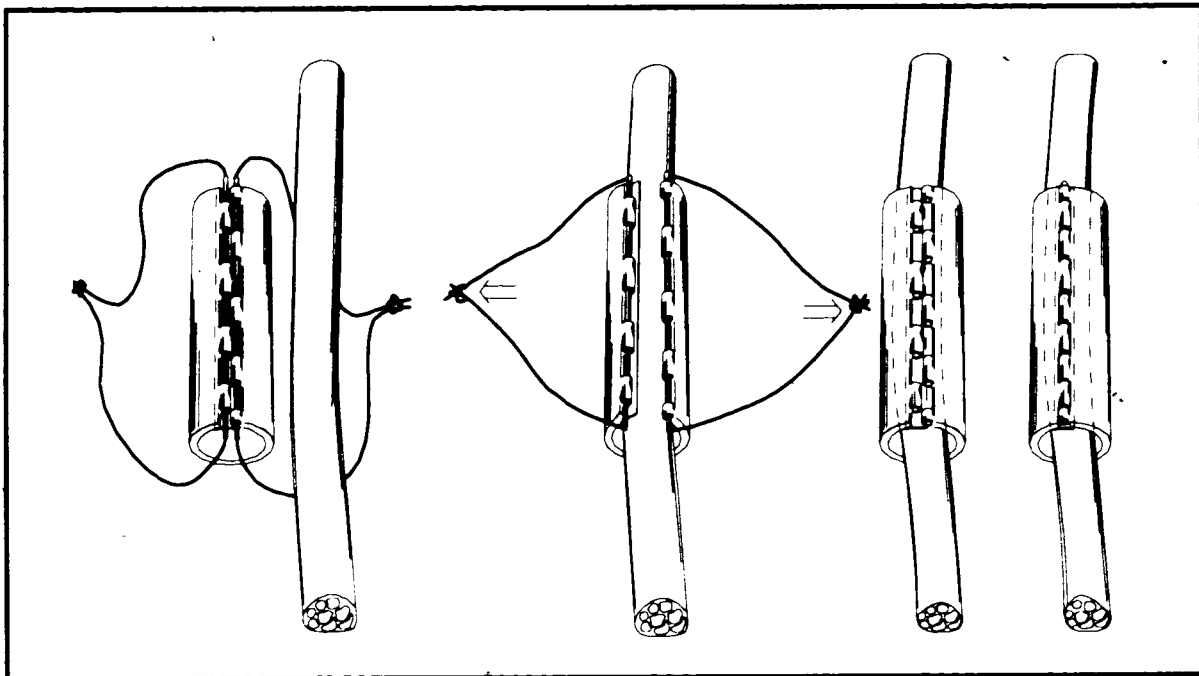
Fig. A4.3: Cross section of a nerve cuff.

Fig. A4.4: Installation procedure for a nerve cuff.

Appendix 5: Calculation Morphometric Measures
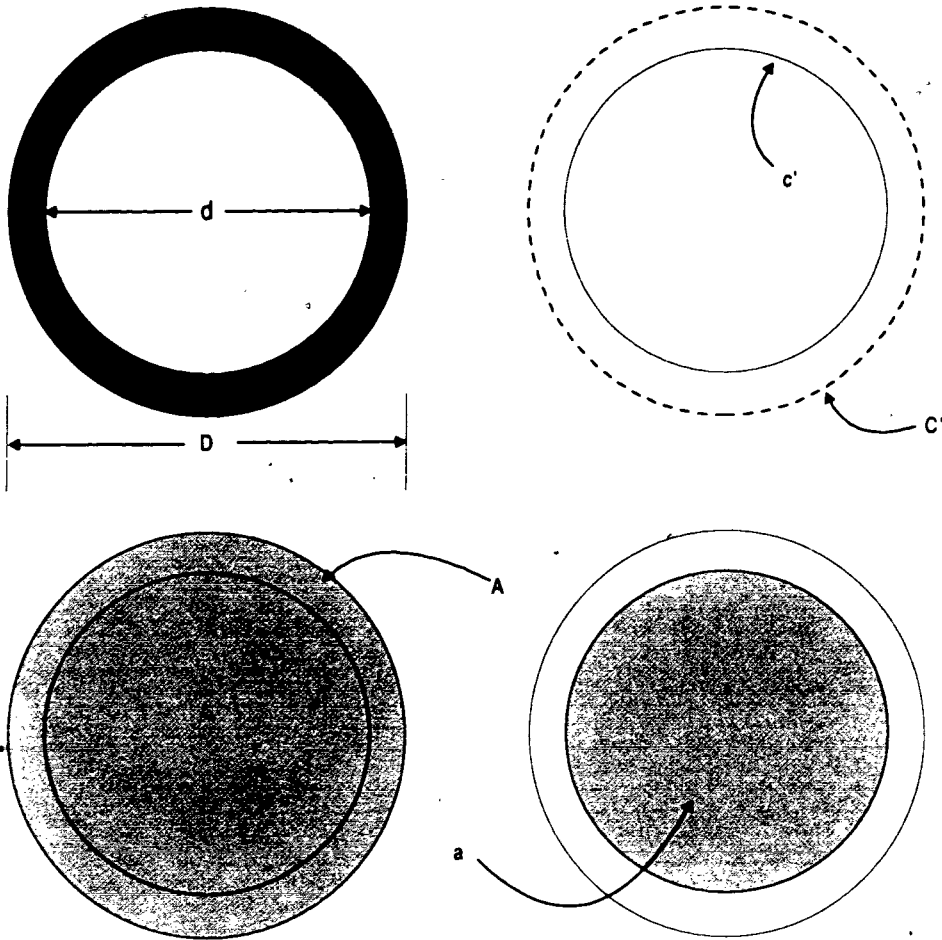
Note: Axons are represented as perfect circles to facilitate their representation.

Measured quantities:

Axon Circumference(c')
Fiber Circumference (C")
Axon Area (a)
Fiber Area (A)

Mathematical derivations:

Diameter Calculated from Circumference:

Axon Diameter (d)=c'/(π)
Fiber Diameter (D)=C"/(π)
Myelin Thickness (m)=1/2(D-d)

Diameter Calculated from Areas

$d = 2\sqrt{a/(\pi)}$
$D = 2\sqrt{A/(\pi)}$
Myelin Thickness (m)=1/2(D-d)

Appendix 6: Macro Programs Used for Nerve Processing

Auto Saving Macro

```
// dcsave.mac
// Macro for saving images in bunches
// David Crouch, Author


iCount=0;                                           // counter
INTEGER iFas=0;                                     //fascicle #

char cNIHNum;                                       // NIH number designation
char cMatch;                                        //combination of all the above

char cNIHNum= prompt ("NIH number?","char");
iFas= Prompt ("Fascicle Number?","integer");

while(true)
{
Acquire();

if (!prompt ("More?"))                              //ask user if they wish to collect more
            break;                                  // breaks out on user cancel

else
        {
        freeze();
        ++iCount;
        cMatch=cNIHNum:totext(iFas):totext(iCount):".tif";
        SaveImage("c:/optimas5/image/dave/":"/":cNIHNum:cMatch);
        SetFont("Helv",12,,,,,500);                 // helvetica text, semi bold at 12
        TextToScreen(cMatch);                       // shows sample number on screen
        MoveScreenItem(,5:5);                       // moves location of text
        print (3.0,,2);                             // prints image with overlaid text in white
        }
}
end;
```

Bulk Filtering Macro

```
// dcbulk.mac
// macro designed to bulk process saved samples
//  David Crouch, Author

INTEGER iA=0;                                    //number of samples to be collected
INTEGER iFas=0;                                        //fascicle #

char cNIHNum;          //. NIH number designation
char cMatch;           //combination of all the above

char cNIHNum= prompt ("NIH number?","char");
iFas= Prompt ("Fascicle Number?","integer");
iA= Prompt ("Number of samples to be collected?","INTEGER");

for (iCount=1;iCount<iA+1;++iCount)
        {
        ROIFullScreen();
        cMatch=cNIHNum:totext(iFas):totext(iCount):".tif";
        OpenImage("c:/optimas5/image/dave/":cNIHNum:"/":cMatch);
        Filters (Median);
        Filters (Median);
        Filters (Median);
        SharpenLow;
        Filters (Median);
        Filters (Median);
        SaveImage("c:/optimas5/image/dave/":cNIHNum:"/processd/":cMatch);
        }
end;
```

Retouching Macro

```
//Dcretuch.mac
//Retouching and area recovery macro
//David Crouch, author

INTEGER iA=0;                              // number of samples to be
collected
INTEGER iFas=0;                                      // fascicle #
INTEGER iCount=1;                          // loop counter
INTEGER iDecision=0;                       // retouch, threshold or save?

char cNIHNum;                              // NIH number designation
char cMatch;                               //combination of all the above

cNIHNum= Prompt ("NIH number?","char");

iFas= Prompt ("Fascicle Number?","integer");

iA= Prompt ("Number of samples to be collected?","INTEGER");

if (!Prompt("Suitable threshold?"))
                    pause();

While (iCount<(iA+1))
{
        cMatch=cNIHNum:totext(iFas):totext(iCount):".tif";
        ImageFileDestinationRoi=0;         //place image onto full screen
        ImageFilePlaceSource=0;                    //user does not place image
        OpenImage("c:/optimas5/image/dave/":cNIHNum:"/Exptl/processd/Fascicle":totext(iF
as):"/":cMatch);

//////////////////////////////////////////////////////////////////
Threshold(96:255);                         /// Must be changed before each session
//////////////////////////////////////////////////////////////////

        Retouching();                              // opens retouching box
        Threshold();
        keyhit();                                          // clears keyboard buffer
        while(keyhit()!=(0x20));       // continues internal loop until spacebar is hit
        CreateArea(,,True);
        Retouching();                              // opens retouching box
        keyhit();                                          // clears keyboard buffer
        while(keyhit()!=(0x20));       // continues internal loop until spacebar
        SaveImage("c:/optimas5/image/dave/":cNIHNum:"/Exptl/Processd/Fascicle":totext(iFa
':cMatch);
```

112

```
            beep(2);
            ++iCount;
    }

beep();
Macromessage("That's it!!");
end;
```

Data Gathering Macro

```
// davegath.mac
// macro connects parents and children and measures parameters from both
// Optimas Corp, primary author; modifications by David Crouch


SetExport(mArHandle,1,TRUE);
SetExport(mArArea,1,TRUE);
SetExport(mArPerimeter,1,TRUE);                                 //dc added

INTEGER
        CON_ConnectivityVariable[,,,,,],                        //5commas
        CON_NumberOfParents=Null,
        CON_ParentHandles=Null,
        CON_ChildHandles=Null;
REAL
        ArParentAreas,
        ArChildAreas,
        ArParentPerimeters,                                     //dc added
        ArChildPerimeters;                                      //dc added

OpenImage("c:/optimas5/images/dave/");
CreateArea(,,TRUE);
MacroMessage(" Lone Parents or Children will cause this macro to fail.\r\n\Hold Shift key
down and click twice on area(s) to remove loners.");
Select();
MultipleExtract(TRUE);
CON_ConnectivityVariable=AreaConnectivity (mArHandle);
CON_NumberOfParents=GetShape (CON_ConnectivityVariable)[0];

For ( i=0; i<CON_NumberOfParents; i++)
{
CON_ParentHandles:= CON_ConnectivityVariable[i,0,,,,]; //Selects Parent
CON_ChildHandles:= CON_ConnectivityVariable[i,1,,,,];  //Select Child
}

ArParentAreas=mArArea[CON_ParentHandles];
ArChildAreas=mArArea[CON_ChildHandles];
ArParentPerimeters=mArPerimeter[CON_ParentHandles];     //dc added
ArChildPerimeters=mArPerimeter[CON_ChildHandles];    //dc added

SetExport(mArArea,1,FALSE);
SetExport(mArHandle,1,FALSE);
SetExport(mArPerimeter,1,FALSE);                                //dc added

Viewbox(ArParentAreas,,ArChildAreas,);
```
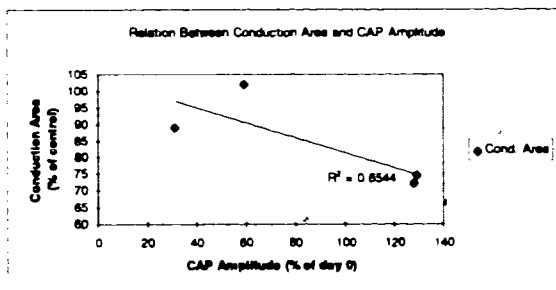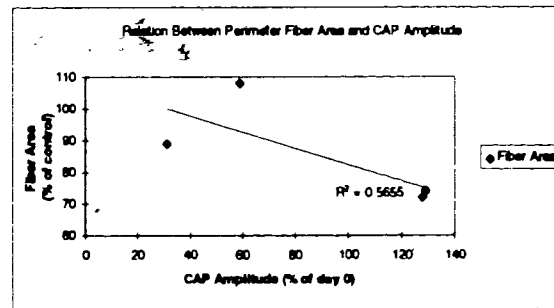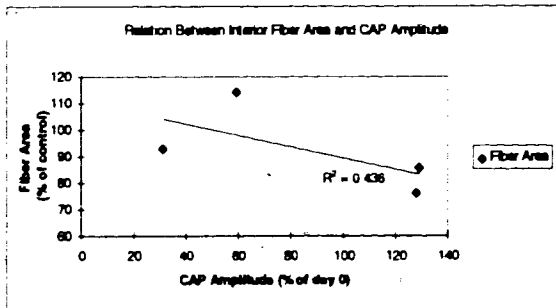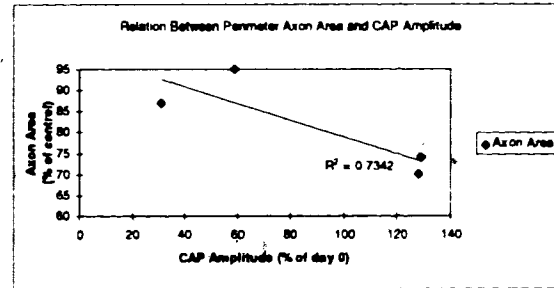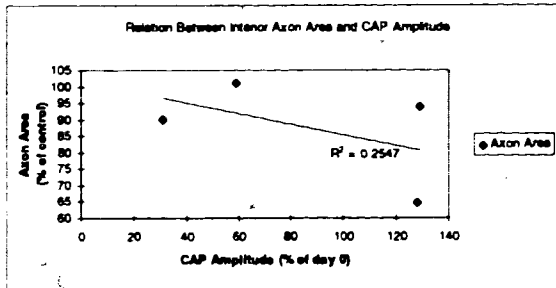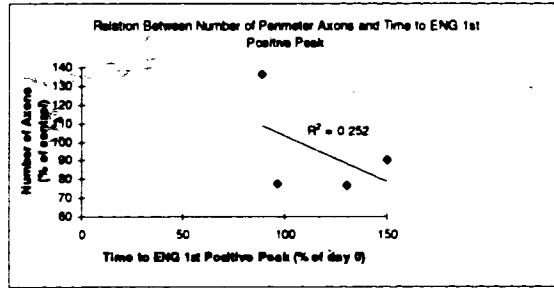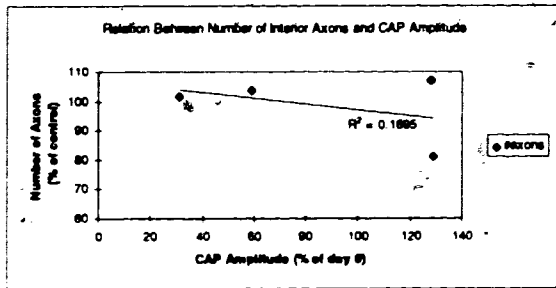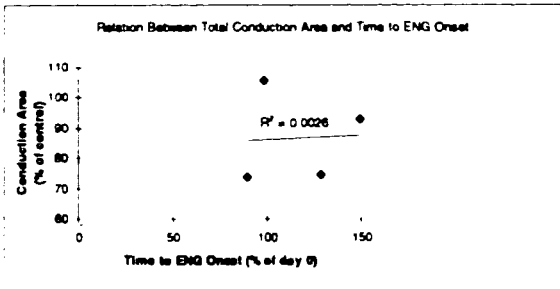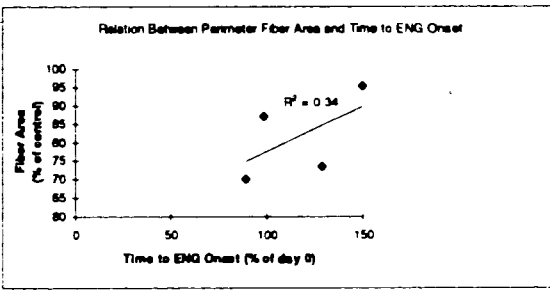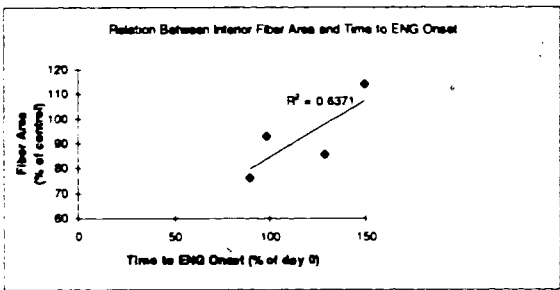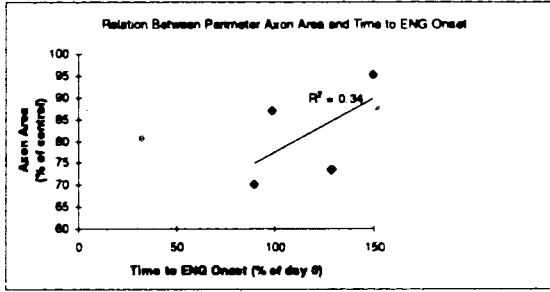
114

//End of Macro

Appendix 7: Additional Correlation Data

CAP Amplitude

Relation Between Number of Interior Axons and CAP Amplitude

Relation Between Number of Perimeter Axons and Time to ENG 1st Positive Peak

Relation Between Interior Axon Area and CAP Amplitude

Relation Between Perimeter Axon Area and CAP Amplitude

Relation Between Interior Fiber Area and CAP Amplitude

Relation Between Perimeter Fiber Area and CAP Amplitude

Relation Between Conduction Area and CAP Amplitude

Time to ENG Onset

Relation of Number of Axons in Interior Zone to Time to ENG Onset

$R^2 = 0.1112$

Relation Between Number of Perimeter Axons and Time to ENG Onset

$R^2 = 0.2607$

Relation Between Interior Axon Area and Time to ENG Onset

$R^2 = 0.7019$

- Axon Area
- Linear (Axon Area)

Relation Between Perimeter Axon Area and Time to ENG Onset

$R^2 = 0.34$

Relation Between Interior Fiber Area and Time to ENG Onset

$R^2 = 0.6371$

Relation Between Perimeter Fiber Area and Time to ENG Onset

$R^2 = 0.34$

Relation Between Total Conduction Area and Time to ENG Onset

$R^2 = 0.0026$

Time to First Positive ENG peak